THE JOURNAL
OF THE
ACOUSTICAL SOCIETY OF AMERICA

Volume 9 Number 4

APRIL • 1938

Loudness, Masking and Their Relation to the Hearing Process and the Problem of Noise Measurement

HARVEY FLETCHER
Bell Telephone Laboratories, Inc., New York, N. Y.

(Received February 15, 1938)

INTRODUCTION

WHEN a person is immersed in a sound wave he experiences the sensation of hearing. Psychologists usually speak of this sensation as the sound. In this sense the sound has three general characteristics, namely, loudness, pitch and quality or timbre. It is only musical sounds which have a definite pitch. The term "quality" contains all the other auditory characteristics not included in the terms "loudness" and "pitch." In recent years there have been attempts to separate quality into the other aspects of the sound such as volume, extension, brilliance, etc. It seems to me that quality and timbre are still very vague terms and in spite of the recent interesting work they are still far from being reduced to a quantitative basis. This is probably because there is such a great variety of things included in the term "quality." On the other hand, pitch and loudness have been reduced to a definite quantitative basis, although the former has a limited application, namely, to musical sounds, while the latter can be applied to every type of sound.

I will discuss experimental and analytical methods used to reduce loudness to a quantitative basis and point out the bearing of the experimental results upon the mechanism of hearing. Before proceeding with this discussion I shall review some of the quantitative terms which will be used.

DEFINITIONS

In dealing in a quantitative way with the sound we will use the terms intensity I, acoustic pressure p, and their relation to the intensity level β; the loudness level L, and the loudness N; the spectrum level B, and noise spectrogram; the masking M, and noise audiogram.

Intensity I

As used in this paper, the intensity I will be used with 10^{-16} watts per square centimeter as a unit. In other words, $I=1$ for the standard reference level of 10^{-16} watts per square centimeter. For example, if I is 10^{9}, then when a free wave passes the point under consideration, 10^{-7} watts of power, or 1 erg per second, pass through each square centimeter of the wave front.

Pressure p

As the wave passes, the acoustic pressure for unit intensity varies with temperature and

atmospheric pressure. These variations are very small compared to the range of values used here, so that for most practical calculations it can be assumed that when I is unity, then p can be taken equal to unity. This also corresponds to the standard threshold for a tone having a frequency of 1000 c.p.s. and corresponds approximately to 0.0002 dyne per square centimeter. With these conventions then

$$I=p^2. \tag{1}$$

Intensity level β

The intensity level β in decibels is then defined by

$$\beta=10 \log I=20 \log p. \tag{2}$$

Loudness level L

For purposes of making comparisons of loudness of various sounds, a reference sound has been adopted by the American Standards Association as a reference standard. This same standard has recently been recommended for adoption to the International Standards Association by an international acoustical conference. This reference sound is a free progressive wave having a frequency of 1000 cycles per second to be received by the listener facing the source of this tone. Its intensity could be defined by giving either I, p, or β, but it has been agreed internationally that it shall be defined by giving the intensity level in decibels. The loudness level of the reference tone expressed in phons is the intensity level of this tone expressed in decibels. The loudness level of any other sound is determined by comparing it to the reference tone, adjusting the latter until the two sound equally loud. Then the loudness level of the reference tone becomes also the loudness level of the sound being measured and is expressed in phons.

Loudness N

Loudness is the magnitude of the auditory sensation produced by the sound. A scale for representing loudness has been found such that units on this scale agree with common experience in the estimates made of the sensation magnitudes. This scale is definitely related to the loudness level scale. Units on the scale are called loudness units, abbreviated LU.

Spectrum level B

When a sound is not musical but is what is ordinarily called a noise then the vibration rates are scattered throughout the audible frequency range and it can be considered as a continuous spectrum. An important noise having a continuous spectrum is the thermal noise which was used in the experiments to be described later. If ΔI is the intensity or power per square centimeter carried by the frequency band between f and $f+\Delta f$, then the spectrum level B at the frequency f is defined by

$$B=10 \log (\Delta I/\Delta f). \tag{3}$$

The actual intensity level β of any band of frequencies between f_1 and f_2 is given by

$$\beta=10 \log \int_{f_1}^{f_2} 10^{B/10} df. \tag{3A}$$

Noise spectrogram

The values of ΔI for a given Δf can be obtained experimentally by means of a noise analyzer. Consequently the values of B at each frequency can be obtained. A curve plotted with the frequency f as abscissae and B as ordinate is called the spectrogram. For purposes of loudness calculations it is not necessary to make Δf smaller than 100 c.p.s.

Overtone structure

If the sound is a musical tone it can be defined by giving the intensity level of the fundamental and of each overtone. Strictly speaking, one should give also the phases between the components, but it has been found that for these steady sounds phases produce only a negligibly small effect on the auditory sensation and in this discussion phase changes are excluded. The overtone structure is usually given in terms of the frequency and intensity levels of the component.

Masking M

Whenever one sound is being heard it reduces the ability of the listener to hear another sound. This phenomenon is called masking. In testing the masking properties of a sound usually pure tones are used as the masked sound. The number of decibels that the threshold level of a pure tone is shifted due to the presence of the noise is called the masking M at the frequency corresponding to that of the pure tone.

Noise audiogram

The values of M for each frequency are determined and the corresponding values of f and M are plotted to form a curve. The resulting curve is called the noise audiogram.

So it is seen that a noise may be defined by giving either its overtone structure, the noise spectrogram or the noise audiogram.

Development of a True Loudness Scale

A true loudness scale must be one such that when the number of units on this scale is doubled, the magnitude of the sensation as experienced by typical observers will be doubled, or when trebled the loudness sensation is trebled, etc. The existence of such a scale is dependent upon the supposition that consistent judgment tests of loudness can be obtained. Experimental tests indicate that such judgments are sufficiently consistent to warrant choosing such a scale. To find the relation between the loudness level and the loudness on the proposed new scale, various types of experiments were performed by investigators in our laboratory and elsewhere.

The general scheme of these experiments is to find experimentally pairs of values of loudness level L_1 and L_2 phons, which correspond to pairs of values of the loudness N_1 and N_2 LU. The first type of experiment is concerned with a comparison of the loudness experienced by a typical observer when listening first with one ear and then with both ears. Since we are dealing with the typical observer, the two ears will be alike in sensitivity. Consequently, if loudness is proportional to the total nerve energy sent to the brain, then it follows that the loudness experienced when using two ears will be double that when using one ear. To obtain such data the sound is first produced at any convenient intensity and listened to with only one ear, and its loudness level measured. Let us call this value L_1. Without changing the intensity of the sound the observer listens with both ears and the loudness level is measured. Let us call its value L_2. If N_1 is the number of loudness units corresponding to listening with one ear and N_2 to that corresponding to listening with both ears, then it is evident that N_2 must be just double N_1. We will again listen with one ear, but increase the intensity of the sound until a loudness level of L_2 is obtained. If now again the intensity of the sound is held constant and we listen with both ears, we will find a loudness level L_4. This must correspond to a loudness N_4 which is four times N_1. And so we might continue throughout the entire intensity range. If we now choose N_1 arbitrarily equal to some convenient number, we will have a set of corresponding values of loudness units and loudness levels from which we can draw a curve giving the relation which we are seeking.

The experiments as outlined could not be carried out because our typical observer was hypothetical. To obtain results corresponding to that which would be obtained by such a typical observer, one must deal with a large group of observers, taking the average value as that corresponding to a typical observer. For this reason, pairs of loudness levels L_1 and L_2 were obtained starting with L_1 at various values throughout the audible range. The points indicated by the open square in Fig. 1 are such observed points. A solid curve is drawn to give the best fit of the observed points corresponding to N_1, $2N_1$, $4N_1$ and $8N_1$. From this curve the proper values of L_1, L_2, L_4, L_8, etc., can be obtained to build the scale in the manner described above.

In the second type of experiment the following procedure is used. A 1000-cycle reference tone is balanced against a pure tone having a frequency far removed from 1000 until they are equally loud. Then the two tones are combined to form a complex tone having two components. Let L_1 be the loudness level of each component alone and L_2 the loudness level of the combination. Since the components were adjusted to produce equal loudness, it is assumed that each is producing the same nerve stimulation and that when they act together they will produce twice the loudness. This hypothesis is reasonable provided in the mechanism of hearing the two sets of nerves do not interfere with each other. It can be shown by experiments on the masking of one tone by another that such interference is negligibly small when their frequencies are widely separated. Consequently, balancing such a two-component tone against the reference tone should give pairs of values of L_1 and L_2 which can be used in the same way as indicated by the one-*vs.*-two ear method described above, that is, L_2 cor-

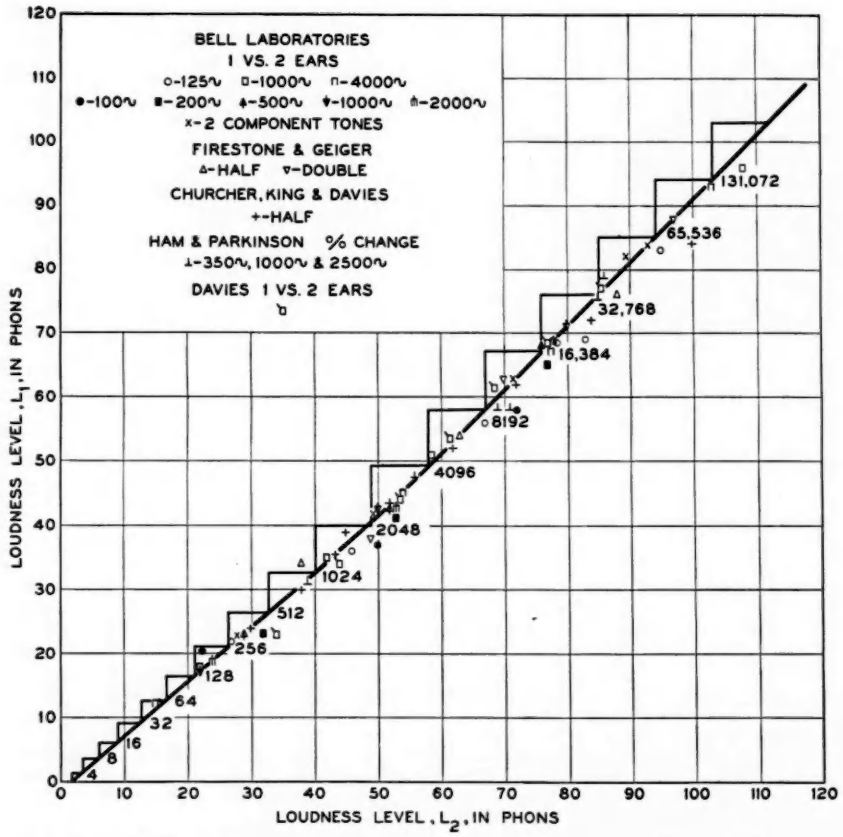

FIG. 1. Experimental values of two loudness levels L_1 and L_2 such that the sound corresponding to the latter is twice as loud as that corresponding to the former.

responds to a loudness number which is just twice that corresponding to L_1. Such observed points are shown in Fig. 1.

In the third type of experiment a typical observer is asked to listen to a sound, first at a loudness level L_1 and then to the same sound when its loudness level has been raised to a value L_2 such that to him the loudness seems to have doubled. The experiment is repeated, starting with another initial value of L_1, and thus a series of pairs of values of L_1 and L_2 are obtained which have the same relation to our loudness scale as those obtained by the first two methods. A much greater amount of data is required by this method because the probable error of a single judgment is very large. However, this method is related more directly to the scale we are seeking than the two preceding ones. Four different investigators[1] in different parts of this country and England have taken a very large number of observations by this method, not only on the

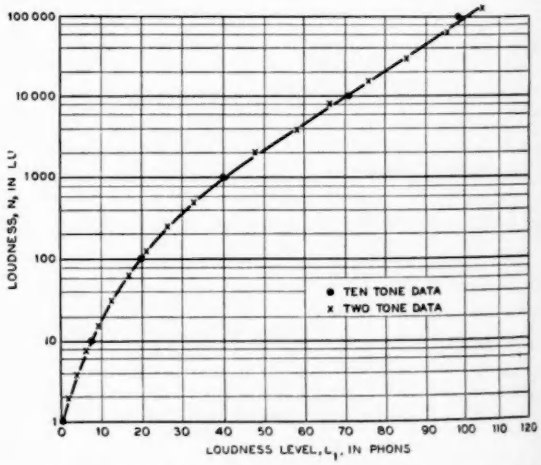

FIG. 2. Relation between loudness level in phons and the loudness in LU.

[1] In these experiments the loudness level was not measured but only the number of db above the threshold. For the 1000-cycle tone this was taken as the loudness level L. For other pure tones the loudness level was computed from our data on the loudness level of pure tones.

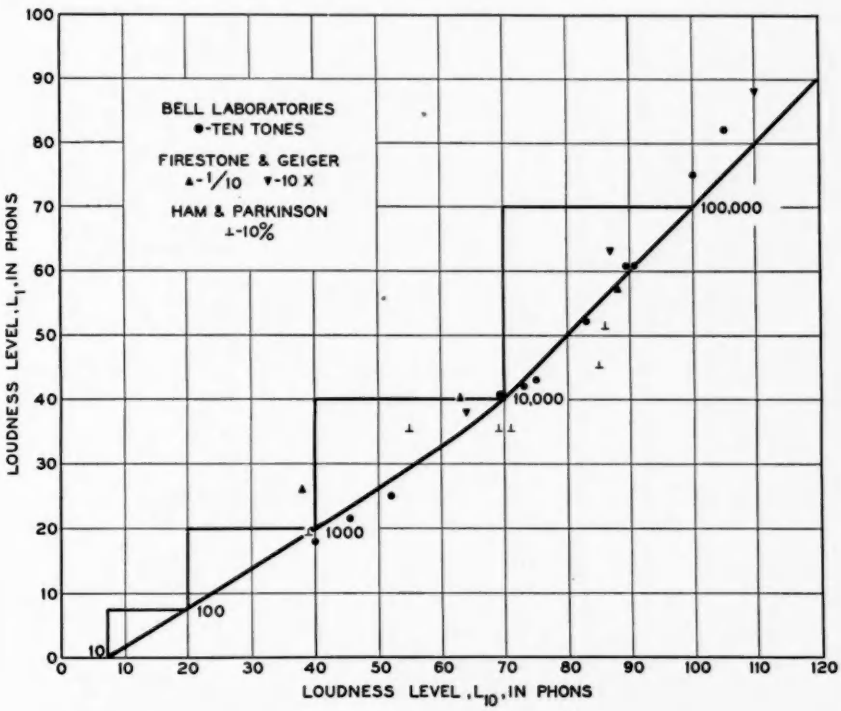

FIG. 3. Experimental values of two loudness levels L_1 and L_{10} such that the sound corresponding to the latter is ten times louder than the former.

1000-cycle reference tone but on many types of tones. The data taken by Laird have been omitted since they were so far out of line from those obtained by the other three groups of investigators, namely, Ham and Parkinson, Firestone and Geiger, and Churcher-King-Davies. Their observations are given in Fig. 1 by the points indicated.

It will be seen that the observed points obtained by these diverse methods fit consistently on one curve, particularly well in the range of loudness usually experienced in everyday life; namely, from $L_2=40$ to $L_2=80$ phons. It was sufficiently consistent to justify choosing the resulting loudness scale as a true loudness scale.

Using this curve in Fig. 1, pairs of values of L_1 and L_2 were taken to construct the curve of Fig. 2 in the following way. It will be seen that a staircase has been erected upon the curve with the corners of the steps lying on a 45 degree straight line. The value of N for $L=0$ was taken as unity. If, then, the sound is adjusted so that the threshold is reached for either ear listening alone, then when listening with both the loudness level is between 2 and 3 phons and the loudness is doubled, or 2. This corresponds to the bottom step. Now if the sound is adjusted so that for each ear alone the loudness level is 2 phons, and then if both ears are used the loudness is raised to 4 LU. This corresponds to the second step. So it is seen that the width of the steps shows the change in the loudness level necessary to double the loudness. The values of the loudness N indicated on each step can now be plotted against the corresponding L to give the desired relation between L and N. This is shown by the curve of Fig. 2.

This same scale can be developed from data obtained by balancing a three-component tone against the reference tone or by judging when a threefold increase in loudness has been produced. Or we could use any other number besides 2 or 3 and get the same scale if it is a real loudness scale. An extreme case would be to use a ten-component tone and use judgment tests for 1/10 and ten times as loud. Tests of this kind have been made which I shall now describe.

A complex tone[2] was generated having ten

[2] The description of this generator is given in the paper by Fletcher and Munson, J. Acous. Soc. Am. 5, 82–108 (1933).

harmonics of a fundamental frequency of 530 c.p.s. The components were each adjusted so that when listened to separately they had the same loudness level L_1 phons. They were then combined into a complex tone, and it was found that the loudness level was raised to a value L_{10} phons. So in this way pairs of values of loudness levels L_1 and L_{10} were obtained starting with L_1 at different intensities of sound. If the patches of nerve stimulation corresponding to each component do not overlap then the complex tone should be ten times as loud as each component. Such pairs of intensities were obtained using a group of observers, and are shown by the points in Fig. 3. Ham and Parkinson, and Firestone and Geiger made judgment tests to find a pair of loudness levels L_1 and L_{10} such that the tone for L_1 was one-tenth the loudness of that for L_{10}. Their results are shown by the points Δ and ∇, respectively. The points are somewhat scattered but I think it is remarkable that the two sets of points determine the single curve within the observational error, for such judgment tests are extremely difficult to make. It is surprising that the agreement is as good as indicated. The judgment tests and the ten-tone balance tests were all made in different laboratories and before any loudness scale of the type discussed here was constructed.

Now the curve of Fig. 3 can be used to construct a loudness scale. In this case the width of the steps of the staircase corresponds to the phons increase necessary to make the sound ten times as loud. The corresponding values of N and L can be used to determine the curve of Fig. 2. The solid curve was drawn so that points on it would yield the same loudness scale as shown in Fig. 2. It is seen that such a curve does indeed fit the observed data. The following equation

$$N=\frac{10^{5/3}I}{(I+10^{5/2})^{2/3}}=\frac{10^{5/3}10^{L/10}}{(10^{L/10}+10^{5/2})^{2/3}} \qquad (4)$$

proposed by Knauss represents approximately the relation shown in the curve of Fig. 2. This reduces to

$$N=I=10^{L/10} \qquad (5)$$

for values of L below 20, and

$$N=10^{5/3}(I)^{1/3}=10^{5/3}10^{L/30}=46\times10^{L/30} \qquad (6)$$

for values of L above 40. This last relation fits the curve accurately, the other two only approximately.

It is important to remember that the values of the intensity I in the above equation refer only to the 1000-cycle reference tone but the values of L can be for any type of sound. The curve of Fig. 2 has been taken as defining the relation between the loudness N expressed in LU's and the loudness level L expressed in phons. The loudness of any other tone, either simple or complex, can be determined by comparing it to this reference tone, and adjusting the intensity of the latter until the two sound equally loud. The loudness of the reference tone thus adjusted is then the loudness of the unknown sound being measured.

The Determination of the Position Coordinate x of the Auditory Nerve Patch Which is Most Excited by a Tone of Frequency f

Besides direct anatomical measurements there are two methods of determining this relation. The first of these was proposed by Wegel and Lane in 1923. It is based upon measurements of the minimum perceptible increments of pitch. A second one is given in this paper and is based upon masking measurements of thermal noise. It is generally agreed that the auditory nerve terminals are spread out along a winding spiral line so that a single coordinate x will define any particular group. This is usually considered to be the array of nerve endings along the basilar membrane. This membrane is about 30 mm long and 1/2 mm wide. It is not necessary to know the actual distances or the distribution of the nerve terminals if we define x as the percent of the total nerve endings that the maximum stimulation passes over as the frequency of a stimulating tone passes from the lowest audible pitch to the pitch corresponding to a frequency f. The position coordinate x thus defined is very convenient and will be used for loudness calculations. The position coordinate then must remain between 0 and 100. The problem then is to find the relation between f and x. Let this relation be expressed by

$$x=\Phi(f). \qquad (7)$$

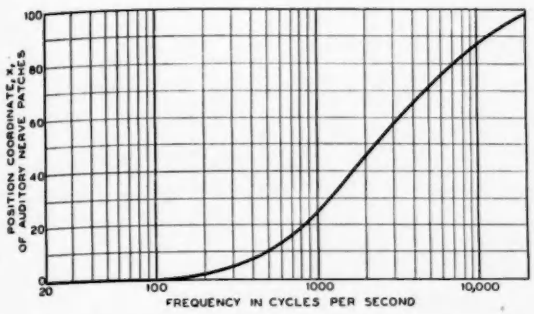

FIG. 4. Relation between the position of maximum nerve stimulation and the frequency of the stimulating tone. Data obtained from minimum perceptible differences in pitch.

The basis of the first method rests upon the assumption that for each minimum perceptible step on the pitch scale the position of maximum stimulation changes over the same number of nerve terminals.

Putting this assumption into an equation

$$\Delta x = \Delta\Phi = (dx/df)\Delta f = \text{constant} \qquad (8)$$

where Δx is the percent of the total nerve endings passed over in a just perceptible change in frequency Δf. Since the Δx is assumed to be always the same, we have the equation

$$\frac{dx}{df} = \frac{1}{\Delta f} A \qquad (9)$$

where A is a constant. Integrating and determining the constant by the condition that $x = 100$ when the frequency goes from the lower limit l to the upper limit u, we have

$$x = 100 \frac{\int_l^f \frac{1}{\Delta f} df}{\int_l^u \frac{1}{\Delta f} df}. \qquad (10)$$

The values of Δf at different frequencies are determined from experiments.

There are difficulties in applying this method as these values of Δf depend upon the intensity level of the tone as well as the frequency. The relation $\Phi(f)$ then also depends upon whether you go through the pitch range on a loudness level contour, a sensation level contour or an intensity level contour. It also depends upon what limits you choose for u and l. Also there is considerable uncertainty[3] that pitch is determined solely by a change in the position of maximum stimulation for the low pitched tones. This problem was discussed by Steinberg[4] in a paper presented before the Acoustical Society. Notwithstanding the difficulties mentioned above, the curve for $\Phi(f)$ which he gave as being the most probable is given in Fig. 4. He showed that this agreed very well with results from animal experimentation.

In the second method results are obtained from masking experiments. Electrical thermal noise is generated in an electrical conductor due to the haphazard movement of the electrons. This electrical noise can be amplified by vacuum tubes and converted into a sound by means of a telephone receiver or loudspeaker. Such an electrical disturbance has the property that the electrical power in any frequency band is proportional to the width of that band. This makes it possible to use thermal noise for building up a continuous spectrum of any desired form. The electrical noise going from a resistance to the amplifier has the same intensity for equal band widths regardless of where the bands are located on the frequency scale. However, by choosing the transmission characteristics of the amplifier and telephone receiver for converting the electrical noise to acoustic noise, one can obtain any desired type of sound spectrum from such thermal noise.

Let us assume that a spectrum of thermal noise is impressed upon the ear, defined by its spectrogram; that is, by giving B for each frequency throughout the audible range. Then we wish to find the stimulation of the nerve patches at the position x. The intensity ΔI contained in the small frequency band between f and $f+\Delta f$ goes mostly to stimulate the patches between x and $x+\Delta x$. There is of course some power going to patches outside this region. Since there are no abrupt changes in the spectrum, the patches outside this small band at x will already be stimulated by power from other frequency bands outside the small band at f. So it seems reasonable to consider that the *major part* of the stimulation in the element between x and $x+\Delta x$ is from the frequency region between f and $f+\Delta f$,

[3] The solution of the problem when Δx is not constant will be dealt with in another paper.

[4] J. C. Steinberg, J. Acous. Soc. Am. **8**, 176 (1937).

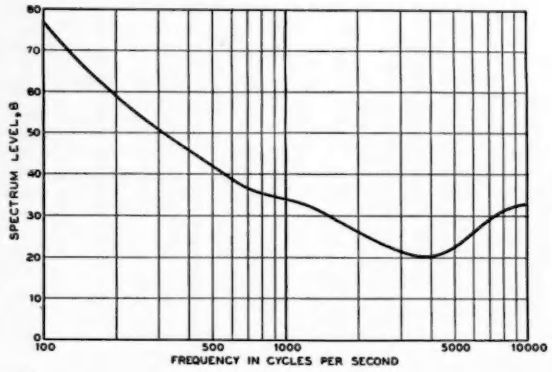

FIG. 5. Spectrogram of noise for producing constant stimulation of the nerve endings at all positions.

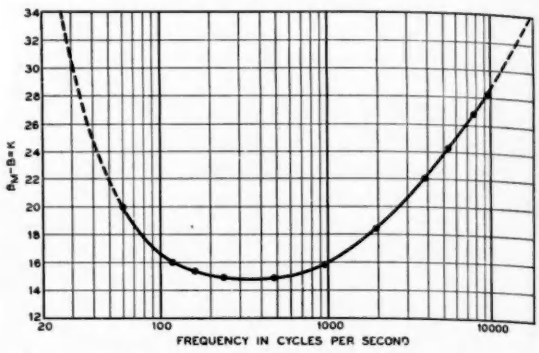

FIG. 6. Difference between the intensity level of the masked tone at each frequency f and the spectrum level of the thermal noise at the same frequency.

and that all the loudness from the patches located between x and $x+\Delta x$ will be due to the intensity coming from the region between f and $f+\Delta f$. When the threshold level is reached the patch of nerves is excited at the position x where the maximum excitation occurs. The acoustic intensity ΔI due to the thermal noise between f and $f+\Delta f$ is then $10^{B/10}\Delta f$. The intensity, when confined to a narrow band of frequencies that is necessary to excite the threshold of hearing, is $10^{\beta_0/10}$, where β_0 is the intensity level theshold for a pure tone of frequency f. This assumes that the intensity is the same whether it is concentrated in a single frequency or spread throughout the band between f and $f+\Delta f$. This assumption has been justified by experimental determination of the threshold for small bands of thermal noise.

For convenience let us call one percent of the nerve endings a patch. Then the values of x corresponding to the whole numbers from 0 to 100 locate each of these patches. Let the power of agitation of a patch be J_x and let J_0 be the power of agitation of the patch for it alone to produce the threshold of hearing. It will be assumed that this power can be spread over all the patch or concentrated in a small part of it and still have the same value for the threshold. This is true because at the threshold the loudness is numerically equal to the intensity. For example, if the intensity is spread over twice as many patches the intensity per patch is halved, and consequently the loudness per patch is halved, but the total loudness remains the same because there are twice as many patches excited. Then the following proportion will hold

$$\frac{J_x dx}{J_0}=\frac{10^{B/10}df}{10^{\beta_0/10}} \quad \text{or} \quad \frac{dx}{df}=\left(\frac{J_0}{J_x}\right)10^{(B-\beta_0)/10}. \tag{11}$$

This would be sufficient to determine the relation between f and x if we knew how J_x/J_0 varied with frequency; or conversely if we knew dx/df we could determine the variation of J/J_0 for any spectrum B since β_0 is known. Whenever the nerve patch is agitated a tone which is normally sensed by this patch will be masked. It seems reasonable to assume that the amount of masking produced can be taken as a measure of its agitation, or at least to assume that when the masking is uniform for all frequencies all of the patches have the same relative agitation, that is, the same value of J_x/J_0. The spectrogram for a thermal noise which will give such a uniform masking has been experimentally determined. It is given in Fig. 5. It was shown in the paper by Fletcher and Munson[5] that the shape of such a spectrum for producing uniform masking is independent of the total noise level used. Since for such a spectrum J_x/J_0 is a constant independent of the frequency, we have

$$x=\left(\frac{J_0}{J_x}\right)\int_0^f 10^{(B-\beta_0)/10}df. \tag{12}$$

The values of the functions B and β_0 at various frequencies can be taken from experimentally determined curves. The quantity J_x/J_0 can be determined from the requirements that x must be 100 when $f=\infty$, which gives

$$\left(\frac{J_x}{J_0}\right)=\frac{1}{100}\int_0^\infty 10^{(B-\beta_0)/10}df. \tag{13}$$

[5] H. Fletcher and W. A. Munson, J. Acous. Soc. Am. 9, 1 (1937).

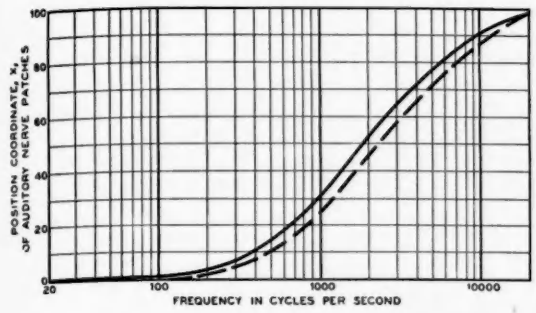

FIG. 7. Relation between the position of maximum nerve stimulation and the frequency of the stimulating tone. Data obtained from masking effects of thermal noise.

This equation then enables one to calculate the relative power of agitation per patch in terms of the noise spectrogram. Combining (12) and (13) we have

$$x = 100 \frac{\int_0^f 10^{(B-\beta_0)/10} df}{\int_0^\infty 10^{(B-\beta_0)/10} df}. \qquad (14)$$

It will be seen that adding a constant to B which is independent of frequency will not change the values of x. Therefore any one of the masking contours shown in Fig. 15 of the paper just cited can be used for the calculation.

Let the difference between the intensity level β_m of the masked tone and the spectrum level B of the thermal noise doing the masking be designated K or

$$\beta_m - B = K. \qquad (15)$$

This difference is constant at any one frequency and independent of B except at very low values of B. Now the masking M is given by

$$M = \beta_m - \beta_0. \qquad (16)$$

Substituting and rearranging we have

$$B - \beta_0 = -K + M \quad \text{and} \quad M = B - \beta_0 + K. \qquad (17)$$

If this is substituted in (14) we obtain, since M is a constant independent of frequency,

$$x = 100 \frac{\int_0^f 10^{-K/10} df}{\int_0^\infty 10^{-K/10} df}. \qquad (18)$$

This is the equation which is most suitable for obtaining the relation between x and f for it does not contain threshold values β_0. The experimental values obtained for K are given in Fig. 6.

It is important to notice that the values of K can be obtained without knowing the amplitude

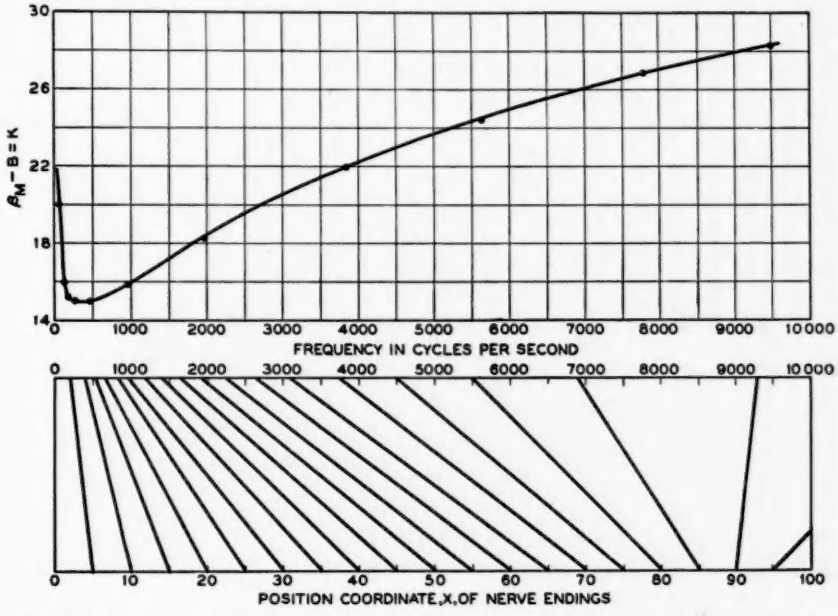

FIG. 8. Chart illustrating how the relation between position coordinate x and the frequency f were obtained from experiments on masking of thermal noise.

frequency characteristics of the amplifiers and head phones used for transferring the electrical noise to acoustic noise. In a noise analyzer the band width is kept constant as the noise spectrum is heterodyned through the audible frequency region. With such a device for producing the noise, it is only necessary to measure the ratio r of the currents or voltages at the telephone receiver terminals for the thermal noise and for the tone being masked. It can easily be shown that Eq. (18) can then be written

$$x=100\frac{\int_0^f r^2df}{\int_0^\infty r^2df}. \qquad (18A)$$

The results of integrating Eq. (18) or (18A) by graphical methods are shown in Fig. 7. The curve from Fig. 4 is shown by the dotted line. There is a fairly good agreement. If pitch changes for low frequencies are not sensed entirely by displacement of maximum stimulation, then the two curves should be slightly separated and in the direction shown. However, the general agreement of these curves with anatomical data gives us considerable confidence in their validity.

If S is the stimulation per patch expressed in decibels above its threshold, then by Eq. (13)

$$S=10\log\frac{J_x}{J_0}=10\left(\log\frac{1}{100}+\frac{M}{10}+\log\int_0^\infty 10^{-K/10}df\right). \qquad (19)$$

The last term was evaluated graphically using the curve of Fig. 5 and was found to be 1.95.

TABLE I.

$L_0=86$ db			$L_0=56$ db		
L	Obs. R.	Calc. R.	L	Obs. R.	Calc. R.
86	1.00	1.00	56	1.00	1.00
82	0.68	0.75	54	0.93	0.85
80	0.53	0.59	52	0.75	0.71
76	0.41	0.45	49	0.55	0.58
71	0.26	0.32	46	0.41	0.47
66	0.20	0.21	41	0.25	0.32
56	0.13	0.10	36	0.11	0.18
46	0.08	0.05			

Consequently the above equation becomes

$$S=M-0.5. \qquad (20)$$

This is an important relation because it states that the stimulation per patch differs by only 0.5 db from the masking of a tone having a frequency f corresponding to the patch position x. This is not exactly true for very low values of M below 15 db or for very high values of M above 70 db because, although the shape of the curve giving K remains constant, its whole position is shifted downward so that S becomes 3 or 4 db less than M at these extreme limits.

This same result can be obtained without using a spectrum producing a uniform masking. Let us assume that the stimulation S and the masking M differ only by a constant C independent of frequency. It is not even necessary to assume that C does not vary with different levels of M. Substituting these values, namely,

$$M-S=C \quad \text{and} \quad M=B-\beta_0+K,$$

into Eq. (13) it becomes

$$dx/df=10^{(B-\beta_0-S)/10}=10^{-K+C}. \qquad (18')$$

If this is integrated we arrive at Eq. (18) with value of $C=0.5$ db. So it is seen that either method leads to a method of evaluating the function $\Phi(f)$ from measurements of the difference K between the intensity level β_m of a masked tone in any frequency region and the spectrum level B of the thermal noise in the same frequency region.

The relations involved in this analysis are illustrated by the chart of Fig. 8. The frequency f and the position coordinate x are plotted linearly along the two lower horizontal lines. The position coordinate line is divided into 20 equal parts so that the positions correspond to 0, 5, 10, 15, 20, etc. These positions of x are connected to the corresponding frequencies -0, 250, 390, 520, 660, etc. Let us assume that the spectrum level B is the same for all frequency regions. Then the amount of power concentrated upon any 5 percent nerve patch, compared to the power concentrated upon the same patch by a single frequency tone which is just masked by the noise, is proportional to the distance between the corresponding frequencies. So it is seen that at high frequencies a much larger amount of

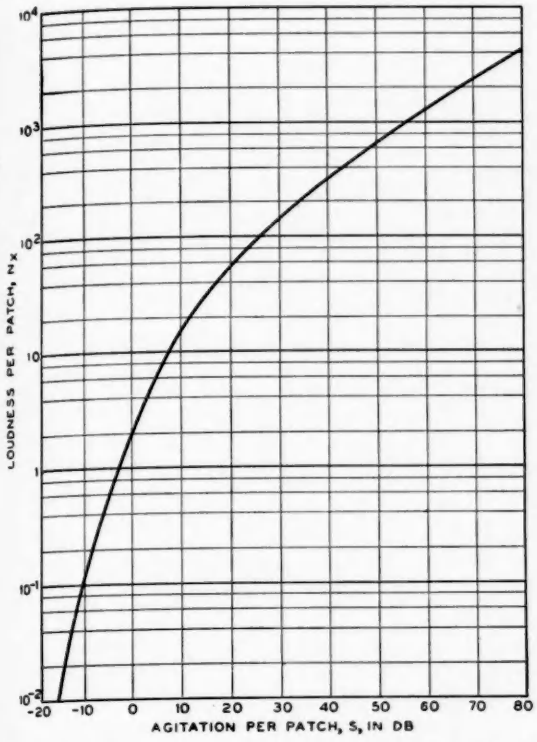

FIG. 9. Relation between the loudness per patch of nerve endings and the stimulation per patch in decibels.

relative power is concentrated upon a 5 percent patch than at low frequencies. Consequently, a greater intensity level β_m for the masked tone is required, as is shown by the curve at the top of Fig. 8. This curve is the same as that in Fig. 6 except that the frequencies are plotted linearly instead of logarithmically. Since for this case B was assumed to be constant, the ordinates of this curve show the relative levels for the masked tone.

One might interpret the curve of Fig. 8 in another way by assuming the noise spectrum to be such that a constant intensity level β_m for the masked tone is produced. Then the relative acoustic power in the masked tone and the thermal noise concentrated upon each 5 percent patch must be the same for all patches. Consequently the quantity $10^{-B/10}\Delta f$ must be constant for all frequency bands. Where the band Δf is large therefore the value of $10^{-B/10}$ must be small. In other words, if the ordinates of Fig. 8 are considered as negative values, then they give the spectrum levels which will just mask a constant intensity level β_m of the masked tone. For such a condition the acoustic power in each of the bands shown is the same. For a large Δf the power per cycle must be small, as is seen to be the case.

Now that we know how to calculate the position coordinate x from f, and the loudness N from the loudness level L, we are in a position to describe several methods of calculating the loudness of a tone or a noise both when listened to by a normal ear and also by a deafened ear.

Comparison of Calculated and Observed Judgments of Fractional Loudness

The loudness function will be first applied to the calculation of fractional reductions in loudness. If L_0 is the initial loudness level and L the loudness level for reducing the loudness to the fractional amount R of the original loudness, then

$$R=N/N_0=10^{(L-L_0)/30} \qquad (21)$$

for values of L greater than 40 db. For lower levels the N/N_0 can be calculated directly from Eq. (6). For example, here is a sample of such data taken by Ham and Parkinson.[6] If the tests are carried out with a 1000-cycle tone, the loudness levels L and L_0 become simply the decibels above the standard threshold pressure 0.0002 dyne per square centimeter. The table shows results upon this reference tone. (Table I.)

The observed values were obtained by asking a large number of observers to set the attenuator so as to produce the tone at levels which seem to them to be reduced by the fractional amounts given. The fact that sets of data of this type do

[6] Ham and Parkinson, J. Acous. Soc. Am. **3**, 511 (1932).

TABLE II.

f	20	100	200	400	800	1000	2000	3000	4000	8000	16000
x	0	1	4	11	25	30.5	5.25	65.5	73	88	98
β_0	72	37	22.5	10	1	0	−4.5	−8	−8	7	30
K	∞	16.7	15.1	14.8	15.5	16	18.6	20.7	22.3	27	32.2
$S-B$	∞	−20.0	−7.0	4.3	14.0	15.5	22.6	28.2	29.8	33.5	6.17

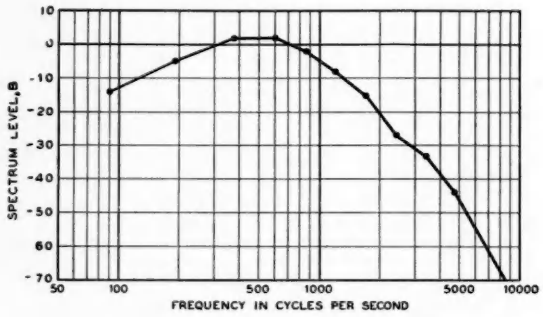

FIG. 10. Room noise spectrogram.

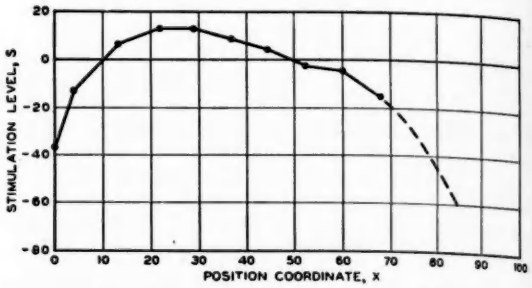

FIG. 11. Stimulation spectrum produced by room noise.

agree with this loudness scale gives us considerable confidence that this is a true loudness scale. Considerable data of this sort have been taken and the calculated values agree very well with those which are measured.

CALCULATION OF THE LOUDNESS FROM THE NOISE SPECTRUM

When a patch containing 1 percent of the total nerve endings in the organ of hearing is stimulated S db above its threshold value it sends out a certain loudness to the brain which we will call N_x. The value of S except[7] at very low or very high values can be obtained by combining (17) and (20), or

$$S=B-\beta_0+K-0.5. \tag{22}$$

The value of N_x should be dependent only upon S and should be independent of the position of this 1 percent of nerve fibers. In other words, it should be independent of the frequency. Consequently

$$N_x=Q(S) \tag{23}$$

where Q is some function which we can determine from our experiments on masking. The total loudness N from 100 percent of the nerve endings is then given by the equation

$$N=\int_0^{100} N_x dx. \tag{24}$$

To determine the functional relationship indicated by (23) a noise spectrum of the shape shown in Fig. 5 is chosen. If such a spectrum is impressed upon the ear it will produce a constant stimulation per patch for all values of x. Consequently, since the nerve endings at various positions are stimulated alike, the loudness N_x from each element is independent of the value of x. For such a spectrum we have the following relation

$$N=N_x\int_0^{100} dx=100N_x. \tag{25}$$

For various values of stimulation per unit length S the corresponding values of N were determined experimentally as outlined above. From these values of N the value of N_x was determined from (25) for each value of S. Then the corresponding values of N_x and S are plotted in a curve to give the desired relation. It is shown in Fig. 9.

As seen from Eqs. (20) and (17), $S-B$ is equal to $K-\beta_0-0.5$ and consequently is always the same function of the frequency for all values of B and therefore can be given in the form of a curve, or in a table. For convenience the corresponding values of f, x, β_0, K and $S-B$ are given in Table II.

By means of this table, the value of S at any of the frequencies given is obtained by simply adding the values of B from the spectrum of the sound to the numbers given in the fifth line. The procedure, then, for calculating the loudness N from Eq. (24) is to find from the noise spectrogram for each frequency f the corresponding value of B. From Table II find the corresponding stimulation level S. With this value enter the abscissae of Fig. 9 to find the corresponding N_x. From Fig. 7, or from Table II, the value of x corresponding to f is found. The point (x, N_x) is then plotted. This is done with enough frequencies to determine a curve going from $x=0$

[7] A more involved method of determining S at all values is given in the paper by Fletcher and Munson already cited.

to $x=100$. The area under this curve gives the value of loudness N which is sought.

The application of this formula is limited to such noises as have essentially continuous spectra. If we use the masking ordinate determined experimentally, then it is shown below that a formula can be obtained which is applicable to all classes of sounds which we have tested, both those having a continuous spectrum and also those having discrete frequencies.

Calculation of the Loudness of Room Noise from Its Spectrum

In trying to simulate conditions under which the telephone is used an artificial room noise has been created which has been used in some experiments at Bell Telephone Laboratories. The spectrogram of this noise is shown in Fig. 10. In Fig. 11 the corresponding stimulation spectrum is shown with S as ordinates and x as abscissae. This is interesting because it shows directly what part of the nerve endings is stimulated most by such a room noise. By using Eq. (24) and the curve in Fig. 9, the loudness level for this noise spectrum was calculated to be 37 db.

If the spectrum shown in Fig. 10 is amplified or attenuated, then similar calculations can be made from the resulting spectrum. In Fig. 12 are shown the values of the calculated loudness level for such spectra. The abscissae give spectrum levels at the frequency 1000 c.p.s. The crosses on the curve give the observed results as obtained by our laboratory technique. Here again it is seen that the agreement is well within the observational error.

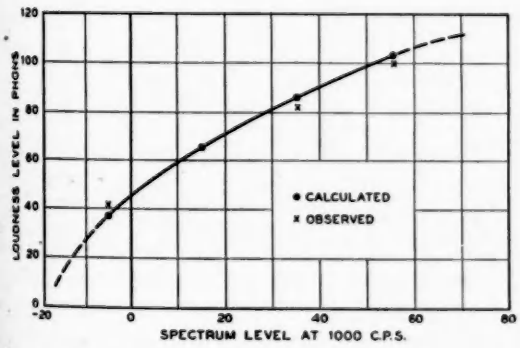

FIG. 12. Comparison of calculated and observed loudness levels for room noise.

Calculation of Loudness from the Masking Audiogram

It has been shown that for every value of the stimulation per unit length S there is a corresponding value of M. Consequently the function N_x can be written as a function of (M) or

$$N_x = F(M). \tag{26}$$

The function $F(M)$ can be obtained directly from the corresponding values of N_x, and M from the same loudness data from which $Q(S)$ was determined. The relation between $F(M)$ and M determined in this way is shown in Fig. 13. Since S and M are approximately equal above 20 db these functions should be approximately equal above this value and are found to be so. Consequently, Eq. (25) may be expressed in the following form

$$N = \int_0^{100} F(M)dx. \tag{27}$$

By means of this formula the loudness can be calculated directly from the masking audiogram determined experimentally. It can be applied to any type of sound in which the masking audiogram is known. It should be applicable to pure

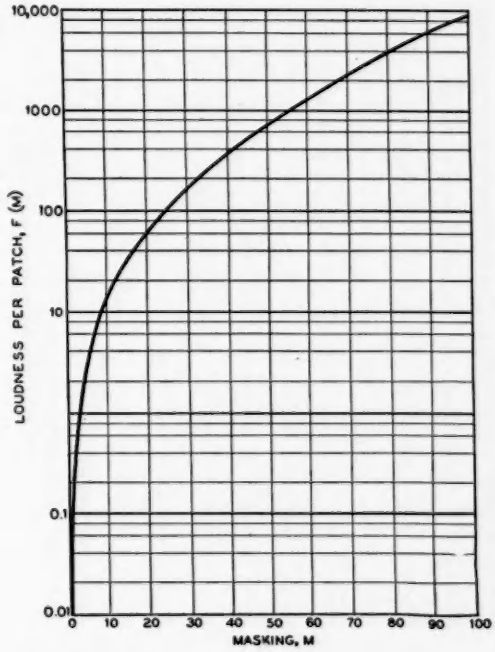

FIG. 13. The relation between the loudness per patch and the masking.

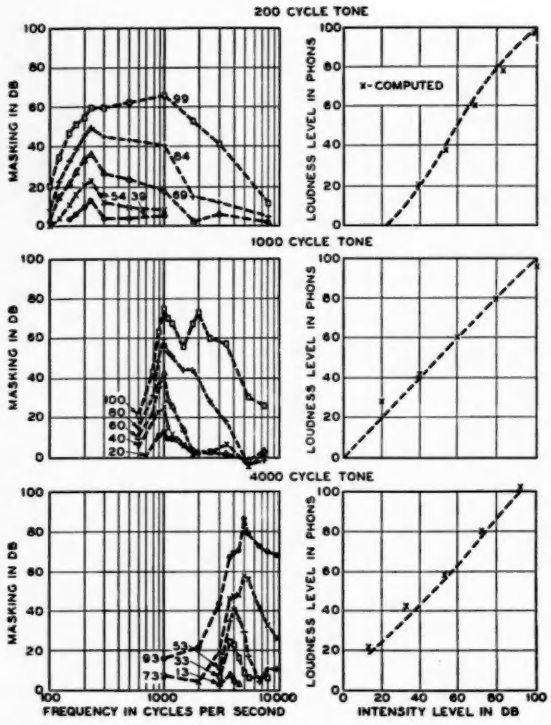

FIG. 14. Comparison between the observed loudness level of pure tones and that calculated from masking data.

tones, or any combination of them. It should be emphasized that Eq. (27) is the only loudness formula which can be universally applied. These statements should probably be somewhat modified to cover only those sounds which are continuous a sufficient time to obtain an audiogram. When the sound is varying, the loudness is varying. There is no doubt that Eq. (27) still applies but the problem of determining the average loudness to correspond to judgment tests is a difficult one. When applied to a discrete frequency spectrum it becomes a tedious job to obtain an accurate audiogram.

CALCULATION OF LOUDNESS OF PURE TONES FROM THEIR MASKING SPECTRUM

A severe test of the general validity of Eq. (27) is the application to masking audiograms of pure tones. The function $F(M)$ was determined by a thermal noise having a continuous spectrum. If it is applicable to a tone having a single frequency, then it seems reasonable to suppose that it will be applicable to a large class of sounds.

Calculations[5] from the masking audiograms of several pure tones were made. Typical results are shown in Fig. 14. These results are for pure tones having frequencies 200, 1000 and 4000 cycles per second. The dotted curves are the ones obtained from experiment and the crosses give the calculated points obtained from the masking audiogram shown on the left-hand side of the chart. It is seen that the agreement is very good. If these audiograms are plotted with x as abscissae and S as ordinates, they will then show directly the stimulation per patch at the various x positions. If this is done it will be seen that the 200-cycle tone covers a much greater percent of the total nerve endings than the 4000-cycle tone.

CALCULATION OF THE LOUDNESS OF COMPLEX TONES FROM THE LOUDNESS OF EACH COMPONENT

When the sound is composed of definite discrete frequency components a different approach to the problem resulted in finding a workable formula which is better adapted for calculating the loudness of such tones. The loudness values for pure tones have been determined experimentally for frequencies and intensities over the entire audible range. The loudness of any combination of these pure tones is calculated from the loudness of its components.

When tones which are sufficiently separated in frequency are impressed upon the ear it has been seen that the number corresponding to the loudness experienced is obtained by adding the loudness numbers of each component tone. The effect of frequency separation is shown in Fig. 15. This shows the results of tests[8] on the combination of ten tones adjusted so that each tone separately has the same loudness as every other component tone. It is seen that when the separation is 500 cycles, the combined loudness is always ten times that of a single component except perhaps for the very high intensities. As the frequency of separation becomes smaller, the intensity where this relation holds also becomes smaller. When the separation becomes as low as 50 cycles this relation fails to hold even for faint sounds. For a 50-cycle separation, the

[8] Experimental apparatus for producing such combinations is described in the paper by Fletcher and Munson, reference 2.

ten tones each having a loudness of 10,000 have a combined loudness of only a little more than twice that of a single component. If ten equally loud components are spaced equally between 2,000 and 2,500 they will also be approximately equally intense tones. Consequently, from a loudness standpoint, the contribution is equivalent to a single tone of 2250 cycles per second which has been increased tenfold in intensity. A tenfold increase in the high intensity range corresponds to $(10)^{\frac{1}{3}}$, or 2.15 times, which agrees with the loudness observations. In other words, for this case each component gave only 0.215, or about one-fifth the loudness that it would have given if allowed to operate on the nerve endings without the interference of the adjacent tones.

In the paper cited above it was shown how to calculate a fraction called b, which was always between zero and unity and which gave the fractional reduction in the loudness contribution for each component due to the interference to its neighboring components. In other words, if N is the loudness number corresponding to the complex tone and N_k the loudness number for its k'th component if acting separately, then

$$N=\sum bN_k. \tag{28}$$

The formula for calculating b is complicated and the reader is referred to the original paper cited above. It is sufficient here to state that b is unity for frequency separations greater than 500 cycles and that all components within a band width less than 100 cycles can be lumped together and treated as a single component. The values of N_k, that is, the loudness of pure single frequency tones, have been experimentally determined for the frequencies and intensities throughout the audible range. The curves in Fig. 16 give a summary of the results obtained. The numbers on the curves give the frequencies of the pure tones. For example, for all pure tones having frequencies between 800 and 2000 cycles the same relation holds between the intensity and the loudness as that given for the reference tone. It will be noticed that for the lowest pitched tone, namely the 50-cycle tone, the intensity variation at the ear which is required in order to reach the threshold of hearing is 500,000 times that required for the reference 1000-cycle tone. It is important, however, to notice how rapidly this tone increases in loudness as its intensity increases. These low frequency tones stimulate practically the entire basilar membrane, even for only small intensities above the threshold, as contrasted with the 1000-cycle tone which stimulates only a very small fraction of the basilar membrane for low intensities. At very high intensities both of these tones stimulate almost the entire basilar membrane.

The following example illustrates the use of these curves for complex tones which have components widely separated in frequency.

Consider a tone having a fundamental frequency of 500 cycles per second and four harmonics, all equally intense, having an intensity of 10,000, that is, having an intensity level of

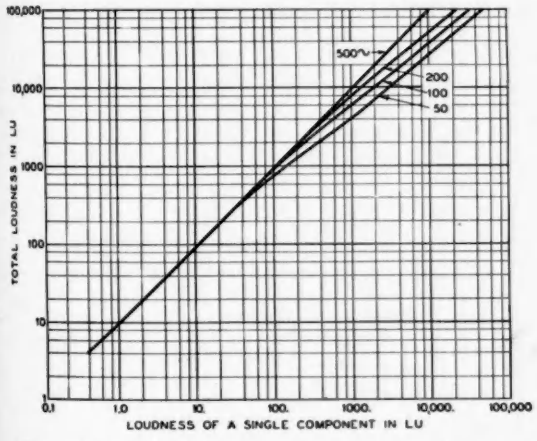

FIG. 15. The relation between the loudness of a complex tone having ten equally loud components, the loudness of each component, and the frequency separation between the components.

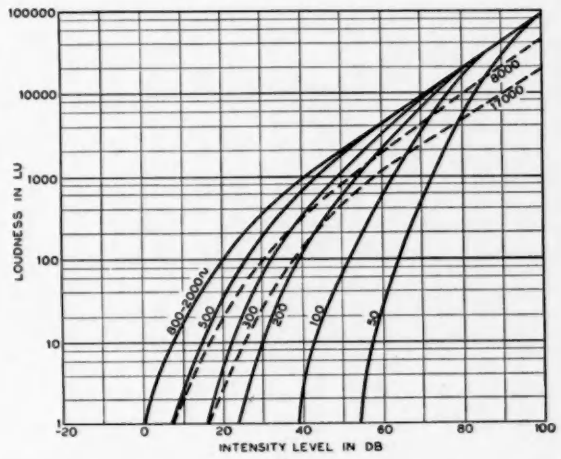

FIG. 16. The relation between the intensity level and the loudness of pure tones.

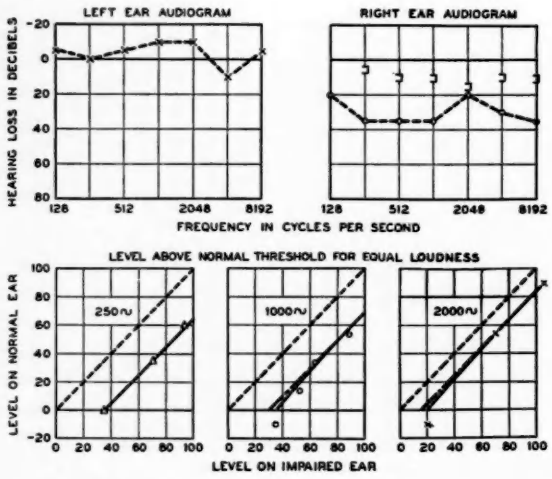

FIG. 17. Comparison between the calculated and observed loudness levels of pure tones for an ear having obstructive deafness.

40 db. The loudness of the components can be determined from the curves of Fig. 16 and are found to be equal to 700, 1000, 1000, 1000, 1000. The combined loudness then is 4700. This loudness corresponds to a loudness level of the reference tone of 62 phons. For a more detailed application of Eq. (28) the reader is referred to the paper already cited.

When the components are so close together that the sound may be considered as a continuous spectrum the above method becomes very complicated to apply and usually gives calculated results which are too high. It has been shown that such noises are better treated by loudness formulae using the spectrum and Eq. (24).

CALCULATION OF THE LOUDNESS OF A SOUND FOR A PARTIALLY DEAFENED EAR

First let us consider a case of pure conductive deafness—one in which the nerve terminals function normally. Let A be the function of frequency defining the audiogram of the deafened ear. Then if M is the masking for a normal ear (that is, an ordinate in the noise audiogram) the loudness experienced by the deafened ear is given by

$$N=\int_0^{100} F(M-A)dx. \qquad (29)$$

If, however, the case is one of nerve deafness, then the loudness for the deafened ear should be given by

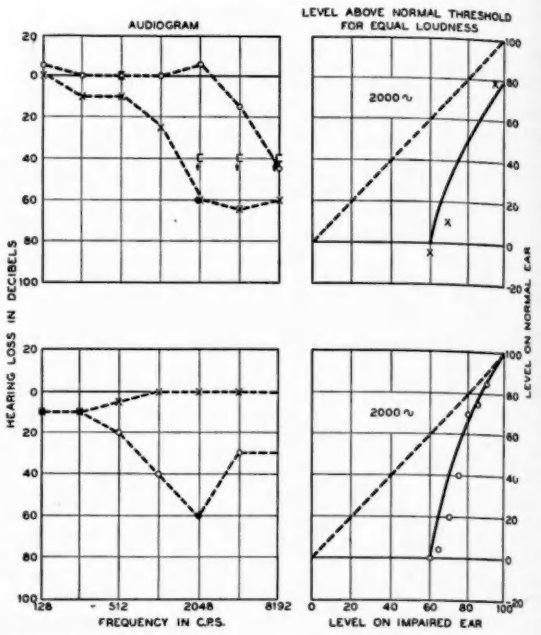

FIG. 18. Comparison between the calculated and observed loudness levels of pure tones for an ear having nerve deafness.

$$N=\int_0^{100} (F(M)-F(A))dx. \qquad (30)$$

In case of mixed deafness

$$N=\int_0^{100} (F(M-A_C)-F(A_N))dx. \qquad (31)$$

In a recent paper[9] Steinberg and Gardner discussed these relations and found indeed that these equations gave calculated results which agreed with experimental observations of partially deafened persons.

In the tests, observers having one deafened and one normal ear, listened to a tone first with one and then with the other ear. The intensity level of the tone on the normal ear was adjusted until it sounded as loud as a fixed level of tone on the deafened ear. By choosing different values of fixed level, the hearing of the deafened ear throughout the intensity range above β_p was studied.

Figure 17 shows a typical case of conductive deafness where the deafened ear hears with reduced loudness at all intensity levels. The ordinates used in these curves and those of Figs. 18 and 19 are levels above threshold. Since here

[9] J. C. Steinberg and M. B. Gardner, J. Acous. Soc. Am. 9, 11 (1937).

we are dealing with pure tones, the relation between loudness level and level above threshold can be obtained from the curves of Fig. 16, the zero loudness levels being interpreted as the threshold levels. The upper charts show the left and the right ear audiograms. The points in the lower charts show the levels on the deafened and normal ears for equal loudness. If both ears were normal, the points would fall on the 45° dashed line through the origin. The displacement of the points to the right of the dashed line gives the hearing loss for the deafened ear which is seen to be the same at all levels. The solid line was calculated from Eq. (29). With this type of deafness the loudness perceived is the same as that perceived by a normal ear with the sound attenuated in db the same as the displacement of these straight lines, or equal to A, the ordinate of the audiogram at 250 c.p.s.

Figure 18 is typical of a case of nerve deafness where the deafened ear tends to hear sounds above the deafened threshold with normal loudness. In this figure, the audiograms are shown by the left-hand charts. In both cases, a threshold loss of 60 db is shown for a 2000-cycle tone. However, when the level is raised 30 db above the deafened threshold, this tone is heard with practically normal loudness. The figures at the right show the experimental data by circles and crosses. The solid curves were calculated from Eq. (30), the values of A being taken from the audiogram of Fig. 18 and the values of M from the masking curve of a 2000-cycle tone. The values of N obtained were converted to loudness level L, and then knowing the frequency of the tone, to the level above threshold. The agreement of the solid lines with the observed points is a striking confirmation of the fundamental theory underlying all these calculations.

Cases of deafness were also observed in which both types occurred in various proportions. The curves of levels for equal loudness on such deafened and normal ears were combinations of the curves shown in Figs. 17 and 18. The occurrence of these two types of deafness can be explained from our picture of loudness previously described.

It is of interest to note that one would expect the hearing loss caused by a masking sound to be of the type resulting from nerve atrophy, if the nerve fibers which are activated by the masking sound are ineffective in contributing to the loudness of a tone heard in the presence of the masking sound. To test this, one ear of an observer was masked by a wide band of thermal noise, extending over most of the audible range.

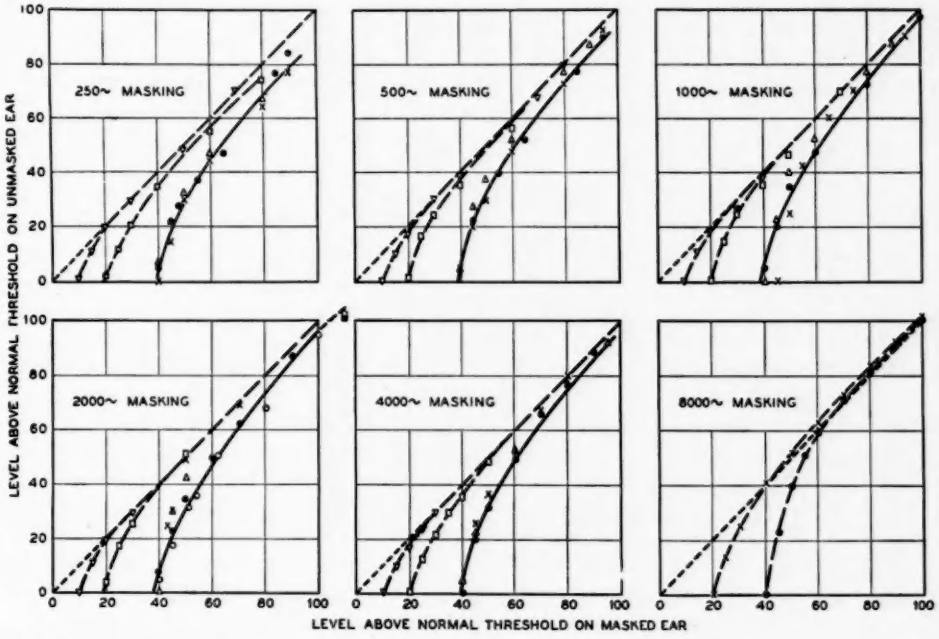

FIG. 19. Comparison between calculated and observed loudness levels of pure tones for an ear immersed in thermal noise.

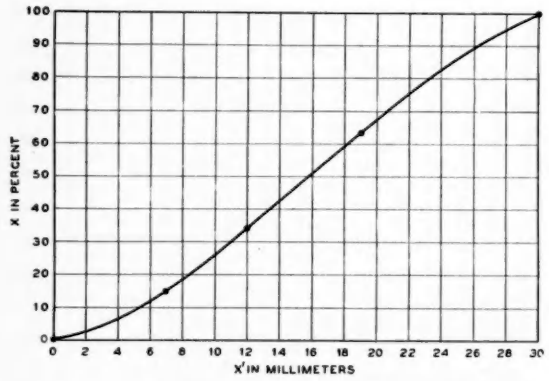

FIG. 20. Relation between the position coordinate x and the distance x' in millimeters along the basilar membrane.

A pure tone heard in the unmasked ear was adjusted to sound as loud as a tone of the same frequency heard in the masked ear. The results are shown in Fig. 19, where it will be seen that the tones heard in the masked ear increase in loudness very much like tones heard in the nerve deafened ear of Fig. 18. The solid lines showing the loudness of various tones when masked 40 db were calculated and are seen to be in good agreement with the observed data.

BEARING OF THESE LOUDNESS RELATIONS UPON QUESTIONS CONCERNING THE HEARING PROCESSES

During the discussion of the material dealt with in the previous sections it has been necessary to frequently refer to the processes involved in hearing. It should be emphasized here again that it was assumed that a sound which produces a constant agitation level above threshold level at all nerve patch positions produces also a constant masking for pure tones of any frequency. By means of this assumption it was shown that the experiment on masking by thermal noise leads to a method of determining the relation between f and x which was given in Fig. 7. The position coordinate x was not taken as distance along the basilar membrane,

TABLE III.

POSITION	x'	COUNT	x
Upper Middle plus Apical	0–7	4200	0–14.5
Lower Middle	7–12	5600	14.5–33.8
Upper Basal	12–19	8500	33.8–63.1
Lower Basal	19–30	10700	63.1–100
Total	0–30	29000	0–100

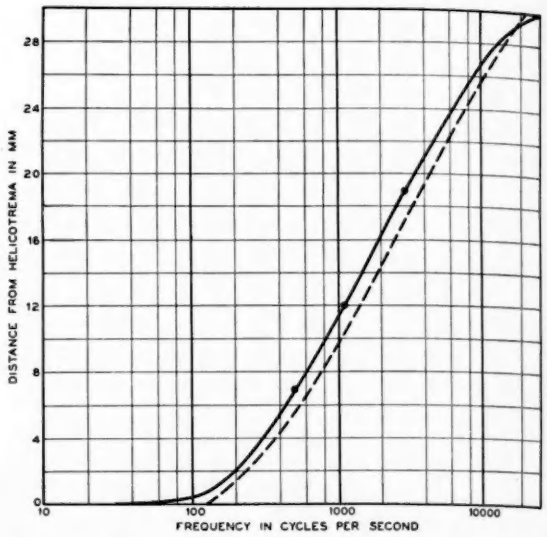

FIG. 21. Relation between the position of maximum response along the basilar membrane and the frequency of the stimulating tone.

as has usually been done, but it is a coordinate which designates a particular set of nerves.

In the interval between x = zero and $x=1$, one percent of the nerve endings which are stimulated by low tones is meant; at the position between $x=1$ and $x=2$ is meant one percent of the nerve endings adjacent to the first patch. In other words, the x values refer to nerve patches in such a way that for equal intervals dx there are an equal number of nerve endings. If the nerves are distributed uniformly on the basilar membrane then the x as used in this discussion corresponds to one percent of the total length of the basilar membrane.

If, however, the nerve endings are not distributed uniformly, then the length dx must be stretched or contracted depending upon whether the nerve density is less or greater than the average. Let x' be the distance from the helicotrema in millimeters.

Guild[10] has made measurements of the number of ganglion cells along the basilar membrane. He divided the cochlea into four parts, namely, (1) upper middle and apical, (2) lower middle, (3) upper basal, (4) lower basal. He made a count of the total number of ganglion cells in each of these parts. They are given in column 3 of Table III. Steinberg has estimated the distance in millimeters along the basilar membrane

[10] Guild, "Correlations of Histologic Observations and the Acuity of Hearing," Acta Oto-Laryng. **17**, 207 (1932).

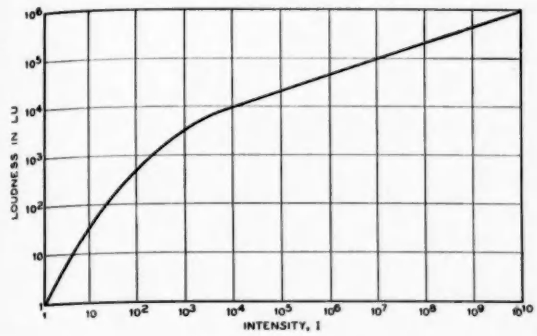

FIG. 22. Relation between the relative intensity of a thermal noise producing uniform masking and the loudness it produces.

for each of these parts to be that given in the column under x'. The corresponding values of x are then easily calculated as the percent of the total cells up to the position corresponding to x'. They are given in the last column.

It is seen that these data on the number of ganglion cells allow us to calculate only three points besides the two end points. These values of x and x' are plotted on Fig. 20 and a smooth curve is passed through the plotted points. Using the relation shown by this curve then the values of x and f from the solid curve of Fig. 7 were transferred to values of x' and f. The values obtained in this way are shown in Fig. 21. The relation between f and x from measurements on the minimum perceptible differences in pitch discussed above is shown by the dotted line in this figure. The close agreement of these two curves is very good evidence of the validity of the interpretation given to the experiments on masking and loudness.

The curve of Fig. 9 gives the loudness when the entire membrane is stimulated uniformly. In Fig. 22 it is replotted, shifting the abscissa so that for the loudness $N=1$ the intensity $I=1$. It will be seen that there is a range of loudness values of about 1,000,000 from the threshold to the highest level that the ear can stand. At low levels the most sensitive nerve endings begin to send discharges to the brain. As the intensity increases more discharges occur from these sensitive nerve endings and also more endings are excited. The curve of Fig. 22, according to my interpretation, is a combination of these two effects. Possibly the steep part of the curve is due principally to the first process and the constant slope part is due to the second process.

It is generally supposed that each nerve fiber cannot discharge more rapidly than 1000 times per second. The 30,000 nerves can then carry 30,000,000 discharges per second. The number N which corresponds to the highest intensity that the ear can stand is about 1/30 this value, which seems to indicate that at the threshold there are about 30 nerve discharges per second. If loudness were proportional to the number of active fibers, as some have supposed, then our loudness numbers could reach only 30,000 instead of 1,000,000. This, it seems to me, is evidence, although not conclusive, that the total number of nerve discharges going to the brain is proportional to the corresponding number on our loudness scale.

SUMMARY

It has been shown how to define loudness and loudness level in a quantitative way. Definite procedures are given for determining experimentally the loudness level of any sound heard by any person. For a typical observer a true loudness scale is developed. The relation of the scale to the loudness level scale is determined experimentally. The scale has been found to be very useful for calculating loudness from the noise spectrogram, the noise audiogram, or the overtone structure of the sound.

The relation between the masking and the loudness produced by a sound has been quantitatively determined and a formula deduced from this relation which has proved useful for calculating the loudness. This formula may be applied with equal success to a normal ear and also to a deafened ear. Evidence has been given that the masking expressed in decibels produced upon any pure tone is equal directly to the agitation of 1.1 percent of the total nerve endings expressed in decibels above the threshold value for such a patch and at the position where such a tone would be sensed. These loudness relations throw light upon some of the important processes involved in hearing. In particular the data from the masking effects of thermal noise were used to calculate the relation between the position of maximum stimulation on the basilar membrane and the frequency of the tone producing the stimulation.

Limits of Audition for Bone Conduction

NORMAN A. WATSON
University of California at Los Angeles
(Received January 31, 1938)

The laboratory facilities and apparatus described in an earlier paper were used to study the normal intensity and frequency limits of audition for bone conduction. The condition of the observer's head to give greatest acuity for pure tones, and the optimal total force of application and area of the vibrator button were found to be essentially the same as for speech sounds. Acuity was found to vary with the position of application of the vibrator; for example, the maximum variation with position of the 1000-cycle threshold was 18 db. A threshold for open canals was determined for the frequency range 80–2000 cycles, without interference from stray air radiation (18 normal observers). Above 2000 cycles air radiation interfered with open canal tests to such an extent that a special technique was devised to obviate its effects. The occluded threshold curve, for a single normal individual, lay below his open canal curve over the range 80–2000 cycles, and also at 10,000 cycles. The usable intensity range for open canals was tentatively determined; it is a maximum of 80–90 db at 1000–2000 cycles. The total audible frequency range for open canals was found to be at least 25–17,000 cycles.

INTRODUCTION

THE normal frequency and intensity limits of hearing by air conduction have been determined accurately by many observers. Fletcher and Munson[1] have delineated the auditory sensation area for binaural listening in a free sound field (for young observers with normal hearing). Several investigators have determined threshold of audibility curves for sound produced in or near the external auditory canal and listened to monaurally. A discussion of their various methods and an average curve have been given by Sivian and White.[2] Wegel[3] has determined the threshold of feeling for monaural listening. These curves of Sivian and White and of Wegel have been extrapolated by Knudsen[4] to give an auditory sensation area for monaural air conduction for young persons with normal hearing. However, comparatively little work has been done on the determination in absolute units of the limits of audition for bone conduction, although relative thresholds of hearing, suitable for testing of hearing, have been obtained by several investigators. Two threshold of hearing curves for bone conduction in absolute units have been determined over limited frequency ranges: one by Knudsen and Jones,[5] in terms of the amplitude of vibration of the vibrator button; and one by von Békésy[6] in terms of the effective amplitude of vibration of the forehead skin compressed over the frontal bone near the point where the vibrator button was applied.

The objectives of the present investigation have been to determine a threshold of hearing curve for bone conduction over as wide a frequency range as possible without interference from stray air radiation, to estimate the useful intensity range for tones within that frequency range, to determine the *total* audible frequency range, and to plot a tentative auditory sensation area for bone conduction.

LABORATORY FACILITIES, APPARATUS AND TECHNIQUE OF TESTING

All the measurements reported in this paper were made in the small soundproof test room of the acoustical laboratory of the University of California at Los Angeles, which has been described in an earlier paper.[7] Thus the tests were free from the influence of external noise and of

[1] H. Fletcher and W. A. Munson, J. Acous. Soc. Am. **5**, 82 (1933), Fig. 4; also see H. Fletcher, Bell System Tech. J. **13**, 239 (1934), Fig. 1.
[2] L. J. Sivian and S. D. White, J. Acous. Soc. Am. **4**, 288 (1933), Fig. 10.
[3] R. Wegel, Proc. Nat. Acad. Sci. **8**, 155 (1922); see also H. Fletcher, *Speech and Hearing*, (D. Van Nostrand, New York, 1929), p. 141, Fig. 70.
[4] V. O. Knudsen, *Audiometry* (The Sonotone Corporation, Elmsford, New York, 1937), p. 6, Fig. 2.
[5] V. O. Knudsen and I. H. Jones, Arch. Otolaryng. **13**, 489 (1931), Fig. 3.
[6] G. von Békésy, Ann. d. Physik (5), **13**, 111 (1932), Fig. 10.
[7] N. A. Watson, J. Acous. Soc. Am. **9**, 99 (1937).

adventitious noise arising within the test room. The induction type electrodynamic vibrator[8] described in the previous paper was used for most of the tests. The driving system for the vibrator is indicated by the block diagram of Fig. 1. It consists of a General Radio beat frequency oscillator, a meter to measure the input current, a voltage divider, attenuators and amplifiers, one of which contains resonance type filter networks. The frequency response characteristics of the vibrator and the driving system are known so that appropriate corrections can be made for their deviation from uniformity. Both the vibrator and driving system are essentially linear over the intensity range used in the tests. The largest overtone in the vibrations of the bone conductor for frequencies above 100 cycles is 35 db below the fundamental, and most of the harmonics are 50 db or more below. The second harmonic of 80 cycles is only 11 db below the fundamental; thus too much weight cannot be given the measurements at that frequency.

The method of determining a threshold was as follows: The observer was seated in the test room with the vibrator against his head and a signal button in his hand. The operator sat at the controls in the adjoining room.[9] By means of them he could change the intensity of the test tone or interrupt it momentarily. The interruption was brought about by breaking the filament supply line to the last stage of the second amplifier. The tubes in this stage were not of the heater type; thus the filaments cooled and heated again very rapidly so that the tone regained its original intensity almost immediately after the filament supply was reconnected following the interruption. The plate supply line and the audio line between amplifiers remained connected; hence there was no "click," either when the tone was interrupted or when it was started again. The operator first presented the tone to the observer at a level definitely above threshold. The observer signaled as long as he heard it. Then the operator interrupted the tone, shifted the attenuator setting to that for a less intense tone, and presented the fainter tone to the observer. (Attenuator changes were made during the time the tone was interrupted so no contact noises would reach the observer.) This process was repeated and the observer's responses noted each time until he failed to signal at two intensities decreasing successively. Then the intensity was increased until he again signaled that he heard at two intensities increasing successively. The procedure was repeated until the operator found the maximum attenuator setting (faintest tone) for which the observer heard the tone a majority of times it was presented. The effective amplitude of vibration of the vibrator button corresponding to this attenuator setting was called the threshold for that observer for the frequency tested. No regular sequence was followed in the time-length of tones or interruptions, as the responses might easily be affected by rhythmic times of tone duration and interruption. With all "clicks" and other extraneous noises eliminated and irregular tone intervals used, the operator could be sure that the tone corresponding to the threshold setting was the real threshold tone for the observer at the time of the test.

Effects of Various Factors on the Bone Conduction Threshold

Before measurements were made for the determination of the average threshold of hearing curve, the effects on the threshold of various controllable factors such as the condition of the observer's head, the position of application of the vibrator, the force of application of the vibrator and the contact area of the vibrator button were studied. It was found that acuity was greatest when the mouth of the observer was

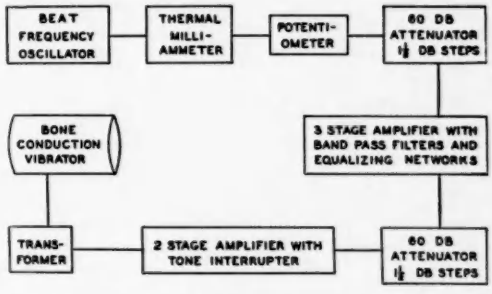
BEAT FREQUENCY OSCILLATOR
THERMAL MILLI-AMMETER
POTENTI-OMETER
60 DB ATTENUATOR ½ DB STEPS
BONE CONDUCTION VIBRATOR
3 STAGE AMPLIFIER WITH BAND PASS FILTERS AND EQUALIZING NETWORKS
TRANS-FORMER
2 STAGE AMPLIFIER WITH TONE INTERRUPTER
60 DB ATTENUATOR ½ DB STEPS

FIG. 1. Block diagram of the driving system for the electrodynamic bone conduction vibrator.

[8] The general appearance of the vibrator and its mode of application to the head are shown by Fig. 7 of reference 7; a schematic cross sectional diagram is given in Fig. 8 of the same paper.

[9] The test room and control room are shown as room 2 and room 1, respectively, in Fig. 4 of reference 7.

closed and his teech touching or clenched, thus making the mandible practically an integral part of the vibrating skull instead of an accessory part, vibrating out of phase with it. Measurements taken with the external auditory canals occluded indicated a very marked lowering of the threshold below that for open canals. Thus it was decided to perform most of the measurements with open canals but later to make similar measurements for occluded canals and to compare the results.

The threshold varied markedly with change of position of application of the vibrator button. For one observer, for example, the 1000 cycle threshold varied 18 db with change of position. The position for greatest acuity was the upper front teeth; that for poorest acuity was along the top midline of the head approximately six inches back from the forehead. With the vibrator button placed at the center of the forehead, just above the position of the frontal sinuses, the acuity was 10 db less than with the vibrator on the upper front teeth, and 3 db less than with the vibrator on the mastoid portion of the temporal bone.[10] In spite of this, the center of the forehead was chosen as the position of application of the vibrator button because (1) it is the most convenient portion of the head for that purpose, (2) the frontal bone at that point is very uniform in density and elasticity over quite a large area, allowing comparatively wide latitude in the location of the button without introducing serious errors in the measurements, and (3) since hearing by bone conduction is essentially a binaural phenomenon, it is advantageous to place the vibrator centrally to provide equal distribution of the vibrations to the two ears when testing persons of normal hearing.

The effect of the variation of the force of application of the vibrator button was tested by taking thresholds with forces of application varying from 85–650 grams-weight for frequencies as low as 125 cycles, and as high as 2500 cycles, which represented the highest frequency that could be used without interference from stray air radiation. The variation in threshold with force of application was found to be small for all frequencies for forces greater than 370 grams-weight—that is, great enough to compress the skin sufficiently to allow it to vibrate in unison with the bones. When the force was decreased the variation in threshold was found to be small for high frequencies (within ± 3 db). For low frequencies, however, the variation was greater; the threshold was raised 10 db for 125 and 250 cycles by the reduction of the force of application to 85 grams-weight. On the basis of these tests the force of application of 370 grams-weight was chosen for further tests.

The effect of variation of the area of vibrator button when applied with a force of 370 grams-weight was next studied. For both open and occluded canals, the variation of threshold with button area at low and medium frequencies was found to be practically negligible (a maximum variation of ± 3 db). For closed canals, however, the larger button areas gave much greater acuity (that is, lower thresholds) at high frequencies. For 3000 cycles, the threshold intensity in db decreased 10 db almost linearly with increase in button area up to 4.75 sq. cm. For 7000 cycles it decreased 24 db up to the same button area. Accurate measurements could not be made at the higher frequencies for open canals because of interference from stray air radiation. Buttons of area less than 0.5 square centimeter were too uncomfortable for the observer when a force of application of 370 grams-weight was used. A compromise among all these factors led to a choice of button area of 0.665 square centimeter.

The unit chosen for measuring the threshold was the effective (that is, root-mean-square) amplitude of vibration of the vibrator button (0.665 sq. cm area) when pressed against the center of the observer's forehead with a force of 370 grams-weight.

The Threshold of Hearing Curve for Bone Conduction

To determine the threshold of hearing curve for bone conduction, thresholds were taken for eighteen observers within the age range 20–28 and of average age 23. Their air conduction hearing lay within ± 5 db of normal, as measured with an accurately calibrated audiometer. They were instructed to place their chins on the sponge

[10] Compare with the differential given by N. H. Kelley, J. Exp. Psych. **21**, 211 (1937), Table III.

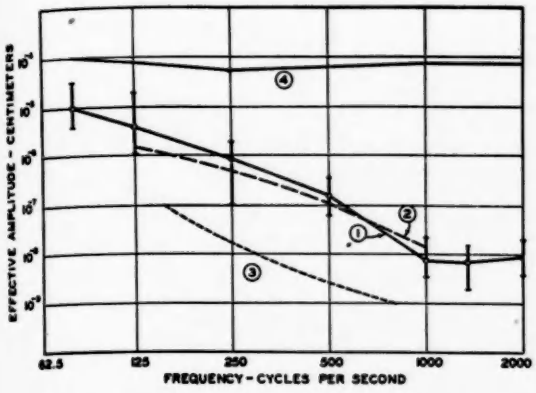

FIG. 2. Threshold curves for bone conduction (open ear canals). Curve 1, average threshold of hearing curve (present investigation). Curve 2, threshold of hearing curve (Knudsen and Jones). Curve 3, threshold of hearing curve (von Békésy). Curve 4, tentative "safe-upper-limit" curve (present investigation). (See area 1, Fig. 5.)

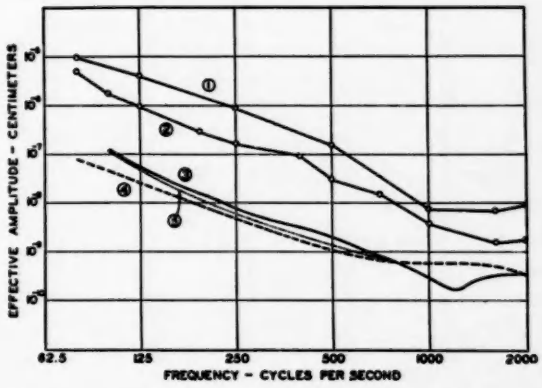

FIG. 3. Comparison of threshold of hearing curves for air and bone conduction (open canals). Curve 1, average bone conduction curve (present investigation). Curve 2, bone conduction curve for a single observer (present investigation). Curve 3, monaural, minimum audible pressure, air conduction curve for a single observer (Waetzmann and Kiebs). Curve 4, average binaural, minimum audible field, air conduction curve (Fletcher and Munson). Curve 5, monaural, minimum audible pressure, air conduction curve (von Békésy).

rubber chin rest and to keep their mouths closed and their teeth touching, but not clenched. For each observer, thresholds were taken at frequencies of 80, 125, 250, 500, 1000, 1500 and 2000 cycles per second. At frequencies greater than 2500 cycles the stray air radiation interfered to an extent which prevented the determination of accurate thresholds. For the frequencies listed above, the stray air radiation thresholds measured with the vibrator just off the head, were at intensities at least 20 db above the bone conduction thresholds, and thus did not interfere with them. The thresholds of the eighteen observers at each frequency were averaged and each arithmetic mean corrected for frequency responses of the vibrator and its driving system. The corrected mean values are shown in Fig. 2 by the circles of curve 1. The variations in threshold among the eighteen observers at the test frequencies are indicated by the vertical bars drawn above and below the circles. The variation is rather large, amounting to more than 20 decibels at some frequencies and more than 10 at all of them. Similar variations have been reported by other workers in bone conduction research. Part of the large total variation may be attributed to inaccuracies of determining individual thresholds. How large a part may be estimated from the following: fourteen thresholds at 1000 cycles were taken for a trained observer over a period of a month and a half with all conditions as nearly constant as possible. Seven of the thresholds were the same, and the extreme range was ± 3 db. The average error for a single determination was 1.1 db. Thus it is clear that most of the total variations arose from the individual skull differences.

The average curve for this investigation (curve 1) lies slightly above that of Knudsen and Jones[5] (curve 2) over most of the frequency range covered by the latter. This separation of a few decibels would be expected, for their measurements were taken on the mastoid portion of the temporal bone while those for curve 1 were taken on the forehead. Curve 1 lies some 30–35 db above von Békésy's[6] curve (curve 3). He measured the effective amplitude of vibration of the forehead skin, compressed over the frontal bone and vibrating with it, rather than the effective amplitude of the vibrator. In another experiment[11] he found that only one to four percent of the vibrations imparted to the skin were transmitted to the skull; one percent transmission would correspond to a 40 db transmission loss and four percent transmission to a 28 db transmission loss. Thus the 30–35 db difference is what one would expect.

In Fig. 3, the average bone conduction curve (No. 1) is compared with the bone conduction curve (No. 2) for a single observer (whose hearing

[11] Reference 6, Figs. 7 and 8.

is somewhat more acute than average) and with various air conduction curves. Curve 3 is a monaural air conduction curve for a single observer, determined by Waetzmann and Keibs,[12] using a method correcting for the absorption coefficient and the transmission factor of the ear drum. Curve 4 is the binaural minimum audible sound field curve of Fletcher and Munson.[1] Curve 5 is the monaural minimum audible pressure curve given by von Békésy[6] in terms of the effective amplitude of vibration of a small capsule placed in the ear canal as a source of sound. The separation of the air conduction and bone conduction curves is determined by the separation given by von Békésy[6] between his air and bone conduction curves at 800 cycles and by the distance of the bone conduction curve of this investigation from von Békésy's. Fletcher and Munson's[1] and Waetzmann and Keib's[12] curves were arbitrarily made to coincide with von Békésy's[6] air conduction curve at 800 cycles. Curve 1 has approximately the same slope as the binaural minimum audible sound field curve over the frequency range 80–500 cycles. Above that frequency the curves converge. The same is true for the monaural curves, although the convergence is not as great. Thus it appears that the minimum audible intensity for bone conduction is not exactly the same function of frequency as that for air conduction.

The frequency range of threshold measurements was restricted by the interference of stray air radiation, in spite of the precautions taken in the design of the bone conduction vibrator to avoid it. To extend the measurements to higher frequencies it was necessary to locate the sources of the stray radiation and to quiet them if possible; if not, to eliminate the effects they produced.

The sound reaching the ears by air conduction was found to have two sources: (1) the sound radiated to the air by parts of the bone conductor other than the button and either conducted as progressive waves to the ear by diffraction around the head or reflected so as to give rise to standing wave patterns in the room with maxima in positions to actuate the air of the external ear canals; (2) the sound radiated to the air from the back side of the vibrator button (or from the observer's forehead) and reflected from the front surface of the vibrator housing so as eventually to reach the ears, either as progressive waves or the maxima of a standing wave pattern.

It was possible to eliminate the effect of these unwanted sounds for any one frequency by the expedients of adjusting the positions of the vibrator and the head of the observer in the room so that his ears were in positions of pressure minima of the standing wave pattern, and of wrapping the vibrator (particularly the front face of the vibrator housing) with loose, highly absorptive material to reduce the sound radiated directly and to absorb the sound reflected from the front face of the housing after it was radiated from the back side of the vibrator button and the observer's forehead. The position of the head and vibrator were adjusted for one frequency (10,000 cycles) by putting an extension on the vibrator rod, raising the vibrator by leveling screws, and moving the observer's head slightly to one side, yet keeping the vibrator button at the same position of the forehead and the observer's chin on the chin rest. Without the special precautions, the open canal bone conduction threshold at 10,000 cycles coincided with the stray air radiation threshold; with the precautions, the bone conduction threshold was 15 db below the stray air radiation threshold. To obtain thresholds at other high frequencies it would be necessary to provide vibrator rod extensions of different lengths, and to reorient the vibrator and the observer's head in the room for each frequency.

(An alternative expedient would be to enclose the vibrator in an absolutely soundproof housing and surround the vibrator rod and button with a soft rubber cylindrical shell mounted on the housing so that it would not touch the rod or button but so that its free flaring end would impinge on the forehead in a circle surrounding the point of application of the vibrator button and thus prevent radiation from the back side of the button. However, such an arrangement would be an extra body pressing against the head and might interfere with the accurate determination of thresholds. For clinical testing, it would be desirable, and has, as a matter of fact,

[12] E. Waetzmann and L. Keibs, Ann. d. Physik (5), **26**, 141 (1936), Fig. 1.

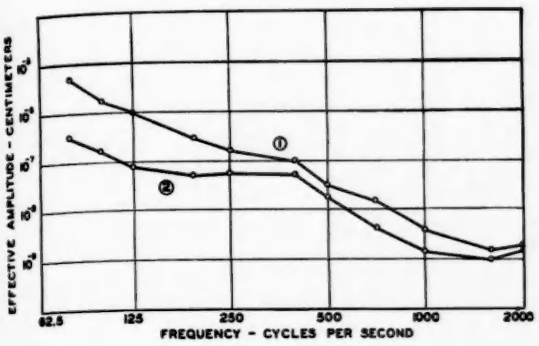

FIG. 4. Threshold of hearing curves for bone conduction (open and closed ear canals, single observer). Curve 1, open canals. Curve 2, closed canals.

already been employed on the bone conduction vibrator of a recent audiometer.[13])

Numerous experimenters have found that the acuity of hearing by bone conduction is increased by occlusion of the external auditory canals. They have found that at low frequencies the separation of the open canal and closed canal thresholds is of the order of 10–20 db, that the curves converge at medium frequencies, and that the separation disappears at frequencies above 2500 cycles.[14] Essentially the same results were obtained in the present investigation when no special precautions were taken to obviate the effects of stray air radiation, as is seen in Fig. 4. Curve 1 is the open canal threshold for a single observer, curve 2 the occluded canal curve for the same observer. There is a separation of over 20 db from 50 to 200 cycles, a decreasing but definite separation to 2000 cycles. Over this frequency range there was no interference from air radiation. Above 2500 cycles the open canal threshold was apparently equal to or even lower than the closed canal threshold; this was caused by the interference of stray air radiation with the open canal threshold. At 10,000 cycles, when the special precautions described above were employed, the open canal bone conduction threshold was 15 db below the stray radiation air conduction threshold and 6 db *above* the closed canal threshold. Thus the phenomenon of increased bone conduction acuity on occlusion of the external auditory canals exists at the high frequency of 10,000 cycles.

[13] I. H. Jones and V. O. Knudsen, Laryngoscope **46**, 523 (1936), Fig. 6.

[14] See reference 5, p. 490; A. G. Pohlman, Ann. Otol. Rhinol. and Laryngol. **39**, 927 (1930); and reference 10.

THE USABLE INTENSITY RANGE AND TOTAL FREQUENCY RANGE FOR BONE CONDUCTION

For the determination of the usable intensity range for bone conduction for the audible frequency range, a large power amplifier was used to drive the bone conduction vibrator, and the intensity of vibrations increased to the point corresponding to the maximum undistorted output of the amplifier. The amplitudes produced under these conditions are shown in Fig. 2 by curve 4. There was no feeling of pain (similar to that elicited by intense air borne sounds) produced for any of the observers at any frequency from 50–12,000 cycles when the vibrator was applied to the center of the forehead for short intervals. However, an application of the vibrator at the high intensity of curve 4 at 1000 cycles for several minutes produced for one observer an unpitched tinnitus (sounding like a rushing air stream) which lasted two days. Hence the intensities indicated seem to be near the limit of the usable intensity range, at least for the middle and higher frequencies. Experience with the testing of speech sounds in which most of the energy is concentrated between 200 and 300 cycles, and with various massage vibrators (low frequency) indicates that the usable intensity is greater at the low frequencies.

From the author's experiments and those conducted by others, the audible frequency range for bone conduction may be set at 20–20,000 cycles.

THE AUDITORY SENSATION AREA FOR BONE CONDUCTION

On the basis of the data just given, a tentative auditory sensation area was constructed for bone conduction for open canals. This is shown in Fig. 5 as area 1. It is compared with the monaural auditory sensation area (No. 2) based on the measurements of Sivian and White[2] and of Wegel;[3] also with the binaural free field auditory sensation area (No. 3) given by Fletcher and Munson.[1] The placement of the pressure level scale (in terms of which area 2 is plotted) with respect to the effective amplitude scale (in terms

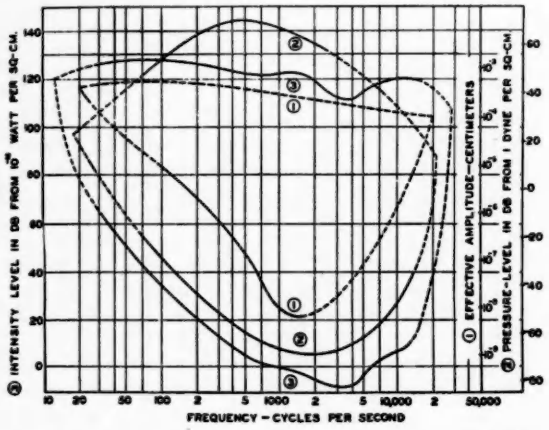
③ INTENSITY LEVEL IN DB FROM 10^{-16} WATT PER SQ-CM.
① EFFECTIVE AMPLITUDE—CENTIMETERS
② PRESSURE-LEVEL IN DB FROM 1 DYNE PER SQ-CM.
FREQUENCY – CYCLES PER SECOND

FIG. 5. Auditory sensation areas. Area 1, tentative bone conduction (present investigation). Area 2, monaural, minimum audible pressure, air conduction (Sivian and White, and Wegel, extrapolated by Knudsen). Area 3, binaural, minimum audible field, air conduction (Fletcher and Munson).

of which area 1 is plotted) was made on the relative placement of the Békésy air conduction curve and the Sivian and White minimum audible pressure curve in Sivian and White's original article.[15] The placement of the intensity level scale (in terms of which area 3 is plotted) with respect to the pressure level scale was determined by the relative placement of the minimum audible pressure data of Sivian and White and the binaural free field data by Fletcher and Munson.[16] The bone conduction area is seen to be smaller than either of the air conduction areas, having approximately the same frequency range as the latter but a smaller usable intensity range. However, it is large enough to include the frequencies and intensities of speech sounds so that speech may be heard as well by bone conduction as by air conduction by persons with normal hearing[17] and so that persons with hearing impairments of the conductive type may utilize bone conduction hearing aids to good advantage.

The author wishes to acknowledge his indebtedness to Professor V. O. Knudsen for suggesting this research and for invaluable help and guidance in carrying it out; to Mrs. Ruth B. Watson and Mr. R. B. Watson, who assisted in many of the tests; to Mr. L. W. Sepmeyer and Mr. Henry Jung for assistance in the design and construction of some of the apparatus used. Acknowledgment is also made to the department of physics of the University of California at Los Angeles for use of its facilities and apparatus and for its financial support of the research.

[15] Reference 2, Fig. 9.

[16] Reference 1, Fig. 2.

[17] Reference 7, Fig. 11.

Periods of Longitudinal Vibration of Steel Cones and Truncated Cones

G. W. PIERCE AND ATHERTON NOYES, JR.
Cruft Laboratory, Harvard University, Cambridge, Massachusetts
(Received October 27, 1937)

THIS paper presents the results of some measurements of the periods of vibration of solid steel cones and truncated cones, excited into longitudinal vibration by magnetostriction. A theoretical investigation is given together with a comparison of observed and theoretical results. Harmonic as well as fundamental modes of vibration were studied.

Modes of longitudinal vibration of the cone

The complete solid cone, illustrated at the top of Fig. 1, was made to vibrate continuously in its natural fundamental longitudinal mode, with a loop of motion at both ends, and its frequency f_1 was determined. The same vibrator was then vibrated in its first dynamic overtone, with a loop of motion at both ends and a third loop of motion intermediate between these two end loops. The frequency of this mode of vibration is designated f_2. Likewise the same vibrator was made to execute its higher dynamic overtones with frequencies f_3, f_4, etc. This cone is designated by specifying its length l, its diameter D_a, with $D_b=0$.

The experiments extend also to the fundamental frequencies and overtone frequencies of a series of truncated solid cones having various lengths l and various diameters D_a and D_b as shown in the lower illustration of Fig. 1.

Materials, dimensions of the vibrators, and measured frequencies

Two samples of steel were employed in the measurements: first a nickel-steel with a sound velocity of 461,200 cm/sec.; and second, a so-called stainless steel with a sound velocity of 538,400 cm/sec. The first happened to be the better magnetostrictive vibrator and gave higher harmonics than the second, but was used up by injudicious cutting so that we did not obtain from it as many separate truncated specimens as we might have done with a better planned use of the material. With the second specimen we proceeded more carefully in successive reductions of length, but were limited somewhat in the harmonic range by the quality of the material. The experimental results of our measurements are given in Table I.

Method of measuring these frequencies

The values of the frequencies of vibration of these vibrators were determined with the aid of the twin magnetostriction oscillator, described in a recent paper[1] by the present authors. The frequencies were obtained by measuring with an audiofrequency meter the difference between the frequencies of the conical vibrators and the known frequencies of a set of standard magnetostrictive rods. These measurements of frequency were not made with extreme accuracy but are generally better than 0.1 percent.

A comparison of observed frequencies and theoretically computed values

It is shown below by a theoretical investigation that the frequencies are related to the diameters of the vibrators by the equation

$$\frac{\pi(2fl/c)}{\tan(2\pi fl/c)}=1+\left(\frac{\pi 2fl}{c}\right)^2\frac{D_a/D_b}{(D_a/D_b-1)^2}, \quad (1)$$

in which l = length of the vibrator, whether a cone or a truncated cone,
D_a = diameter of the large end,
D_b = diameter of the small end,
f = frequency, whether fundamental or overtone,
c = velocity of longitudinal sound waves in the cone.

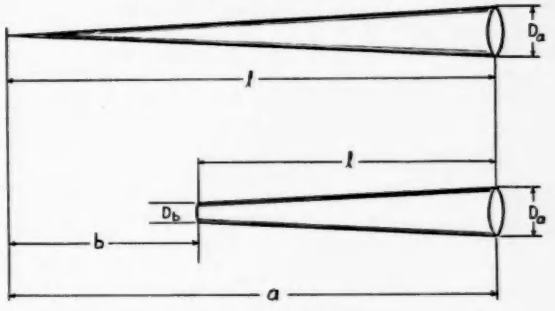

FIG. 1.

[1] J. Acous. Soc. Am. 9, 185 (1938).

This quantity c is a function of the ratio of diameter to length of the specimen. The function is not known exactly for the cones, but for a uniform cylinder, if v=the velocity obtained with a rod of diameter small in comparison with its length, the velocity c in cases where this condition is not fulfilled is,[2]

$$c=v\left\{1-\frac{n^2\pi^2\sigma^2D^2}{8l^2}\right\}^{\frac{1}{2}} \text{ approximately;} \quad (2)$$

[2] For experimental verification see David S. Muzzey, Jr., Phys. Rev. **36**, 935 (1930), which gives references to

TABLE I. *Materials, dimensions and observed frequencies.*

MATERIAL	LENGTH CM	LARGE DIAMETER D_a CM	SMALL DIAMETER D_b CM	OBSERVED FREQUENCIES CYCLES PER SECOND	D_a/D_b
Nickel-Steel, v=461,200 cm/sec.	14.08	1.261	0.139	21,030 36,520 51,800 67,360 83,200 98,870	9.075
Nickel-Steel, v=461,200 cm/sec.	11.50	1.261	.343	22,810 41,810 61,110 80,700 99,960 118,960 137,990	3.68
Nickel-Steel, v=461,200 cm/sec.	9.025	1.261	.542	27,150 51,800 76,690 101,380	2.33
Stainless Steel, v=538,400 cm/sec.	15.42	1.271	0+	24,160 41,470 58,450	∞ -
	14.37	1.271	.127	24,310 42,100	10.0
	13.94	1.271	.160	24,480 42,680	7.95
	13.64	1.271	.182	24,640 43,170	7 0
	13.24	1.271	.2125	24,880 43,970	6.0
	12.71	1.271	.254	25,290 45,170	5.0
	11.88	1.271	.317	26,110 47,500	4.0
	10.58	1.271	.424	28,120 52,400	3.0
	9.565	1.271	.501	30,250 57,380	2.51
	8.02	1.271	.6325	35,100 67,940	2 01
	5.297	1.271	.846	51,580	1.5
	15.42	1.266	.464	18,950 35,810 52,910	2.73

where n = an integer defining the mode of vibration,
D = diameter of the cylindrical rod,
σ = Poisson's ratio.

The second term in the brace of (2) is small in comparison with unity.

In the case of the cones and truncated cones we shall assume that we may replace D^2 of the cylindrical case by $(D_a^2+D_b^2)/2$, giving

$$c=v\left\{1-\frac{n^2\pi^2\sigma^2(D_a^2+D_b^2)}{16l^2}\right\}^{\frac{1}{2}}, \text{ approximately.} \quad (2a)$$

This assumption is probably not quite correct over the whole range of our observations as given in Table I.

Equation (1) is a theoretical equation giving $2fl/c$ (theoretical) as a function of the diameter-ratio D_a/D_b; while from our observed values of Table I we have calculated $2fl/v$, and by the use of (3) obtained $2fl/c$ (observed) for various given values of D_a/D_b.

It is somewhat simpler to compare $2fl/nc$, observed and calculated, as is done in Fig. 2. In the curves of Fig. 2 the diameter-ratio D_a/D_b is plotted as abscissae and $2fl/nc$ calculated by Eq. (1) as ordinates, giving the lines of the curves, for $n=1$ (fundamental), $n=2$ (first dynamic overtone), etc. The corresponding observed values of $2fl/nc$ are plotted as crosses or circles. The crosses are for the nickel-steel specimens and the circles for the stainless steel specimens.

Agreement between observed and calculated frequencies

It is seen in Fig. 2 that for the fundamental mode of vibration ($n=1$) and for the first dynamic overtone ($n=2$) the observed frequencies fall on the calculated curves with the exception of the points at $D_a/D_b=2.33$ where the observed frequencies are lower than the calculated by about 0.2 percent for $n=1$ and $n=3$. This departure, while a little greater than the errors of frequency measurements, is probably not greater than the inhomogeneity of the material

theoretical treatment by Pochhammer, Chree, Love, Rayleigh and others.

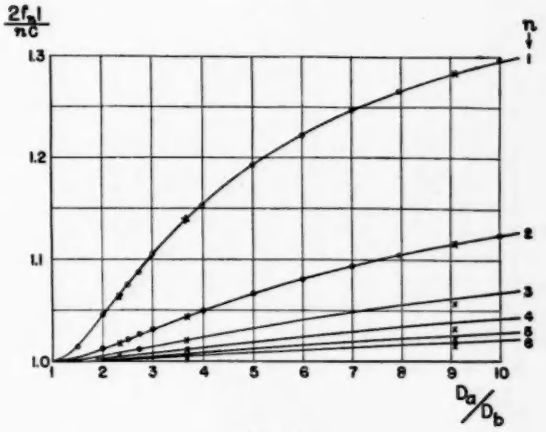

FIG. 2.

or the errors of measurement of mechanical dimensions of this specimen.

On the other hand, for the higher dynamic overtones, $n=3$ to $n=6$, and especially for large values of D_a/D_b the observed values are lower in frequency than the calculated values by as much as 0.5 percent, whence it appears that the equations (1) and (2) though approximately correct are not quite exact for high overtone vibrations of truncated cones which have a large ratio of diameter of large end to diameter of small end.

Frequencies of complete cone

We attempted to prepare a complete cone; i.e., to make $D_b=0$. In this case Eq. (1) becomes

$$\tan \pi 2fl/c=\pi 2fl/c. \quad (3)$$

The roots of this equation[3] are

$$2fl/c=1.4303,\ 2.4590,\ 3.4709,\ 4.4774,\ 5.4818,\ 6.4844 \quad (4)$$

corresponding to $n=1, 2, 3, 4, 5, 6$, respectively.

With our attempted complete cone we obtained experimentally for $n=1$, 2, and 3, respectively,

$$2fl/c(\text{observed})=1.384,\ 2.375,\ 3.355. \quad (5)$$

The specimen was made of the stainless steel and would not oscillate at the higher overtone modes. It is seen that the observed values (5) are

[3] Love, *The Mathematical Theory of Elasticity*, third edition, (Cambridge University Press, 1920) p. 289. Rayleigh, *Theory of Sound*, second edition, Vol. 1, (Macmillan, 1894), p. 334 has also these values (4) but with 4.4774 misprinted 4.4747.

less than the computed values (4) by about 3.5 percent. However, mechanical measurements showed that the small end of the specimen was in fact not a true point with a uniform taper to the end. It is found that if we compute from the observed frequency relations of (5) by Eq. (1), the values for the diameter-ratio D_a/D_b, we obtain $D_a/D_b=30.4$, 28.6, 28.7, respectively, for $n=1$, 2, and 3 of Eq. (5). This means that the observed and calculated values of $2fl/c$ agree if the cone actually had an effective small-end diameter D_b equal to about 1/29 of $D_a=0.044$ cm. Actually the tip diameter was certainly less than this, but calculations from other geometrical measurements showed that a complete cone having the general taper of this one should have had a length of 15.90 cm, whereas the actual length was only 15.42 cm. That is, the cone tapered somewhat more rapidly near the tip than elsewhere. Now, had the taper been perfect with a resulting length of 15.90 cm, the frequency would have been very nearly unchanged. See Table I for frequency changes due to cutting off the cone tip. Hence $2fl/c$ would have been about 3 percent greater than the values we obtained by using a value of 15.42 cm, and this would have brought the values of (5) into close agreement with (4).

Theoretical derivation of Eq. (1)

In a brief search of the literature we have not been able to find the general Eq. (1). Accordingly, we here give a theoretical treatment of the problem, based on parts of Chapter XIII of Love's *Mathematical Theory of Elasticity*.[3] In that chapter on page 297, for propagation of waves in elastic solid media, Love gives the equation of motion in the form

$$(\lambda+\mu)\left(\frac{\partial\Delta}{\partial x},\frac{\partial\Delta}{\partial y},\frac{\partial\Delta}{\partial z}\right)+\mu\nabla^2(u,v,w)=\rho\left(\frac{\partial^2u}{\partial t^2},\frac{\partial^2v}{\partial t^2},\frac{\partial^2w}{\partial t^2}\right) \quad (6)$$

In this equation u, v, w are components of displacement (not velocity) and

$$\Delta=\frac{\partial u}{\partial x}+\frac{\partial v}{\partial y}+\frac{\partial w}{\partial z} \quad (7)$$

as pointed out on p. 281 and p. 299 of Love's book. By differentiating the three equations of (6) respectively by x, y, and z and adding the results Love obtains

$$(\lambda+2\mu)\nabla^2\Delta=\rho(\partial^2\Delta/\partial t^2). \quad (8)$$

Love next points out that, if certain curl components vanish, this equation may be written

$$c^2\nabla^2\phi=\partial^2\phi/\partial t^2, \quad (9)$$

where

$$c=((\lambda+2\mu)/\rho)^{\frac{1}{2}} \quad (10)$$

is the velocity of propagation of the disturbance and ϕ=a potential function, not the usual velocity potential of Rayleigh, but a function whose gradient is the particle *displacement*, with components designated in Love as u, v, w.

Keeping Love's definition of ϕ we shall change his notation for displacement and let ξ=the particle displacement in the direction of r drawn from the vertex of the cone.
Then for motion only in the direction r,

$$\xi=\partial\phi/\partial r. \quad (11)$$

Love points out on p. 298 that, if the motion is irrotational and if ϕ is a function of r and t alone, it satisfies the equation

$$\phi=\frac{f(r-ct)}{r}+\frac{F(r+ct)}{r}, \quad (12)$$

with f and F denoting arbitrary functions. c is the velocity of the wave.

If now as usual we restrict these arbitrary functions to sinusoidal functions of the time we have

$$\phi=\frac{A\sin\omega(t-r/c)}{r}+\frac{B\sin\omega(t+r/c)}{r}. \quad (13)$$

Love next discusses the components of traction per unit area designated by him $-X_\nu$, $-Y_\nu$, $-Z_\nu$ in any normal direction drawn toward the surface, and obtains at the bottom of his p. 300

$$\rho c\left(\frac{\partial u}{\partial t},\frac{\partial v}{\partial t},\frac{\partial w}{\partial t}\right)=-(X_\nu,Y_\nu,Z_\nu).$$

In our notation, since these normal traction components become pressure, we may write

$$p=\rho c(\partial\xi/\partial t). \quad (14)$$

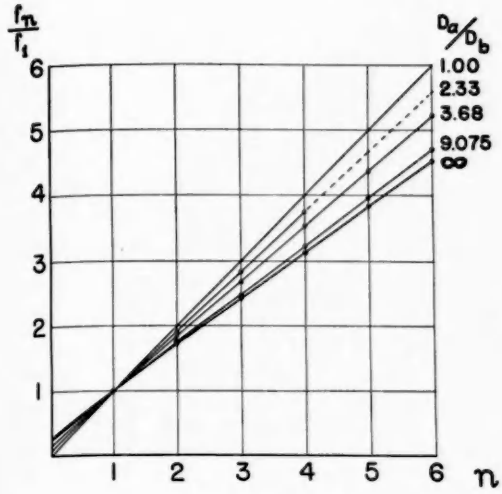

FIG. 3.

Now employing Eqs. (11), (14), and (13) we obtain

$$p=\rho c(\partial/\partial t)(\partial/\partial r)\phi$$
$$=\rho c\omega\left[\frac{-A\cos\omega(t-r/c)}{r^2}+\frac{A\omega\sin\omega(t-r/c)}{cr}\right.$$
$$\left.-\frac{B\cos\omega(t+r/c)}{r^2}-\frac{B\omega\sin\omega(t+r/c)}{cr}\right].$$

Expanding the sums and differences in this equation we obtain

$$p=\frac{\rho c\omega}{r}\left[\left\{-\frac{A+B}{r}\cos\frac{\omega r}{c}-(A+B)\frac{\omega}{c}\sin\frac{\omega r}{c}\right\}\cos\omega t\right.$$
$$\left.-\left\{\frac{A-B}{r}\sin\frac{\omega r}{c}-(A-B)\frac{\omega}{c}\cos\frac{\omega r}{c}\right\}\sin\omega t\right] \quad (15)$$

If now $r=a$ at the large end of the cone, p must be zero at $r=a$; whence
either

I. $A+B=0$ and $\tan\omega a/c=\omega a/c$
or (16)
II. $A-B=0$ and $\tan\omega a/c=-c/\omega a$.

If also $r=b$ at the small end of the cone, p must be zero at $r=b$; whence
either

I. $A+B=0$ and $\tan\omega b/c=\omega b/c$
or (17)
II. $A-B=0$ and $\tan\omega b/c=-c/\omega b$.

We shall now combine (16) and (17), using the combination formula

$$\tan(x-y)=\frac{\tan x-\tan y}{1+\tan x\tan y},$$

obtaining from I of (16) and I of (17),

$$\tan\left(\frac{\omega a}{c}-\frac{\omega b}{c}\right)=\frac{\omega a/c-\omega b/c}{1+(\omega^2ab)/c^2}; \quad (18)$$

or, likewise, if we use II of (16) and II of (17), we obtain

$$\tan\left(\frac{\omega a}{c}-\frac{\omega b}{c}\right)=\frac{-c/\omega a+c/\omega b}{1+c^2/(\omega^2ab)}$$
$$\frac{\omega a/c-\omega b/c}{1+(\omega^2ab/c^2)},$$

which is the same as (18).

It only remains to change the form of Eq. (18) by use of the notation indicated in Fig. 1;

$$b/a=D_b/D_a, \quad a-l=b, \quad \omega=2\pi f.$$

which substituted into (18) gives, on inversion,

$$\frac{\pi(2fl/c)}{\tan(\pi(2fl/c))}=1+\left(\frac{\pi 2fl}{c}\right)^2\frac{D_a/D_b}{\{D_a/D_b-1\}^2}. \quad (19)$$

This is the Eq. (1), which we have employed above and found (cf. Fig. 2) to be approximately checked by the experimental values of frequencies f for different lengths l and diameter ratios D_a/D_b of the conical vibrators.

Method of calculation of curves of Fig. 2

The curves drawn in Fig. 2 were calculated from Eq. (1) using the value of c given in (2a). It is seen that if D_a/D_b, l and v are given the solution of (1) for frequency f is not simple. On the other hand if l and v are known we may introduce various values of f and compute D_a/D_b. This latter method was adopted and $2f_nl/nc$ was then plotted *vs.* the computed values of D_a/D_b to give the curves of Fig. 2.

For a given ratio of the end diameters the dynamic overtone frequencies are nearly linearly related to the overtone number n

It is an interesting and curious result that values of f_n/f_1, plotted in Fig. 3 against the overtone number n give nearly a straight line for

each fixed value of D_a/D_b. Except in the case of the top curve for a cylindrical rod ($D_a/D_b=1$) these nearly straight lines do not pass through the origin. This means that with the cones and truncated cones as vibrators and for any given value of D_a/D_b the overtone frequencies are not integral multiples of the fundamental frequency, but that the difference of frequencies of successive overtones ($f_{n+1}-f_n$) of a given cone or trunctted cone is nearly a constant quantity for $n=1, 2, 3, 4\ldots$.

The top and bottom curves of Fig. 3 were calculated from Eq. (1), with omission of the slight correction factor for the change of c with n as given in Eq. (2a). The top curve for $D_a/D_b=1$ is accurately straight with slope unity; and the bottom curve for $D_a/D_b=$infinity is given by the values of Eq. (4), from which, on division by the first number

$$f_n/f_1=1,\ 1.719,\ 2.427,\ 3.130,\ 3.833,\ 4.534$$

with differences

$$(f_{n+1}-f_n)/f_1=0.719,\ 0.708,\ 0.703,\ 0.703,\ 0.701.$$

The three intermediate lines of Fig. 3 are taken from the curves of Fig. 2 computed from Eq. (1), and the circles on the lines are the observed values with the nickel-steel set of truncated conical vibrators. Similar results were also obtained for the set of stainless steel vibrators. The worst departure from rectilinearity is in the set of computed values of the preceding paragraph.

This approximately linear relation is inherent in Eq. (1) as well as in the observed vibration frequencies, as may be shown independently but with some difficulty by a mathematical examination of Eq. (1). In this examination it is best to employ the series expansion of an antitangent. The treatment of this problem is not here given.

Comparisons of theory and results with theory of conical air columns

In one of the sections above we have pointed out the absence of literature on solid conical vibrators. On the other hand there is considerable theoretical material on the vibration of conical air columns. Lord Rayleigh,[4] assuming certain limitations as to smallness of diameters of a truncated conical pipe filled with air, *with both ends of the conical pipe closed*, finds theoretically for the air column an equation that leads to our Eq. (1). The condition imposed by Lord Rayleigh is that the *velocity* of the vibrating column is zero at the ends of the column, whereas with our solid steel vibrators it is the *pressure* at the two ends that is zero. In this case of *pressure zero* at the two ends Lord Rayleigh obtains for conical air columns the same result for frequency as for *cylindrical* air columns; namely (in our notation), $\sin(\omega l/c)=0$. This is far from true of our vibrators, except in the special case of $D_a/D_b=1$, when our equations give the same results. Barton[5] and Stewart and Lindsay[6] have arrived at the same results as Rayleigh. Barton also describes briefly some elementary experimental work in confirmation of the theory of Rayleigh.

Of course there is a difference between our vibrators and the air-column vibrators of Rayleigh, in that his air-columns were constrained against sideways velocities by the conical tubes containing the air, while our rods were unrestrained against sideways motions. It seems, however, that neither Rayleigh and others nor we have introduced the condition of restraint or unrestraint into the theoretical treatment.

Summary

We have checked by experiment the relation given by Eq. (1) for the vibration frequencies of cones and truncated cones, as a function of their end diameters. For the fundamental and first overtone the agreement is very good; for the higher overtones, for which the diameter of the vibrator is more important in comparison with the wave-length of the vibration, the theory is less closely checked by experiment, though the departure is not great.

We have found that for cones, truncated cones and uniform cylinders the frequency differences between successive overtones is nearly constant, but that only in the case of narrow uniform cylinders are the overtone frequencies exact integral multiples of the fundamental frequency.

[4] Rayleigh, *Theory of Sound*, Vol. II, (1894), p. 281.

[5] Barton, *Textbook on Sound*, (1919) pp. 251–262.

[6] Stewart and Lindsay, *Acoustics*, (1930) pp. 79–83.

The fundamental frequency of a truncated cone of fixed length is always higher than the frequency of a uniform cylinder of the same length and material, and is a function of the ratio of the end diameters; the ratio of the fundamental of a truncated cone to the fundamental frequency of a cylindrical rod of the same length and material changes from 1.000 to 1.4303 as the ratio of the end diameters changes from 1 to infinity. The curves of Fig. 2 relate these frequency ratios, for fundamental and for overtones, to the diameter ratios.

A theoretical derivation of the fundamental equations and a discussion of the departure of the results from theoretical results by Rayleigh and others for conical air columns are given.

The Role of the Speaker Impedance in Resonance in a Closed Pipe

WILLIAM D. PHELPS
Research Division, RCA Manufacturing Company, Camden, New Jersey
(Received August 31, 1937)

An analysis is made of a standing wave resonance system consisting of an eight-foot iron pipe with an eight-inch dynamic speaker at one end and a movable iron piston at the other. Considering the speaker both as a source and as an impedance, expressions are derived for the phase shift, φ_1, of the pressure wave at the speaker, and for the pressure amplitude in the tube. The relation connecting l and λ at resonance is found to be $l=(n+\varphi/2\pi)\lambda/2$, placing the speaker at a distance $(\varphi/4\pi)\lambda$ from the first particle velocity node. (Contrast this equation with the relation $l=n\lambda/2$ for a tube rigidly closed at both ends.) Initial resonance frequencies and a pressure-frequency curve are computed for comparison with experimental data. The possibility of using the resonance conditions for measuring the impedance of diaphragms is pointed out.

INTRODUCTION

IN order to obtain high sound pressures for investigating amplitude distortion in microphones, a standing wave resonance system was built. It consists of an eight-foot iron pipe ten inches in diameter, and a five-sixteenths inch wall with an eight-inch dynamic speaker at one end and a movable iron piston at the other (see photograph, Fig. 1). The microphone is supported from the piston. Use of the apparatus revealed that the relation between the length l of the tube and the wavelength λ at resonance is certainly not given by the formula $l=n\lambda/2$, where n is a whole number 1, 2, 3, etc. Also, a rapid variation of pressure at resonance with resonance frequency in the region of the speaker resonance was noted. Present treatments of the problem[1-3] of forced vibrations in a tube have failed to properly take into account the effect of the source on the resonance phenomena.

THEORY

Before outlining a mathematical analysis of the problem, an intuitive picture of resonance in the tube will be considered. The speaker at any time t_0 sends down the tube a pressure pulse of phase θ. The pulse reaches the end of the tube closed with a rigid piston, suffers no phase change on reflection, and arrives back at the speaker at a time t in the same phase θ. If, on reflection at the speaker, it suffers a phase change φ, it now is of the phase $\theta+\varphi$. But in order for re-enforcement with the pulse now going out from the speaker and resonance to occur, the speaker must go through the phase $n2\pi+\varphi$, n integral, while the original pulse is traveling the length of the tube and back. This reasoning leads to the conclusion that $\omega(t-t_0)=2\omega l/c=n2\pi+\varphi$ or $l=(n+\varphi/2\pi)\lambda/2$ as the resonance condition, where c is the velocity of sound and the other terms have been previously defined. Further analysis is necessary to determine the function φ, the pressure amplitude in the tube, and to verify the relation connecting length and wavelength at resonance.

Assuming undamped plane wave propagation in the tube (see Fig. 2) let the particle velocity and pressure in the wave traveling to the right be represented by

$$\dot{\xi}_1=A_1\epsilon^{-ikx}\epsilon^{i\omega t}, \tag{1}$$

$$p_1=\rho_0 cA_1\epsilon^{-ikx}\epsilon^{i\omega t}, \tag{2}$$

and the corresponding quantities in the wave to the left be represented by

$$\dot{\xi}_2=A_2\epsilon^{+ikx}\epsilon^{i\omega t}, \tag{3}$$

$$p_2=\rho_0 cA_2\epsilon^{+ikx}\epsilon^{i\omega t}. \tag{4}$$

One wishes to know the phase shift in the incident pressure p_2 when reflected at the speaker. Since the amplitude of p_2 is reduced on reflection, and since[4] $|p_2|=|p_1|$, it follows that p_1 is made

[1] Stewart and Lindsay, *Acoustics*, p. 57.
[2] Lamb, *Dynamical Theory of Sound*, p. 174.
[3] Crandall, *Theory of Vibrating Systems and Sound*, p. 103.
[4] See Eq. (13).

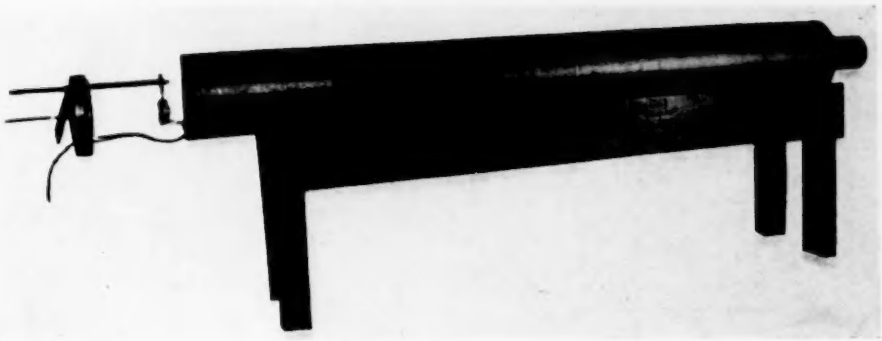

FIG. 1. The standing wave resonance system.

up of two components. If p_1' represents the contribution to p_1 of the speaker as a source and p_1'' the pressure reflected by the speaker as an impedance, then for a steady state

$$p_1'+p_1''=p_1 \tag{5}$$

and the phase shift is given by the expression $(p_1''/p_2)_{x=0}$. For convenience in evaluating p_1''/p_2 one may, without loss of generality, assume for the moment that $p_1'=0$, i.e., that the voice coil current is zero, then $p_1''=(p_1)_{x=0}$ and hence from Eqs. (2) and (4)

$$(p_1''/p_2)_{x=0}=A_1''/A_2. \tag{6}$$

Also from the boundary condition on volume currents at $x=0$

$$S_2(A_1''-A_2)\epsilon^{i\omega t}=S_1\dot{\xi}_S, \tag{7}$$

where $\dot{\xi}_S$ is the cone velocity. The equation of motion for the speaker is

$$p_1''+p_2=-Z_{A1}S_1\dot{\xi}_S, \tag{8}$$

where Z_{A1} is the speaker impedance in acoustic ohms including damping due to the electrical circuit.

Again from Eqs. (2), (4), and (7) Eq. (8) becomes

$$\rho_0 c(A_1''+A_2)\epsilon^{i\omega t}=-Z_{A1}S_2(A_1''-A_2)\epsilon^{i\omega t}, \tag{9}$$

whence

$$(p_1''/p_2)_{x=0}=(Z_{A1}-Z_A)/(Z_A+Z_{A1}) \tag{10}$$

or

$$(p_1''/p_2)_{x=0}=B\epsilon^{i\varphi}, \tag{11}$$

where

$$\varphi=\tan^{-1}(2Z_AX_{A1})/(R_{A1}^2+X_{A1}^2-Z_A^2)$$

is the phase shift in pressure amplitude on reflection at the speaker, $Z_A=\rho_0 c/S_2$, $Z_{A1}=R_{A1}+iX_{A1}$, and

$$B=[(R_{A1}-Z_A)^2+X_{A1}^2]^{\frac{1}{2}}/[(R_{A1}+Z_A)^2+X_{A1}]^{\frac{1}{2}}$$

is the ratio of the reflected to the incident pressure amplitudes.

As the next step, the pressure amplitude in the tube as a function of frequency, speaker impedance, and pipe constants will be determined. From the conditions imposed on the volume currents at the two ends of the tube, one finds at

$$x=0$$

$$S_2(A_1-A_2)\epsilon^{i\omega t}=S_1\dot{\xi}_S. \tag{12}$$

At $x=l$

$$(A_1\epsilon^{-ikl}-A_2\epsilon^{ikl})\epsilon^{i\omega t}=0$$

or

$$A_2=A_1\epsilon^{-i2kl}. \tag{13}$$

One should note that while Eqs. (7) and (12) are of the same form, they are for different conditons; namely, for $F=0$, and for $F=F_0\epsilon^{i\omega t}$, respectively. Also, the equation of motion for the speaker becomes

$$F=S_1^2(Z_{A1}-iZ_A\cot kl)\dot{\xi}_S, \tag{14}$$

where $-iZ_A\cot kl$ is the input impedance of the

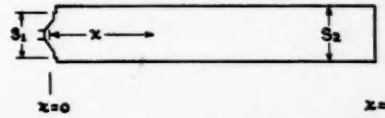

FIG. 2. Diagram of the standing wave resonance system.

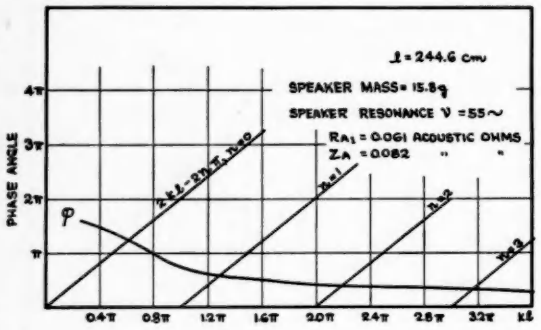

FIG. 3. Determination of the initial resonance frequencies of pipe and speaker, $R_{A1} < Z_A$. φ is the phase shift by the speaker.

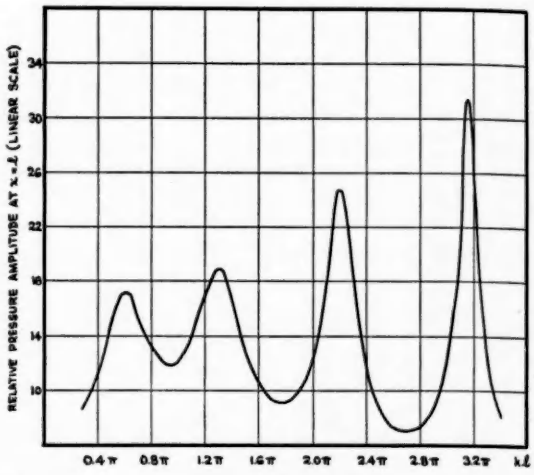

FIG. 4. Calculated pressure-frequency characteristic for the first four peaks. The resonance frequencies are accurately given by the phase change on reflection at the speaker. Note the peak value trend in the region of the speaker resonance frequency.

closed tube.[5] From Eqs. (12), (13), and (14) one finds

$$A_1 = \epsilon^{ikl} F_0 / 2S_1S_2[i \sin kl\, Z_{A1} + Z_A \cos kl]. \quad (15)$$

Hence the pressure amplitude at any distance x is

$$|(p_1+p_2)|_{x=x} = \left| \frac{\rho_0 c \cos k(l-x) F_0}{S_1S_2[iR_{A1} \sin kl + Z_A \cos kl - X_{A1} \sin kl]} \right|. \quad (16)$$

From Eq. (16) one may easily derive the resonance condition on k, l, and φ. For a given value of k the pressure amplitude is a maximum at a pressure loop when l is such that the absolute value of the complex denominator is a minimum. Considering the denominator as a function of l and minimizing, the resonance condition is found to be

$$\tan 2kl = 2Z_A X_{A1} / (R_{A1}^2 + X_{A1}^2 - Z_A^2). \quad (17)$$

Comparing Eqs. (17) and (11) it is seen that

$$\tan 2kl = \tan \varphi \quad (18)$$

or

$$2kl = 2n\pi + \varphi. \quad (19)$$

Eq. (19) derived on the basis of maximum amplitude is identical with the relation arrived at intuitively on the basis of phase alone. It emphasizes the importance of phase reenforcement of the reflected and generated pressure at the speaker for high pressures in such a system.

Having derived equations showing the effect of the speaker on the resonance frequencies of the system, and on other aspects of the problem, it is instructive to graphically illustrate some of these by curves. If the pipe length and cross-sectional area and speaker impedance are known, then Eq. (19) and the expression for φ in Eq. (11) enable one to compute the resonance frequencies. In Fig. 3 these are given by the intersection of the curves φ and $2kl - 2n\pi$, both considered functions of kl, for the first four resonance frequencies of the system. Table I shows a comparison of the calculated and measured values of kl at resonance. With the exception of the first one, the agreement is not bad.[6]

Using Eq. (16) the frequency characteristic (see Fig. 4) of the pressure amplitude at a loop, say at $x=l$, has been plotted for kl in the region of the speaker resonance frequency assuming constant voice coil current. The speaker resonates at $kl = 0.78\pi$. It is to be noted that the magnitude of the peaks increase with k while

TABLE I. *Comparison of calculated and measured kl at resonance, $kl = 1.42\pi\nu 10^{-2}$.*

kl	
CALCULATED	MEASURED
0.62π	0.8π
1.30π	1.38π
2.20π	2.20π
3.16π	3.24π

[5] Olson and Massa, *Applied Acoustics*, p. 35.

[6] In this and subsequent computations the contribution to R_{A1} due to damping in the cone suspension has been neglected.

the minima decrease. While this peak value depends on a number of factors as given by Eq. (16), the rise is explicable in the fact that the phase shift by the speaker decreases with increasing k, causing the cone to approach a particle velocity node. The decrease in the minima is due to the increasing speaker impedance. In Fig. 5 is plotted, for comparison with Fig. 4, a pressure-frequency characteristic obtained with a pressure microphone placed at $x=l-2.54$ cm. No corrections have been applied. With the exception of the first peak the curves in the two figures are similar.

Discussion

One is now in a position to answer the question: Is the speaker at a particle velocity node?

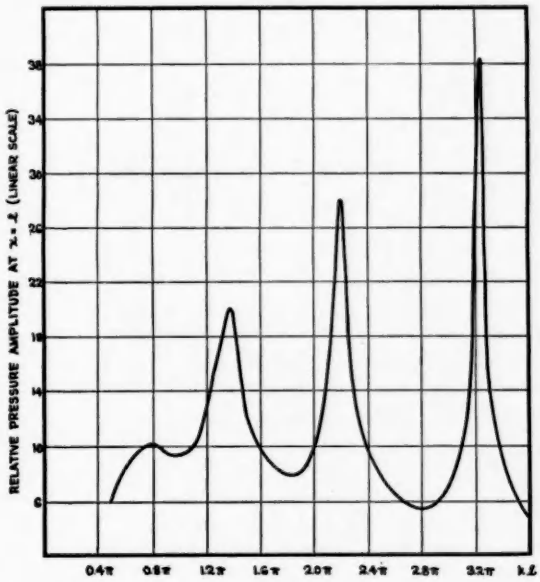

Fig. 5. Experimental pressure-frequency characteristic of the system described taken with a pressure microphone.

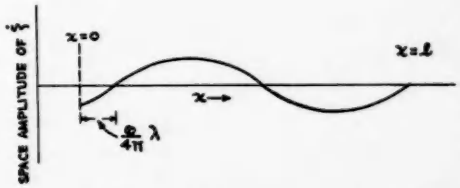

Fig. 6. Representation of the space amplitude of the particle velocity along the tube at resonance, $n=2$. The speaker is located at $x=0$.

The answer is that it is not in general. The distance from the speaker to the first node is equal to $(\varphi/4\pi)\lambda$. This condition is illustrated in Fig. 6, for example, where $n=2$.

It should also be noted that the speaker absorbs some of the incident wave as well as changes its phase on reflection.

Since the speaker impedance enters into the resonance phenomena, it is to be expected that resonance might be used to measure the impedance of diaphragms. An examination of Eq. (17) substantiates this statement. By measuring k, l, and Z_A, R_{A1} and X_{A1} may be computed.

Conclusions

1. The speaker shifts the phase of the reflected wave by an angle φ thereby making the resonance condition $l=(n+\varphi/2\pi)\lambda/2$ in contrast with the condition $l=n\lambda/2$ for a tube rigidly closed at both ends.

2. The speaker is at a distance $(\varphi/4\pi)\lambda$ from the first particle velocity node.

3. The pressure amplitude is dependent on speaker impedance and phase shift.

4. The resonance Eqs. (17) and (18) offer a method for measuring speaker and microphone impedance.

Absolute Sound Intensity in Liquids by Spherical Torsion Pendula

ELIAS KLEIN
Naval Research Laboratory, Washington, D. C.
(Received August 18, 1937)

These experiments demonstrate the use of spherical radiometers to determine the energy density in an acoustic field. It is shown that the theoretical work of King is applicable to the measurement of radiation pressure in liquids. Considering the torsion pendulum as an absolute instrument, pressure microphones are calibrated as secondary standards.

INTRODUCTION

THE object of this paper is to describe a method for absolute sound intensity measurements in liquids; and to indicate means of calibrating pressure microphones in terms of fundamental units. This investigation is based entirely upon the well-known phenomenon of acoustic radiation pressure which postulates a nonlinear character to the wave progressing in a fluid medium.

In the realm of high frequency acoustics, particularly in liquids, the radiometer is almost indispensable as a measuring instrument. This device, in its various forms, responds to the steady continuous pressure existing in a sound field. The alternating pressures commonly associated with sound propagation phenomena are only indirectly involved in these measurements. The relation between the two types of pressures is

$$R_p=\frac{(\gamma+1)}{2}\frac{p^2}{\rho c^2}, \qquad (1)$$

where R_p is the radiation pressure which a radiometer evaluates; γ is the ratio of the specific heats; p is the r.m.s. oscillatory pressure; and ρc is the acoustic resistance of the medium in which the pressures are measured. In air $R_p \doteqdot 0.8 \times 10^{-6} p^2$, while in water $R_p \doteqdot 0.44 \times 10^{-10} p^2$. In other words, one dyne per square cm of oscillatory pressure in air yields less than a microdyne of radiation pressure; whereas, in water the same unit of r.m.s. pressure (1 dyne/cm^2) produces less than half a ten-thousandth of a microdyne in radiation pressure. This indicates the magnitudes which are involved in radiation pressure experiments.

Radiation pressure is associated with the momentum of wave motion and is measured by the impact of the wave upon an obstacle. One may regard radiation pressure as a rectified component (second order in magnitude) of the oscillatory motion which a vibrating source imposes upon the medium. This increment in static pressure in a sound field is due to the nonlinear relation existing between pressure and density. Indeed, if it were possible to generate an acoustic wave disturbance and so influence the medium that it would respond only to a linear law of force, then there should be no momentum propagated and no radiation pressure detectable. However, the results of many investigators[1] have demonstrated not only the presence of radiation pressure, but have verified its quantitive relation to the energy density per unit volume, E, of the medium, namely

$$R_p=(\gamma+1)E/2. \qquad (2)$$

THE PRESENT PROBLEM

The general procedure of all radiometric determinations is to place an obstacle in the path of the wave train, which obstacle causes a change in the propagated momentum and itself experiences a reaction. Usually, this disturbs the sound field and makes absolute measurements unreliable. A primary requisite of any measuring device is that its influence upon the domain under observation shall be either entirely negligible or exactly calculable. Therefore, the obstacle must be of such geometric form as to introduce (a) no noticeable distortion into the sound field; or (b) its reflective and refractive effects should be definitely known. Both phases of this problem

[1] Dvorak, Pogg. Ann. **57**, 42 (1876); Meyer, Phil. Mag. **6**, 225 (1878); Zernow, Ann. d. Physik **21**, 131 (1906); Rayleigh, Scientif. Papers, V, 41 and 262; Weaver, Phys. Rev. **15**, 400 (1920); Altberg and Holtzman, Physik. Zeits. **26**, 49 (1925).

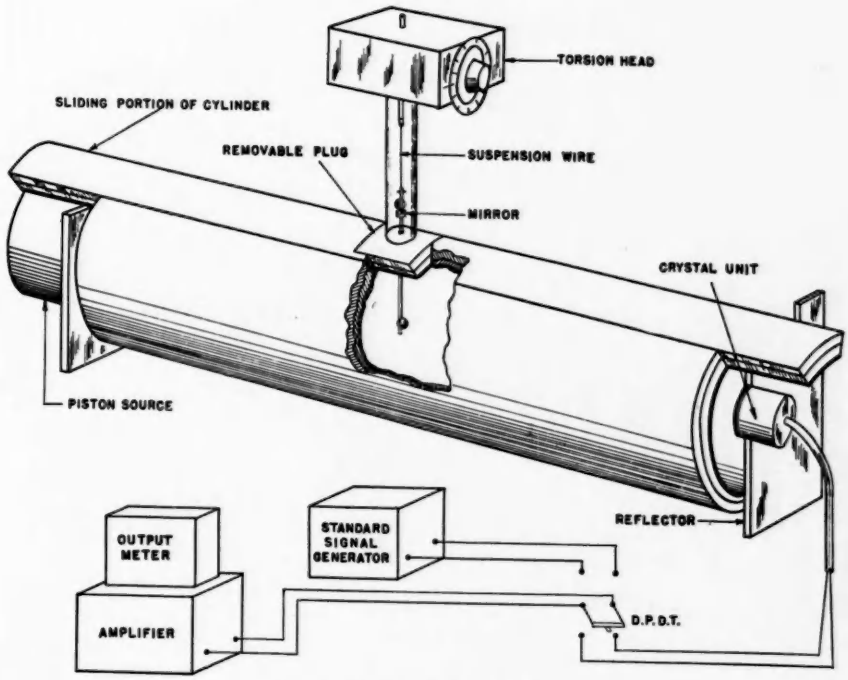

FIG. 1. Radiometer assembly.

are being investigated; however, for the present,[2] the discussion is confined to spherical torsion pendula as related to (b).

Accordingly, sound energy is allowed to fall upon solid spheres of various sizes comparable to the wave-length in the medium. The acoustic field is symmetrically distorted by the obstacle. The latter reflects some of the incident energy, while a portion of it may unite behind the sphere so as to form a shadow. An exact knowledge of the scattering and diffraction effects of spheres when subjected to acoustic radiation pressure has been made available in a theoretical development by L. V. King.[3] Following this mathematical treatment precise calculations have been made herein for the total force exerted upon spherical obstacles in plane stationary wave systems. The results of these computations are compared with a series of experiments which show reasonable quantitative agreement with King's analysis.

EXPERIMENTAL METHOD AND APPARATUS

The methods of producing plane stationary waves in liquids at high frequencies are quite well known. Nevertheless, certain of the precautions taken are noteworthy. Fig. 1 is a composite

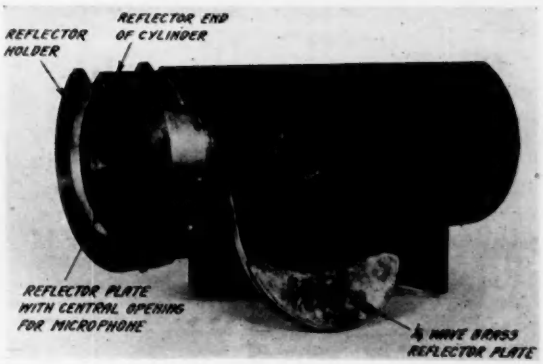
REFLECTOR HOLDER
REFLECTOR END OF CYLINDER
REFLECTOR PLATE WITH CENTRAL OPENING FOR MICROPHONE
¼ WAVE BRASS REFLECTOR PLATE

FIG. 2.

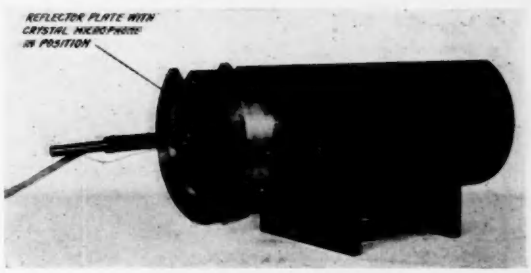

FIG. 3.

[2] Correlation of the two methods is already in progress with encouraging results, as demonstrated at the Washington meeting, May 3, 1937.

[3] L. V. King, Proc. Roy. Soc. **A147**, 212 (1934).

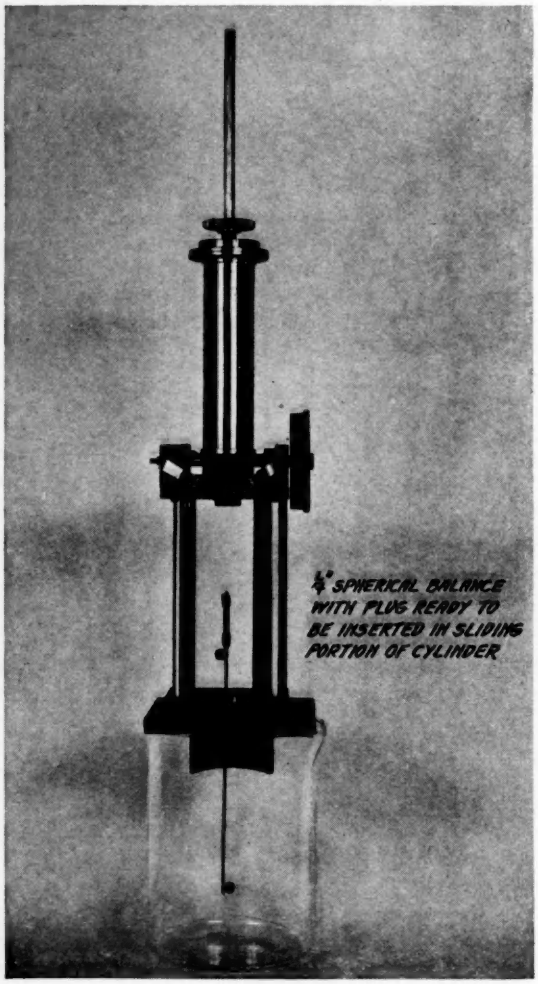

FIG. 4.

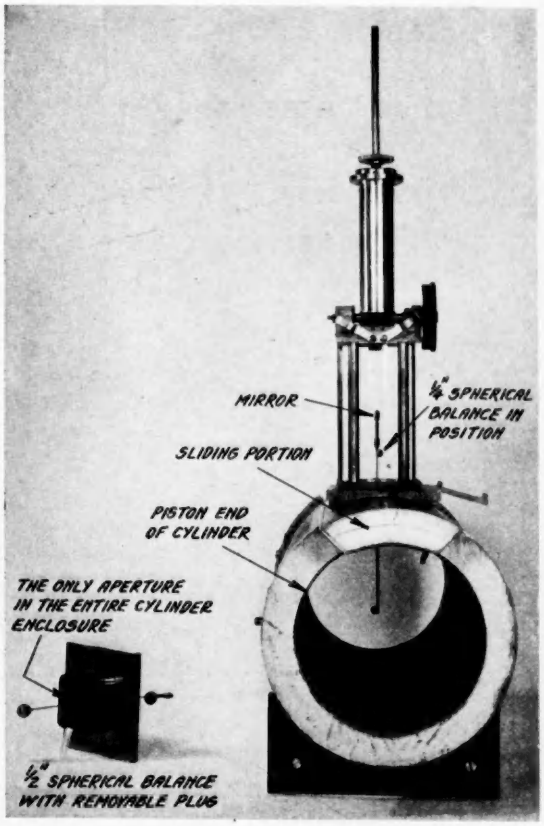
MIRROR
1/4" SPHERICAL BALANCE IN POSITION
SLIDING PORTION
PISTON END OF CYLINDER
THE ONLY APERTURE IN THE ENTIRE CYLINDER ENCLOSURE
1/2" SPHERICAL BALANCE WITH REMOVABLE PLUG

FIG. 5.

sketch of the principal parts of the apparatus. A nonresonant crystal quartz sound generator (piston type) fills one end of a rigid cylindrical tube, six inches in diameter. The other end, about 2 feet away is closed by a machined reflector. The latter is so arranged as to function either as a complete reflector or as a reflector minus a central plug. The microphone to be calibrated is placed in the hole left by removing the plug, about $1\frac{1}{2}''$ diameter (Fig. 2 and Fig. 3). The tube and associated parts are completely immersed in a tank of distilled water. Acoustically the length of the tube is adjustable by providing telescopic movement between the piston source and the rigid tube. Also the microphone position can be regulated in the reflector opening so that the pressure upon the microphone is a maximum. By this means, sharply defined nodes and antinodes are established within the cylinder. These are essential in absolute determinations of radiation pressures in standing wave systems. Moreover, the nodes and antinodes should be fixed in space relative to the closures of the tube. To maintain these conditions, the temperature of the water tank, which houses the apparatus is kept fairly constant; also, the frequency and voltage of the electrical oscillator which actuates the sound source are carefully controlled.

A spherical torsion balance (Fig. 4 and Fig. 5) is employed to explore and evaluate the radiation pressure generated within the tube. The pressure is exerted only upon the measuring sphere which is kept at all times exactly on the axis of the cylinder. The sphere visible above the cylinder acts merely as a counterpoise. The center of each sphere is at a fixed distance from the axis of

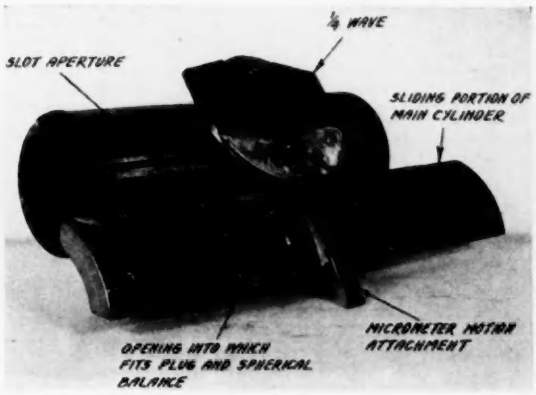
¼ WAVE
SLOT APERTURE
SLIDING PORTION OF MAIN CYLINDER
MICROMETER MOTOR ATTACHMENT
OPENING INTO WHICH FITS PLUG AND SPHERICAL BALANCE

FIG. 6.

suspension. A force causing the measuring sphere to turn is balanced by the torsion of the wire. A scale and mirror are employed to indicate the angular deflections. The photograph shows the $\frac{1}{4}''$ spherical suspended system ready to be placed into the sliding portion of the tube. Alongside are the $\frac{1}{2}''$ spheres to indicate the plug fitting and to show the only opening of consequence through which energy from the inside of the tube may escape to the surrounding water.

Before extending the description of these experimental details, it is reasonable to inquire as to the need for such elaborate precautions to minimize energy flow from the tube. The necessity for eliminating leakage and diffusion of sound through openings was proved by tests with a series of slots parallel to the axis of the tube. The slots[4] (one such is shown in Fig. 6) varied in width from $\lambda/10$ to $\lambda/4$. The results showed considerable distortion and asymmetry in the standing wave system inside the cylinder due to energy transmission through the apertures. This was evident from the radiation pressure curves when plotted in a manner similar to Fig. 7, Fig. 8 and Fig. 9. The ideal condition should present a sinusoidal distribution of R_p along the axis of the cylinder. Unfortunately, the errors

[4] In this connection it is interesting to recall that the amount of sound energy which passes through an opening is considerably out of proportion to the area of the opening. For example, see Wintergest and Knecht, V.D.I. 76, 777, (1932).

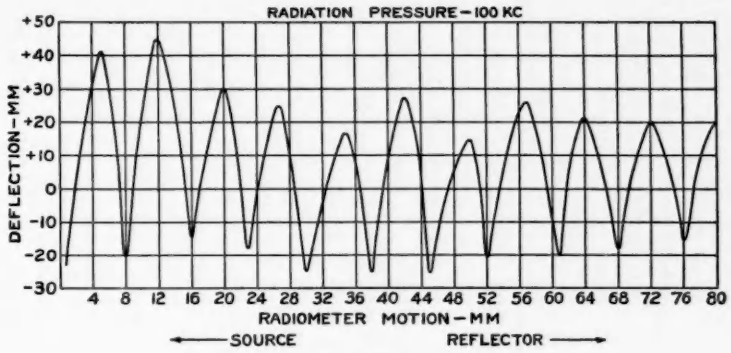

FIG. 7

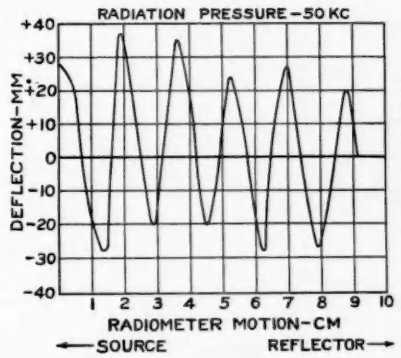

FIG. 8

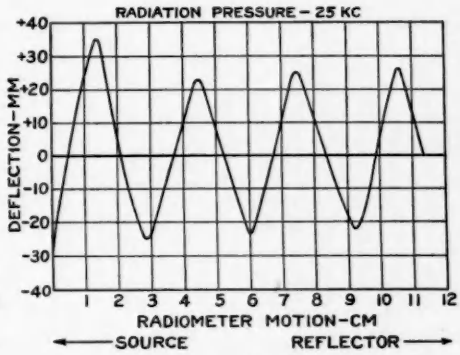

FIG. 9

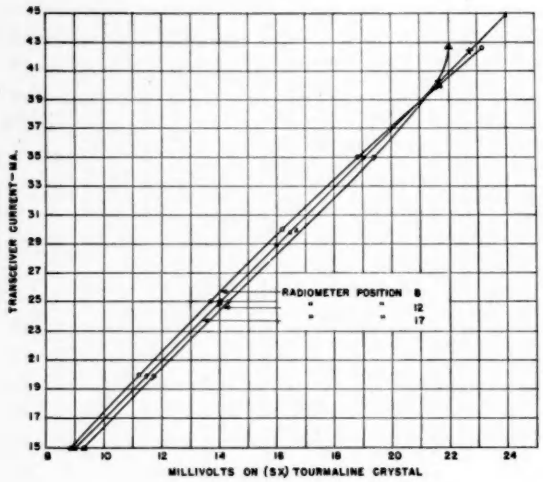

FIG. 10.

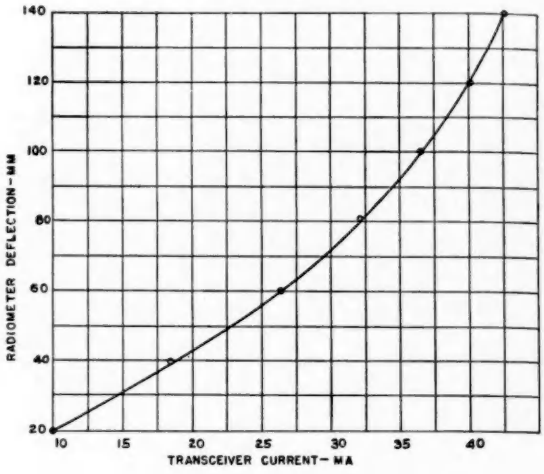

FIG. 11.

introduced into radiation pressure measurements by the presence of pseudo-stationary waves due to an apparent attenuation in the medium are not readily calculable. Therefore, apertures of any sort were carefully avoided in the design of the present cylindrical enclosure. Also a serious effort was made to have as nearly a perfect standing wave system as is practically realizable in distilled water contained in a tube.[5]

The latter is over $1\frac{1}{8}$ inches in thickness and is composed of three concentric layers of different metals. The inner shell is of $\frac{1}{16}''$ brass while the outer shell is $\frac{1}{2}''$ bronze. Hot molten lead was poured between these two cylinders so as to form a tubular sandwich of brass-lead-bronze which machined as a single cylinder about 3 ft. long. The sector shown in Fig. 6 as the sliding portion of the main cylinder was cut from the original length of tubular-sandwich, and is about 6″ longer than the lower portion of the tube over which it travels on guides. The rectangular plug through which the spheres are joined (Fig. 5) is also part of the original cylinder. Bronze spheres were used in these experiments. A nickel tube about 0.05 inches in diameter joins the two spheres. The suspensions are 0.001″ tungsten wire supporting the $\frac{1}{4}''$ sphere and 0.002″ carrying the $\frac{1}{2}''$ spheres.

[5] Radial oscillations may become very troublesome at certain frequencies despite the tube design and construction. (Field, Can. J. Research **5**, 131 (1931).) In these tests it was necessary to provide an inner lining for the main cylinder in order to break up at some frequencies supposed radial oscillations.

MEASUREMENTS AND DATA

In these experiments acoustic radiation pressure data serve a twofold purpose. The energy density of the incident wave may be evaluated. At the same time a pressure microphone is calibrated as a secondary standard. The two sets of observations are made simultaneously by independent observers. Deflections of the spherical torsion pendulum are noted at different points

TABLE I.

FREQUENCY IN KC	VALUE OF $\alpha = ka$ FOR SPHERES OF		DEFLECTION-AMPLITUDE IN CM OF SPHERES		Δ FROM FIG. 12		EXPT. $8.5\,\delta_2/\delta_1$	THEORY Δ_2/Δ_1	APPROXIMATE	
	$\frac{1}{4}''$	$\frac{1}{2}''$	$\frac{1}{4}''$	$\frac{1}{2}''$	$\frac{1}{4}''$	$\frac{1}{2}''$			R.M.S. PRESSURES IN DYNES/CM² UPON CRYSTAL MICROPHONES	MILLIVOLTS RECORDED BY MICROPHONES
25	0.332	0.665	2.90	1.95	0.030	0.162	5.70	5.40	0.4×10^5	10
50	0.665	1.33	5.40	2.30	0.162	0.542	3.62	3.34		
75	1.00	2.00	1.95	0.18	0.412	0.207	0.783	0.503	to	to
100	1.33	2.66	2.61	0.22	0.542	0.357	0.718	0.608		
122.5	1.63	3.26	2.15	0.35	0.175	0.30	1.38	1.71	2.0×10^5	100

along the axis of the cylinder. These readings, obtained either by using the torsion head or by the direct deflection method, are taken one to three mm. apart depending upon the frequency of the emitted sound. Examples of such data are shown in Fig. 7, Fig. 8 and Fig. 9.

The voltages impressed upon the microphone located in the reflector plate are measured while the deflections of the sphere are recorded in its various positions. Fig. 10 illustrates the general relationship existing between the received voltages and the current amplitude of the source at constant frequency. The three curves indicate three different locations of the radiometer, and suggest the likely effect of the suspended system position upon the r.m.s. pressure developed at the reflector.

From Fig. 10 it will be noted that the piston-source amplitude varies directly with the alternating pressures as registered by the microphone. On the other hand, the same current-amplitude of the piston source is proportional to the square root of the radiometer deflection, shown by the experimental curve in Fig. 11, and implied in Eq. (1).

Table I represents averages of considerable data gathered primarily for the purpose of testing King's theory, and to ascertain the suitability of the spherical torsion balance for absolute measurements. Although a sufficient number of check determinations by other methods has now been made to establish these results quantitatively, yet they lack in ultimate precision and refinement when regarded as standard values. Therefore, the different columns merely indicate certain observed and calculated quantities. They also show estimates of other magnitudes dealt with experimentally.

Theory and Calculations

The general expression for the mean radiation pressure on a sphere in a plane stationary field, as developed by King is:

$$\bar{P}=\pi\rho_0/A^2/\sin 2kh\left[\frac{1}{\alpha^3}\frac{F_0F_1+G_0G_1}{H_0^2H_1^2}\alpha^2-\frac{2}{\alpha^5}\frac{(F_1F_2+G_1G_2)}{H_1^2H_2^2}\left\{\alpha^2-3\left(1-\frac{\rho_0}{\rho_1}\right)\right\}\right.$$
$$\left.+\sum_{n=2}^{\infty}(-1)^n\frac{(n+1)}{\alpha^{2n+3}}\frac{(F_{n+1}F_n+G_{n+1}G_n)}{H^2{}_{n+1}H_n{}^2}\{\alpha^2-n(n+2)\}\right]. \quad (3)$$

$\bar{P}$ is the total force acting on the sphere of radius a; ρ_0 and ρ_1 are the densities of the liquid and sphere respectively. $|A|$ is the complex amplitude of the wave; h, the distance from the center of the sphere to the nearest velocity node; $k=2\pi/\lambda$ wave-length; and $\alpha=ka$. F_n, G_n and H_n are related

$$H_n{}^2=F_n{}^2+G_n{}^2, \quad (4)$$

where $H_n{}^2$ is expressible in a Bessel series. (3) may be written as

$$\bar{P}=\pi\rho_0|A|^2\Delta\sin 2kh, \quad (5)$$

where Δ represents the numerical equivalents of the series in the square bracket [ ] for different values of $(\alpha=ka)$.

Now the mean total energy density in the incident wave is

$$E=\tfrac{1}{2}\rho_0k^2|A^2|.$$

Therefore, $$\bar{P}=(2\pi E/k^2)\Delta\sin 2kh. \quad (6)$$

Expression (6) is used to evaluate experimental results. Δ was calculated in terms of Bateman's or Bessel functions, and is represented graphically[6] in Fig. 12. Another form of (3) for the total force on a sphere is

$$\bar{P}\equiv F=\pi a^2\bar{E}\sigma\sin 2kh, \quad (7)$$

where σ is a function of $(\alpha=ka)$ and the density ratio (ρ_0/ρ_1).

Calculations of σ in Eq. (7) were carried out by Sivian and O'Neil[7] for the measurement of aerial sound intensities. Comparing (6) and (7), a relation between σ and Δ is obtained, *viz.*

$$\sigma=(2/\alpha^2)\Delta. \quad (8)$$

Fig. 13 shows a comparison of the Bell Labora-

[6] The calculations were made and checked with the helpful cooperation of Dr. M. Sasuly and Mr. H. Hedinger.

[7] The author is indebted to the Bell Laboratories for permission to publish expression (7) and the solid curve in Fig. 13 for comparison.

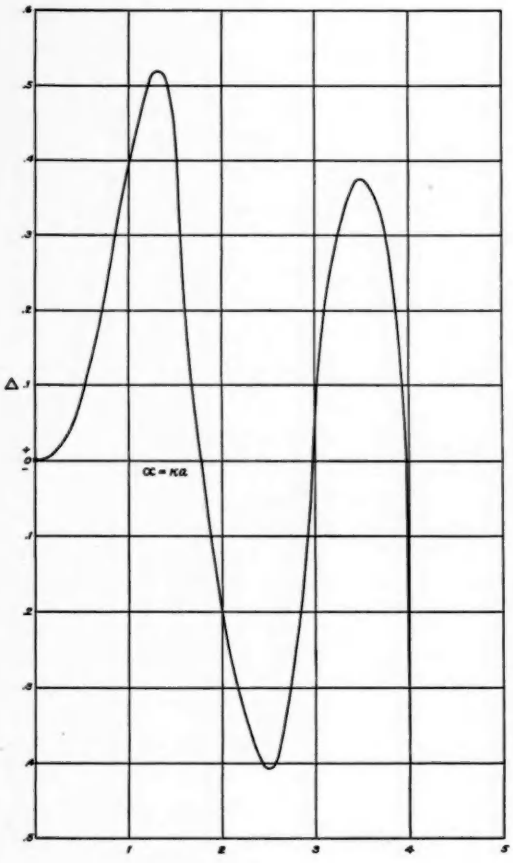

FIG. 12.

tories calculations of σ with its values derived from (8). It should be observed that the solid σ curve was computed with the assumption that $\rho_0/\rho_1=0$, quite legitimate for aerial waves. In the Δ calculations, the experimental value of $(\rho_0/\rho_1=1/8.8)$ was used. Different series and distinct methods were employed in evaluating σ and Δ, respectively. These curves bring to light the experimental fact that in a stationary wave much larger radiation pressure is exerted on a sphere whose value of α is relatively small. Theory also predicts that for the same maximum amplitude of sound, the measuring sphere of small α experiences a considerably greater magnitude of radiation pressure in a standing wave system than it does in a progressive wave. For larger values of α, however, the conditions are reversed. That is, radiation pressure is greater in a progressive wave.

To reduce experimental data, either equation (6) or (7) is suitable provided, of course, the values of Δ and σ are available for different ranges of α. Although (6) is consistently used in the present calculations, the physical significance[8] of the factors involved is more apparent in (7). Rewriting the latter in terms of radiation pressure, R_p, we have

$$R_p \equiv F/\pi a^2 = E\sigma \sin 2kh. \qquad (7')$$

This expression states first of all that in a plane stationary wave in which the mean energy density is E, the radiation pressure acting upon a spherical obstacle is generally less (depending upon σ which is always less than unity) than the energy density in the neighborhood of the sphere because of scattering and diffraction.

Secondly, the radiation pressure is a periodic function of the position of the sphere relative to the particle velocity nodes and loops. Moreover, the periodicity is double that of the standing wave pattern. This dependence of radiation pressure upon the location of the sphere was theoretically predicted by King and amply verified in these experiments.

In reducing the data to numerical values, the average of the radiation pressure amplitude was used for a given series of deflections. Thus (6)

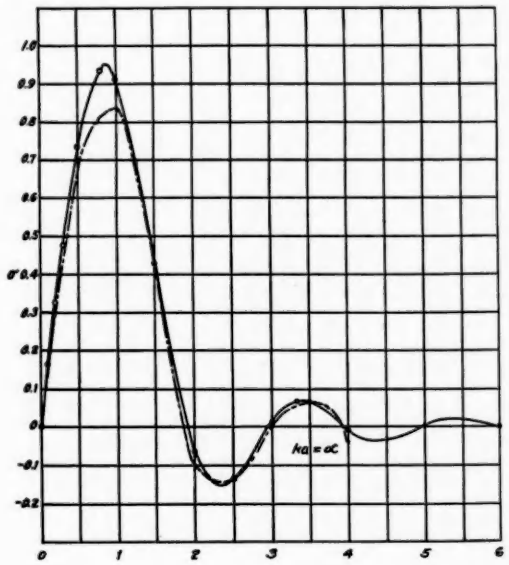

FIG. 13. Solid curve, Bell Laboratories calculation; broken curve. N.R.L. reduction from $\sigma=2\Delta/\alpha^2$.

[8] For further explanation see Appendix.

becomes

$$P=(2\pi E/k^2)\Delta. \tag{9}$$

Now the torque acting upon the sphere due to radiation pressure is balanced by the twist in the suspension after the system turns through a resultant angle δ or

$$Pl=s\delta, \tag{10}$$

where l is the distance from the center of the sphere to the axis of rotation; and s is the torsion constant of the suspension. Combining (9) and (10); and solving for the energy density, we have

$$E=s\delta k^2/2\pi\Delta l=2\pi s\delta/\lambda^2\Delta l. \tag{11}$$

It is reasonable to expect that E would remain fixed while operating at one frequency with the same power into the piston source; and, maintaining all other experimental conditions constant (except the torsion balance size). That being true, the different diameter spheres should experience a torque according to

$$s_1\delta_1/\Delta_1 l_1=s_2\delta_2/\Delta_2 l_2, \tag{12}$$

where the subscripts 1 and 2 correspond to the factors associated with the $\frac{1}{4}''$ and $\frac{1}{2}''$ spheres, respectively. Rewriting, there results

$$(s_2 l_1/s_1 l_2)\delta_2/\delta_1=\Delta_2/\Delta_1. \tag{13}$$

The coefficient of the ratio of deflections is made up of predetermined experimental constants, the value of which is 8.50. Therefore, the validity of (3) may be tested for various frequencies by the aid of (13), provided that E does not change during the investigation of any one frequency. This procedure was followed for the frequencies recorded in the table. Columns 8 and 9 show the approximate agreement between theory and experiment. By a series of motional impedance measurements associated with this project, as well as by certain piezoelectric studies, the assumption that E remains constant was further justified. Column 10 suggests the limits of alternating pressures exerted upon the crystal microphone located in the reflector plate while column 11 gives the approximate voltages developed by several microphones.

Discussion and Conclusion

It is desirable to point out some likely sources of error which were not considered in this series of experiments. Their effects upon the absolute values of radiation pressures are still to be ascertained. Consequently, estimates of accuracy are omitted until a number of influencing factors are made more determinate.

Although noticeable in most of the curves similar to Fig. 7, Fig. 8 and Fig. 9, the attenuation of the signal in the medium between the source and radiometer was neglected in the computations. Incidentally, this type of radiometer might be readily adapted to absorption measurements in liquids.

Nor was any attempt made to correlate the size of the tube with the high frequencies used for optimum radiation pressures. The data available need more study. Furthermore, absolute results obtained from acoustic measurements in liquids contained in tubes with beamed sources require careful interpretations.

The spheres used were assumed to be "rigid." Preliminary calculations based upon the physical properties of the spheres showed that neither their spheroidal nor their radial modes of natural mechanical vibration frequencies were close to the excited acoustic frequencies. Nevertheless, the discrepancies observed between theory and experiment at 75 and 100 kc lead one to suspect that a nearby mechanical resonance in the $\frac{1}{4}''$ sphere may have caused some trouble.

These and other attending difficulties notwithstanding, the method described for absolute acoustic determinations in liquids gives a plausible answer to the question "How Much Sound?".

Appendix

The physical significance of an equation, however pertinent, is not quite acceptable as an explanation of a phenomenon which is vaguely understood. Thus, while discussing the paper at the Washington meeting, there arose two questions concerning radiation pressure in stationary fields.

(1) If a stationary wave is equivalent to two progressive waves of the same frequency and amplitude, traveling in opposite directions, why is the sphere (or any other symmetrical obstacle), when placed in this sound field, not subject to equal and opposite forces?

(2) How does a standing wave system of one frequency

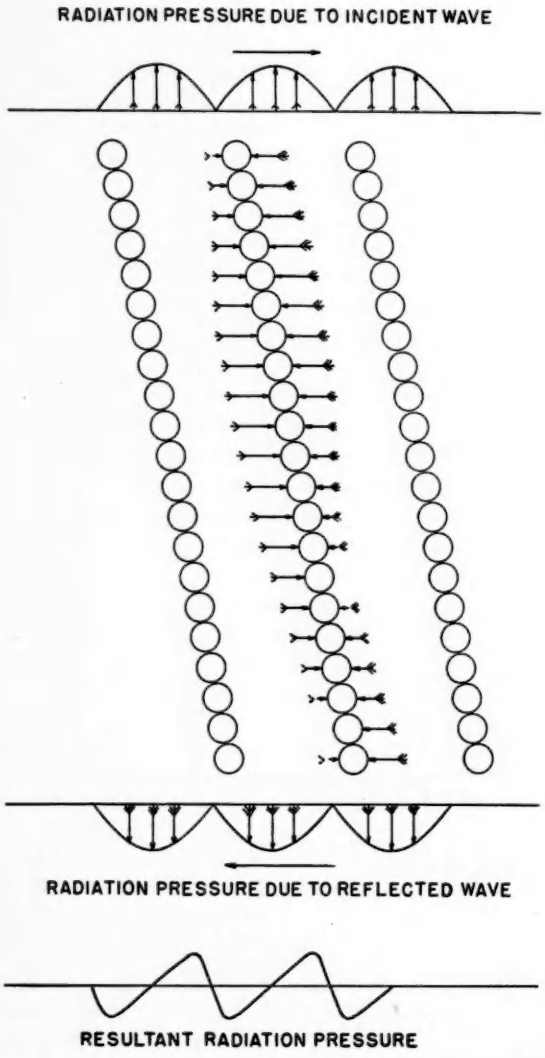

FIG. 14. Relation magnitudes of pressure components on sphere in successive positions with reference to the stationary wave system.

and presumably free from harmonics cause the sphere to react with twice the frequency of the sound generated?

The following is an attempt at a graphical description of the phenomena fully portrayed in mathematical language by King.

Consider two plane progressive (identical) waves moving in opposite directions. Let these constitute the resolved components of the actual stationary wave system. Each of these progressive longitudinal waves carried with it a certain amount of momentum which is always directed away from the source. This is sketched in Fig. 14 as a rectified component of the wave train. Each group of segments may be regarded as an increment in static pressure of the medium. In magnitude, it fluctuates from point to point with the wave.

Now suppose that an infinitely thin metallic disk (say a section of a larger sphere) of sufficient wave front area to be considered an obstacle were used as a radiometer. Equal streams of momenta would fall on each surface of the disk, due to the oppositely traveling waves, and the obstacle should remain at rest. In other words, the rate of change of momentum on either side of the disk is equal and opposite and no motion will result. However, if the same disk be extended to finite thickness, comparable to the wavelength, then there will be positions along the wave train where the two faces of the disk, normal to the direction of propagation, are subjected to unequal changes in momenta and motion will ensue. The occurrence of such points is depicted by the aid of a half-inch sphere in successive locations on the axis of a plane stationary field. The arrows represent the component magnitudes of radiation pressures exerted. Those on the left with two barbs, for the incident wave; and, on the right the single barbs show the reflected wave. The resultant effect of the two is plotted in the lower portion of the drawing.

Following this graphical analysis it becomes apparent how the periodicity of the pendulum deflections is twice that of the standing wave system. The same conclusion might be drawn from considerations of the energy density in a stationary wave. For, let an incident plane wave, of sine-law distribution and energy density E, be reflected at the end of a tube to form a standing wave system. Upon plotting the energy density of the stationary wave against distance along the axis of the tube, it will be found that:

(1) The energy density in the stationary wave fluctuates between zero and $4E$.

(2) The fluctuations have double the periodicity of the stationary wave.

Tones Produced by a Wire Placed in an Ignited Gas Jet

J. J. Coop
Indiana University, Bloomington, Indiana
(Received August 16, 1937)

It was found that a wire placed in an ignited gas jet would produce a tone when the velocity of the gas reached a critical value. The tone was amplified by use of a second wire and by use of a photoelectric cell. The relation between the diameter D of the wire, the diameter O of the orifice, the distance d of the wire from the orifice and the critical velocity U_i for the initiation of the tone was found to be of the form $OU_i=kd/D+C$, where k and C are constants. This equation is not linear for values of d less than one centimeter. It appears that a similar relation exists for the critical velocity U_f at which "flaring" starts. The products OU_i/ν, where ν is the kinematic viscosity, were found to be nearly the same for the two gases used. At any distance of a wire from the orifice the frequency of the tone was found to be a linear function of the efflux velocity of the gas. The expression for the frequency was found to be of the form $N=k/D(U-U_0)$, where k is a constant and U_0 is the velocity intercept. The quantity $D(dN/dU)$ has an average value of about 0.047 for wire diameters between 0.04 and 0.1 cm. For a constant frequency the relation between the orifice velocity and the distance was found to be of the form $U=Kd^n$, where n is approximately $\frac{1}{2}$; $nO^{\frac{1}{2}}$ is a constant and $KO^{\frac{1}{2}}$ nearly constant. An approximate relation between frequency, velocity, and distance is given by $N=kU/d^{\frac{1}{2}}+C$, where k and C are constants. A thin metallic sheet placed against the wire on the downstream side prevents the production of the tone. As the distance between this sheet and the wire is varied the tone ceases at a critical distance, which is a function of the velocity and the diameter of the wire. For a fixed velocity this critical distance is proportional to the square root of the diameter of the wire. It was concluded that the tone is an Aeolian tone modified by the flow of one stream into a similar fluid at rest. An equation of the form $N=kU/D$ was derived on the basis of the Bernard-Karman vortex theory. By comparing experimental with theoretical results it was concluded that for an ignited jet the density varies inversely as the distance from the orifice.

WHILE studying the action of a sensitive flame the writer found that a wire placed in the gas flame would, under certain conditions, produce a musical note. A study of this phenomenon was made and the purpose of this paper is to describe the results of this investigation.

Theory

The tones produced by an obstacle placed in a fluid stream are commonly known as Aeolian tones. In the ordinary Aeolian tone phenomena the wire is moving with respect to a fluid of infinite extent. In the case here considered the wire is in a stream flowing into a similar fluid at rest.

In either case vortices are shed alternately from the sides of the obstacle and are carried down the stream in two rows. This procession of alternate vortices was first noted by Mallock[1] and studied independently by Bernard[2] in 1908. The stability of this vortex system has been investigated mathematically by Karman.[3]

In Fig. 1 let l be the distance between two consecutive vortices in the same row, and the separation of the two rows by h, and let a be the "stagger" of one row upon the other. Karman found that there were two conditions of equilibrium for the system, namely: $a=0$, and $a=l/2$. The system is unstable for the case $a=0$, while for the case $a=l/2$, maximum stability exists for $h/l=0.28$.

The application of the Karman theory to the case here considered is very similar to that for jet tones given by Kruger and Schmidtke.[4] The frequency of the tone is the number of vortices leaving one side of the wire in one second. This is given by $N=u/l$ where N is the frequency, u is the velocity of the vortices relative to the wire, and l is the distance between consecutive

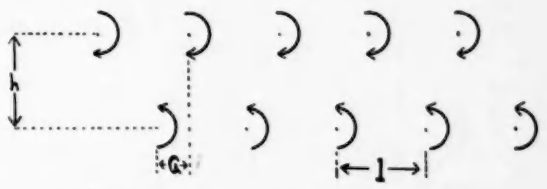

FIG. 1. Parallel rows of alternate vortices.

[1] Mallock, Proc. Roy. Soc. **9**, 262 (1907).
[2] Bernard, Comptes rendus **147**, 839, 970 (1908).
[3] Karman, Ann. d. Physik **44**, 801 (1914).
[4] Kruger and Schmidtke, Ann. d. Physik **60**, 701 (1919).

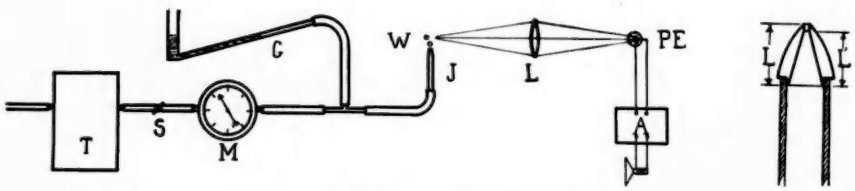

FIG. 2 (left) AND FIG 3 (right).

vortices in the same row. Now u must be proportional to the stream velocity U so that $u=aU$ where a is a constant. Also the distance between consecutive vortices must be proportional to the diameter of the wire so that $l=bD$ where D is the diameter of the wire and b is a constant. Then the frequency N is given by

$$N=u/l=aU/bD,$$

or
$$ND/U=a/b=a \text{ constant.} \qquad (1)$$

This relation was found by Strouhal,[5] who rotated a stretched wire about an axis parallel to its length. The tones observed were harmonics of the wire. In the case to be considered here the wire does not vibrate and the frequency of the tone is continuously variable.

DESCRIPTION OF APPARATUS AND METHOD

The platinum wires were supported at one end in a micrometer, which permitted distances of 0.0005 cm to be read. The efflux velocity of the gas was calculated from the relation $U=Q/At$ where Q is the volume of gas passing through the orifice in a time t, and A is the area of the cross section of the orifice. The volume of the gas was measured by a standard 0.1 cu. ft. meter made by the American Meter Company. In general the time was taken for a complete revolution of the index, although the dial was divided into 100 divisions and thus could be read to 0.001 cu. ft. The meter was calibrated by the aspirator bottle method, after which the water level was adjusted to compensate for the water removed by the gas. A diagram of the apparatus is shown in Fig. 2.

Between the gas meter and the gas main a 35 liter reservoir was used to reduce the pressure fluctuations. The pressure was varied by means of a regulating valve placed between the reservoir and meter. As these experiments were conducted in a constant temperature room the error in volume measurements, due to temperature variations, was very small, since the usual variation was less than 2°C.

While velocities were not calculated from pressure data it was found convenient at times to obtain the velocities from a pressure velocity curve previously determined by direct measurement. The jet consisted of a brass pipe 12.5 cm long, with an inside diameter of 0.66 cm, into one end of which could be placed removable nozzles. All nozzles except the one marked (g) (glass) were made of brass. The design of the nozzles is shown in Fig. 3. The length of the taper L' was 1.6 cm. The length of the channel, $L-L'$, was about 2 mm. The nozzle with diameter $O=0.907$ mm was made with a taper length of 0.3 cm and channel length of 1.1 cm.

The frequency of the note emitted by the wire was determined by obtaining zero beat with an audio oscillator. A General Radio oscillator type 377B was used. In practice it was found convenient to set the oscillator at a desired frequency and to vary the gas pressure on the jet to secure resonance.

METHOD OF AMPLIFYING TONE

It was found that the intensity of the tone emitted by the wire was greatly increased when a second wire was placed in the flame above the first, or sound initiating wire. Best results were obtained when the second wire was placed parallel to the first wire at a distance of about 2 cm downstream and about halfway between the center of the burning jet and the visible boundary. By projecting the light from this wire, which was a bright red, onto a photoelectric cell further amplification was possible. An audio amplifier with a voltage amplification of 50,000 was used in connection with the photoelectric cell.

[5] Strouhal, Ann. d. Physik **5**, 216 (1878).

A cathode-ray oscilloscope connected to the photoelectric cell through the amplifier showed that the oscillation was a sine wave and that the position of the second wire did not affect the frequency except to introduce, or to amplify, the first overtone when placed very close to the first, or sound initiating wire.

When the light from the flame was projected onto the photoelectric cell little effect was produced if the wire was less than about 1 cm from the orifice, while for greater distances a large output was obtained from the cell. When projecting the light of the flame the second wire was removed from the flame.

Action of Wire in Flame

If a wire whose diameter is nearly that of the orifice is moved slowly across an ignited jet, having the proper efflux velocity, a critical point will be reached near the center of the jet at which a musical tone will be heard. The space in which the tone continues is of the order of one-tenth of the visible diameter of the flame and varies with the distance from the orifice and the orifice velocity of the gas. The frequency of the tone varies as the wire is moved across the jet, an effect which produces the largest source of error in this study.

Since the width of this critical region decreases with the velocity the method used was to move the wire backwards and forwards across the center of the jet while reducing the velocity. The final setting was made for a clear tone near the center of the jet. When all measurements are carefully made the entire apparatus may be reassembled and a reading repeated with an average variation of about two percent. Occasional variations of four or five percent were observed.

Critical Velocities

If after placing the wire in position in the flame the velocity is slowly decreased, by decreasing the pressure, a point will be reached where the tone ceases. By increasing the velocity again the tone starts almost exactly at the same velocity at which it stopped. The tone continues at a velocity slightly less than that required to start it. In practice the average velocity at which slight fluctuations in gas pressure would cause the tone to start and stop was taken to be the velocity of initiation U_i.

As the velocity is increased beyond the value for initiation the frequency increases to a critical point at which one or more subharmonics start. These subharmonics are usually accompanied by a characteristic change in the shape of the flame. If the velocity is increased beyond this point the changes in shape and the number of subharmonics become increasingly rapid until finally the separate tones merge into the characteristic "flare." This critical velocity is called the flare velocity with wire and is designated by U_f. The results for the initiation and flare velocities are given in Table I and are shown in Fig. 4, where critical velocities are plotted against orifice diameter. In these tables D is the diameter of the wire, d is the distance of the wire from the orifice, and O is the diameter of the orifice. The data in Table I were obtained while using artificial gas. Table II shows the results of a similar experiment using natural gas from the supply at Lexington, Kentucky.

After the wire is removed from the flame a still further increase in velocity brings the jet into the condition in which it is sensitive to sound. A further increase in velocity causes the flame to break down into the familiar flaring or turbulent condition. The results for these critical velocities for sensitivity and flare are shown in Fig. 4. All data plotted in Fig. 4 were obtained using artificial gas.

While the curves shown in Fig. 4 are not exactly hyperbolae this is very nearly the true relation for the initiation of the tone, using artificial gas. If it is assumed that the kinematic viscosity ν is constant then OU/ν is constant, that is, this transition corresponds to a definite

Table I. *Initiation and flare velocity.*

$D = 0.0484$ cm $d = 0.05$ cm

O mm	U_i m/sec.	U_f m/sec.	OU_i cm²/sec.	OU_f cm²/sec.
1.779	7.15	18.14	127.0	323
1.689	7.53	19.42	126.8	330
1.420	8.80	23.50	125.0	332
1.169	10.47	27.60	122.2	325
0.907	13.90	34.45	126.2	317
0.797	16.21	38.40	129.0	307
Average			126.3	322

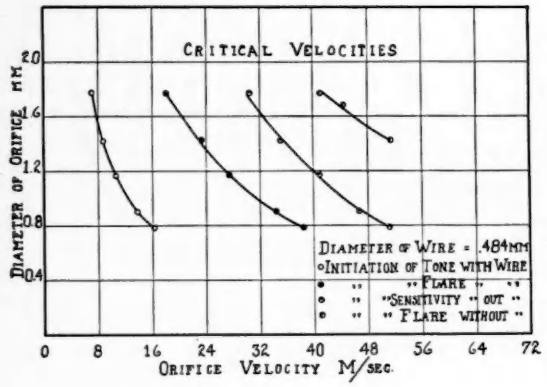

FIG. 4.

Reynold's number. Since the kinematic viscosity is a function of temperature it may be that each of these transitions correspond to a definite Reynold's number. If the kinematic coefficient of viscosity were known for each of the gases used, this relation could be tested. Since the composition of the artificial gas used does not remain constant the value of the kinematic coefficient as calculated from the average composition must be considered only an approximation. The calculated value is 0.23 at 24°C. The corresponding value of ν_m for methane, the main constituent of the natural gas used, was 0.167. For the same temperature the following relation is to be expected if the Reynold's number for a given transition is constant:

$$(OU)a/0.233=(OU)m/0.167.$$

From Tables I and II the products OU_i for artificial and natural gas are, respectively, 126.3 and 95.4. These values substituted into the above equation give 542 for artificial gas compared with 565 for natural gas.

INITIATION VELOCITY AS A FUNCTION OF ORIFICE DIAMETER AND DISTANCE OF WIRE FROM ORIFICE

An examination of Fig. 5 shows that there is a linear relation between the distance of the wire from the orifice and the initiation velocity. When the wire is at distances greater than about one centimeter the equation which gives the relation between d and U_i is

$$d=mU_i+K \qquad (2)$$

where $m=dd/dU$. Table III gives the values of m and the ratio O/m_i for different orifice diameters. The fact that the quantity O/m_i appears to be a constant is a very striking result.

Using the average value 0.550 for O/m_i the following equation is obtained,

$$O/m_i=O(dU/dd)=0.55. \qquad (3)$$

Eq. (3) becomes, on integrating,

$$OU_i=0.55d+OU_0. \qquad (4)$$

While further data are needed on this point it appears that the d intercepts of the lines in Fig. 5 are constant. Using the average value of -2.49 found in Table III Eq. (4) becomes,

$$OU_i=0.55d+1.37. \qquad (5)$$

By use of Eq. (5) the velocity of initiation may be calculated for any orifice diameter and for any distance of the wire from the orifice, when using a wire whose diameter is 1.01 mm. The equation, of course, is limited to the linear portion of the curves shown in Fig. 5, and to the assumption that the d intercepts are constant. A similar equation appears to hold for the flare velocity, in fact, the initiating and flare lines for a given orifice are almost parallel, as is indicated in Table III. A flare line is shown in Fig. 10. The determination of the flare velocity becomes increasingly difficult as the distance of the wire from the orifice is increased.

INITIATION VELOCITY AND DIAMETER OF WIRE AS A FUNCTION OF THE DISTANCE OF THE WIRE FROM THE ORIFICE

In Fig. 6 the initiation velocities for wires of different diameters were plotted as a function of the distance from the orifice. The results of a

TABLE II. *Initiation and flare velocity—natural gas.*

$D=0.084$ CM $d=0.05$ CM

O mm	U_i m/sec.	U_f m/sec.	OU_i cm²/sec.	$O^{\frac{1}{2}}U_i$	OU_f
1.779	6.20	9.44	111	82	168
1.420	7.30	12.88	103	89.5	183
1.169	7.60	14.70	89	82.2	171.5
0.797	9.80	20.90	78.6	88	166
Average			95.4	85.4	172.1

study of these curves are given in Table IV. In this table m_w is dd/dU, or the slope of the line. The intercepts on the velocity axis appear to be a constant for a given orifice, although the linear relation is not valid near the orifice. The shape of the curves near the orifice is shown more clearly in Fig. 5. The convergence of these initiating lines on the velocity axis indicates that near the orifice the velocity for the initiation of the tone is independent of the diameter of the wire. A further study of these critical velocities was made by placing the wires at a distance of 0.05 cm from the orifice. For this distance both the velocity of initiation and the flare velocity are nearly independent of the wire diameter. The initiating velocity tends to increase for wires smaller than about 0.4 mm.

In addition to the common intercept indicated in Table IV another striking result is that the ratio D/m_w is very nearly constant for a given orifice. These relations may be expressed by the equation,

$$D/m_w = D(dU/dd) = \text{a constant},$$

or
$$DU_i = kd + c. \tag{6}$$

For the particular orifice, $O = 1.169$ mm. Eq. (6) becomes

$$U_i = 0.415d/D + 12.6. \tag{7}$$

The essential difference between Eqs. (4) and (6) is, that for different orifices the common intercept is on the d axis while for different wire diameters the common intercept is on the U or velocity axis.

Combined Effect of Diameter of Orifice and Diameter of Wire on the Initiation Velocity

The two equations, (5) and (7), may be combined into a single equation. Since the diameter

Table III. *Initiation and flare velocities vs. orifice diameters; D = 1.01 mm.*

O cm	m_i	d_0 (intercept)	O/m_i	m_f (flare line)
0.1779	0.313	−2.23	0.568	0.29
.1420	.275	−2.68	.516	.26
.1169	.210	−2.57	.557	.18?
.0907	.163		.558	
Average		−2.49	.550	

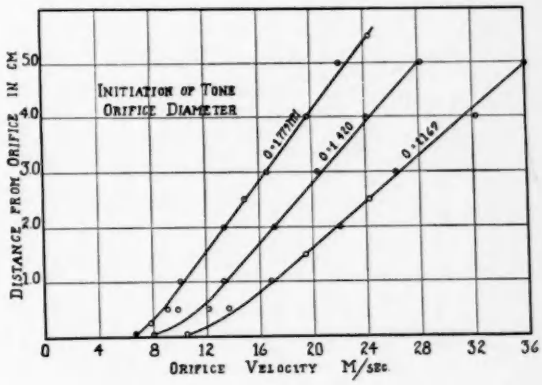

Fig. 5.

of the wire used in obtaining Eq. (5) had the value $D = 0.101$ cm it follows that for any orifice diameter O_1 the constant k in Eq. (6) is given by the relation

$$(D/m_w)_{O_1} = 0.101/m_{i_1}. \tag{8}$$

For example if the ratio D/m_w is desired for an orifice whose diameter is 0.097 cm the value of m_i for this orifice taken from Table III gives the ratio 0.101/0.163 or $D/m_w = 0.620$, which is in good agreement with the average value of 0.602 given in Table IV.

By substituting the corresponding value of m_i from Eq. (3) into Eq. (8) the following equation results

$$OD/m_w = OD(dU/dd) = 0.055. \tag{9}$$

Eq. (9) becomes, after integrating,

$$ODU_i = 0.055d + C. \tag{10}$$

In evaluating C in the above equation it is to be observed that when $d = 0$ then $OU_i = OU_0 =$ a constant, independent of D the diameter of the wire, with the exceptions mentioned. The average value of OU_0 was found to be 1.41, where U is measured in m/sec. and O in cm. (The value of the intercepts for the orifice whose diameter is 0.0907 cm was not included in this average due to its construction.) With the substitution of the value of C, which is $C = 1.41D$, Eq. (10) becomes

$$OU_i = 0.055d/D + 1.41. \tag{11}$$

This equation is surprisingly simple in view of the fact that the actual velocity and viscosity are both unknown functions of the distance d. There is some reason to expect that the con-

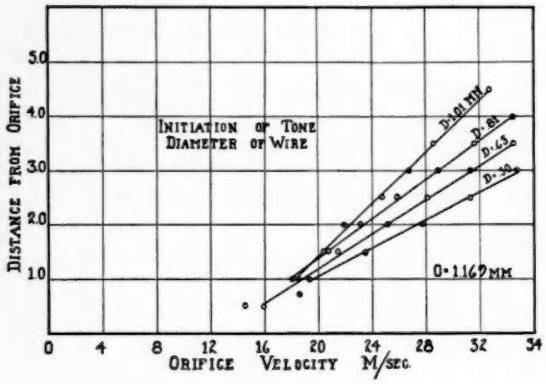

FIG. 6.

stants in the above equation would depend on the construction of the jet as well as they would depend on the nature of the gas.

FREQUENCY OF THE TONE

The frequency of the tone depends on the velocity of the gas, the diameter of the orifice, the diameter of the wire, and the distance of the wire from the orifice. It has been found that whatever the distance of the wire from the orifice, the frequency is a linear function of the orifice velocity of the gas. This feature is clearly shown in Fig. 7, where the frequency is plotted as ordinates against the orifice velocity, in meters per second, as abscissae. It is observed that the slope decreases with the orifice distance of the wire so that the equation of these lines is of the form

$$N=f(d)U-g(d), \qquad (12)$$

where $f(d)$ represents the variation of the slope with distance and $g(d)$ stands for the variation of the velocity intercept with distance. The direct determinations of these functions is made difficult by the variation of the slope depending on the position of the wire with respect to the center of the jet.

An examination of these curves shows that lower frequencies are observed at greater distances from the orifice. While the entire range of frequencies between the initiation of the tone and the beginning of flaring is not shown in Fig. 7 it is a general rule that the frequency range for any distance of the wire from the orifice is about two octaves. The most noticeable feature of Fig. 8 is the abrupt change in slope, which appears at about the same frequency at the various distances. A study of these slopes is given in Table V.

For $O=1.169$ mm and $D=1.01$ mm an average of four values of m'/m gave 1.70. For $O=1.420$ and $D=1.01$ mm the average of five such ratios of m'/m was 1.45. While no definite conclusions can be drawn, it appears that when a change in the slope occurs the ratio m'/m is approximately constant. The cause of these breaks is unknown and their appearance is quite erratic. It was noted that when breaks occurred in a family of curves like those shown in Fig. 7 they appeared in consecutive curves.

FREQUENCY OF TONE AS A FUNCTION OF VELOCITY AND DIAMETER OF WIRE

When the wire is placed very near the orifice it may be assumed that the velocity of the gas passing the wire is equal to the efflux velocity. The frequency velocity curves for wires of different diameters placed at a distance of 0.05 cm from the orifice are shown in Fig. 9. These curves resemble those obtained by Strouhal[6] for Aeolian tones from wire of different diameter, and they are almost identical with the curves obtained by Kohlrausch[7] for jet tones from circular orifices. The results of a study of these and similar curves are given in Table VI. In this table the slope (dN/dU) is measured in vibrations per cm/sec.

A comparison of the values of dN/dU for $D=0.101$ cm suggests that the value 0.736 in column II of Table VI is in erorr and the product $D(dN/dUO)=0.074$ was not included in the average. Data from wires smaller than 0.04 cm are not included in the averages given in Table

TABLE IV. *Initiation velocity and diameter of wire.*

	$O=1.169$ MM			$O=0.097$ MM		
D cm	m_w	D/m_w	U (intercept)	m_w	D/m_w	U (intercept)
0.101	0.240	0.420	13.9	0.159	0.636	22.5
.081	.182	.445	12.3	.143	.568	23.3
.063	.158	.400	12.3	.104	.602	22.9
.050	.128	.395	12.1			
Average		.415	12.6		.602	22.9

[6] Strouhal, Ann. d. Physik **5**, 216 (1878).
[7] Kohlrausch, Ann. d. Physik **13**, 545 (1881).

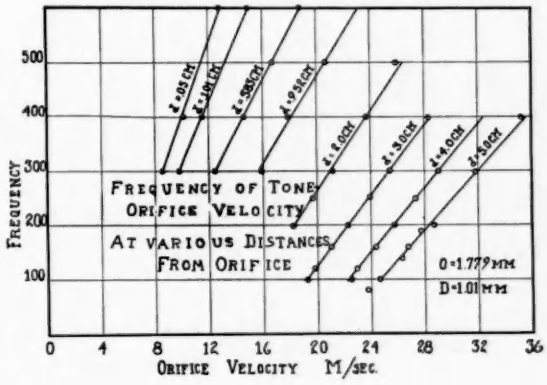

FIG. 7.

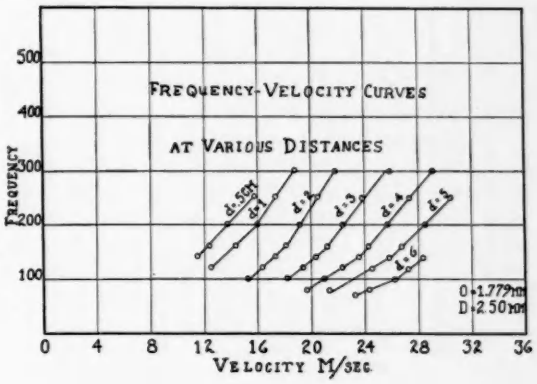

FIG. 8.

VI. Kohlrausch[7] measured the frequency of the tone produced by a jet of air streaming into air and found the products $O(dN/dU)$ to lie between 0.04 and 0.06. Also, he found that these products decreased with the diameter of the orifice, the values being almost identical with those given for wires of the same diameter, as given in Table VI.

These results tend to show that for the same efflux velocity the frequency of a tone from a wire of diameter D is almost the same as that for a jet of the same diameter. It must be noted, however, that no tones were observed without placing some obstacle in the stream. Even when the light from a burning jet was focused onto a photoelectric cell using an amplification of 50,000 no tone was heard.

The equation for these lines is the same as that given by Kohlrausch for jet tones,

$$N=k/D(U-U_0), \tag{13}$$

where O is replaced by D. In this case U_0, the velocity intercept, is nearly a constant for the lines in Fig. 9. However, other data tends to show that U_0 becomes larger for very small wires. The approximate equation for the lines shown in Fig. 9 is

$$N=(0.048/D)U-660, \tag{14}$$

where U is measured in cm/sec. and D is measured in cm.

While not enough data were taken to show the general relation of the quantity $D(dN/dU)$ to the diameter of the orifice, it was found that for $D=0.0484$ cm at a distance $d=0.05$ cm the same velocities produced corresponding frequencies for the four jets whose diameters were 0.797, 0.907, 1.009, and 1.169 mm. The common frequency range for these jets was 1000–2000. For larger wires other data tended to show that the quantity $D(dN/dU)$ is slightly greater for smaller orifice diameters. A difficulty encountered in making this comparison is that a given wire diameter gives consistent results for only a very small range of orifice diameters.

Approximate Relation Between Frequency, Velocity, and Distance

A simple method for studying the relation of frequency to the distance of the wire from the orifice is to move the wire up or down in the jet and to determine the frequency at various distances while keeping the orifice velocity constant. The difficulty here is that the new setting required for each reading introduces new errors of position with respect to the center of the stream. While no simple relation was found, a rough approximation is $Nd=$a constant.

In an attempt to overcome the difficulties mentioned above, a frequency velocity curve was

TABLE V. *Slopes of frequency velocity curves from Fig. 8.*

$O=1.779$ MM		$D=2.50$ MM	
d cm	m' (upper slope)	m (lower slope)	m'/m
1.0	35.7	24.2	1.47
2.0	37.0	22.2	1.66
3.0	31.2	19.2	1.62
4.0	29.9	15.6	1.91
5.0	24.3	15.4	1.58
6.0	19.0	10.3	1.84
Average			1.68

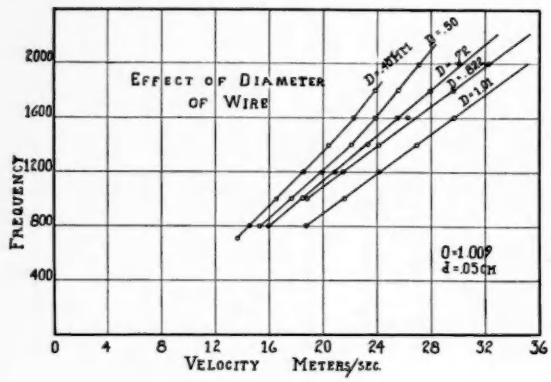

Fig. 9.

determined at various distances from the orifice, as shown in Fig. 7. From these curves distance velocity curves at constant frequencies were constructed for four orifice diameters. For each orifice it is obvious that all possible constant frequency curves must be bounded by the initiation and flare lines for that orifice, as shown in Fig. 10.

In studying these curves log U was plotted against log d, as shown in Fig. 11. For values of d greater than about 1 cm the resulting curves are linear. In this region the relation between velocity and distance for a constant frequency may be expressed by

$$U_N = Kd^n, \tag{15}$$

where U_N is the orifice velocity required to give a frequency N at a distance d. In this same manner four equations for four different orifice diameters were determined. Values of n varied from 0.395 to 0.629. In most cases the value was not far from 0.5. It was found that when different orifice diameters produced the same frequency the constants in Eq. (15) were related to the orifice diameter O by $nO^{\frac{1}{2}}$=a constant and by $KO^{\frac{1}{2}}$=a constant. By substituting for K its value in terms of N an approximate relation was found to be of the form

$$N = U/(Bd^{\frac{1}{2}}) + (100 - A/B), \tag{16}$$

where A and B are constants for a given orifice diameter. The slopes of the lines similar to those shown in Fig. 7, should then be given by $dN/dU = 1/Bd^{\frac{1}{2}}$. While this equation shows the general nature of the change of slope with distance, the actual decrease of the slope with distance is less than that predicted by this formula.

Nature of Tone

The variation of the frequency of the tone as a function of the distance, at constant orifice velocity, is somewhat similar to the relation which exists in the case of edge tones. In the edge tone phenomena there is no interaction between the vortices after they strike the edge. If the wire acted as an edge in the jet, then a thin sheet or wedge placed behind it so as to form a continuous wedge with the wire as the apex, should not prevent the production of a tone.

To test this condition a metal sheet 0.025 cm thick and 1.9 cm wide was placed behind the wire. It was found that when the sheet was slowly moved toward the wire or away from it in the direction of the stream the tone ceased and started again at a definite distance from the wire. This critical distance varies with the velocity and the diameter of the wire and perhaps with the diameter of the orifice, though this relation was not examined. A graph of the relation between the distance for the cessation of the tone and the efflux velocity for a given wire and orifice diameter is shown in Fig. 12. The equation of this particular curve is given by

$$z = 19/U^{1.1}, \tag{17}$$

where z, the edge distance, is measured in millimeters and U is measured in meters per second.

At a constant velocity this critical distance varies with the diameter of the wire. The values of z for various wire diameters at a constant velocity of 22 meters per second are given in

Table VI. *Diameter of wires and slopes of N-U curves.*

O=1.009 mm (g)	d=0.05 cm		O=1.169 mm		O=1.169 mm	d=0.247 cm	
D cm	dN/dU	$D(dN/dU)$	dN/dU	$D(dN/dU)$	D	dN/dU	$D(dN/dU)$
0.101	*0.736*	*0.074*	0.538	0.054	0.1010	0.542	0.055
.082	.734	.060	.558	.046	.0814	.604	.049
.072	.841	.046			.0635	.755	.048
.050	.897	.045	.823	.041	.0509	.838	.043
.048	1.010	.049					
040	1.025	.041	.973	.039	.0407	1.050	.043
.032			1.22	.038	.0330	1.057	.033
.025					.0254	1.305	.033
Average		.048		.045			.047

Table VII. If the sheet is placed in contact with the wire and then moved in a horizontal plane the tone starts again at a definite distance X from the center of the wire. These values are given in Table VII.

An examination of Table VII shows that for wire diameters larger than 0.40 mm the relation between z and D may be expressed by

$$D^{\frac{1}{2}}/z = \text{a constant.} \qquad (18)$$

Under the conditions given in Table VII the value of this constant is 1.73, hence Eq. (18) may be written as $z=0.576D^{\frac{1}{2}}$. The ratio X/D increases as D decreases. The abrupt increase in the value of z as the diameter of the wire approaches the thickness of the sheet is very apparent.

These results tend to show that the tone is produced by an oscillation in the stream immediately behind the wire, as is the case in the Aeolian tone phenomenon. In general, the investigators studying Aeolian tones in gases have had to depend on the tone produced by the wire, which was in resonance with the shedding of the vortices. In these experiments the wire does not vibrate and the tones studied were observed only when the gas was burning.

When the wire was heated to a bright red glow by an electric current a very faint tone could be heard. It is believed that the oscillations are present in the unignited gas and that the tone in an ignited gas is due to the miniature explosions produced by the formation of vortices behind the wire. The formation of an eddy behind an obstacle in the flame would certainly bring about a mixture more suitable for combustion. It appears that the action of the amplifying wire is due partly to increased mixing of the gas as an eddy strikes it and partly due to the change in temperature of the wire produced by this agitation.

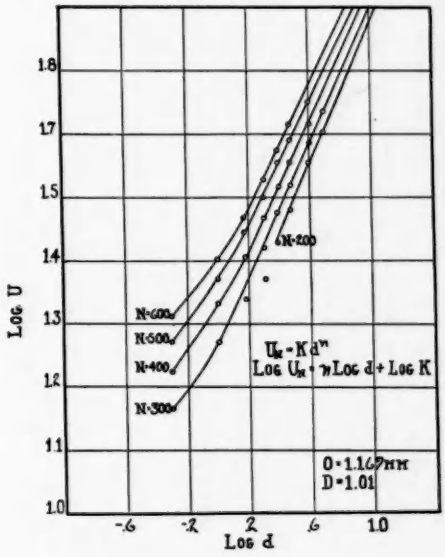

FIG. 11.

The action of the amplifying wire suggests that the tone produced by the first, or sound initiating, wire may be due to its amplifying action on the vortices emitted by the orifice. However, in moving the amplifying wire in the stream there is no change of frequency with the distance from the source, while there is a change of frequency if the distance of the first wire from the orifice is changed.

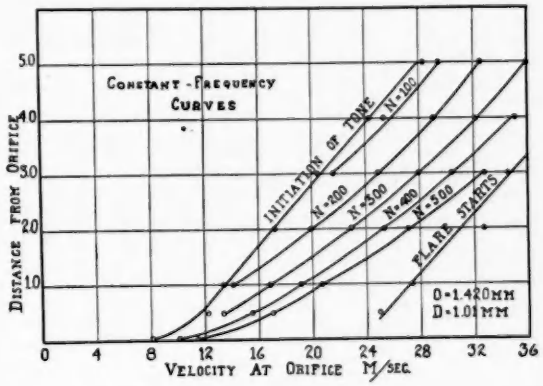

FIG. 10.

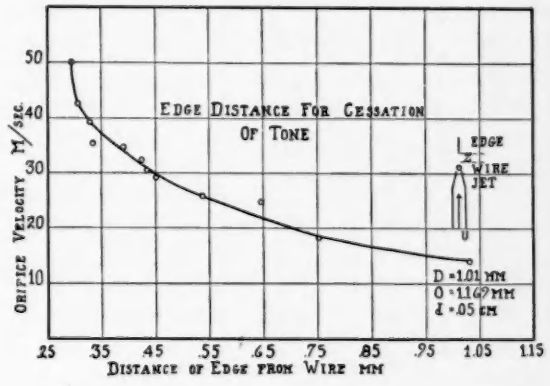

FIG. 12.

Discussion of Results

Several points could be cleared up if the actual velocity of the gas passing a wire at a distance d from the orifice could be determined accurately. If it be assumed that the frequency for a given wire and orifice depends only on the velocity of the gas as it passes the wire, then the factor d^n in Eq. (15) should give the rate of decrease of actual velocity with distance. It may be of value to consider the nature of flow in a jet.

For the small pressures used it may be assumed that the total pressure of the gas remains constant. It follows that the decrease in velocity is due to frictional stresses alone. While fresh masses of air will be dragged into the jet the momentum I of the stream must be constant, or

$$I = \int\int dr U^2 dA = \text{a constant}, \tag{19}$$

where r is the density of the gas and A is the area of the cross section of the stream. From this relation

$$r_1 U_1^2 A_1 = r_2 U_2^2 A_2. \tag{20}$$

Observation shows that a jet is conical in shape, so that

$$A_1/A_2 = d_1^2/d_2^2. \tag{21}$$

With this substitution Eq. (20) becomes

$$U_2/U_1 = (d_1/d_2)(r_1/r_2)^{\frac{1}{2}}. \tag{22}$$

Table VII. *Variation of edge distance with wire diameter.*

O = 1.169 mm		U = 22.0 m/sec.		d = 0.05 cm	
D mm	z mm	$D^{\frac{1}{2}}$	$D^{\frac{1}{2}}/z$	X mm	X/D
1.01	0.576	1.004	1.74	1.03	1.020
.826	.559	.908	1.63	.872	1.055
.76	.510	.872	1.71		
.50	.397	.707	1.78	.595	1.190
.40	.340	.632	1.80	.495	1.235
.32	.750	.566	0.75	.530	1.655
.25	.760	.500	0.66	.580	2.320

For an unignited jet $r_1 = r_2$ and the velocity decreases inversely as the first power of the distance, or Eq. (22) may be written,

$$U' = k/d. \tag{23}$$

Taking the approximate value of n in Eq. (15) to be $\frac{1}{2}$ then Eq. (16) indicates that for an ignited jet the rate of decrease of velocity with distance may be expressed by

$$U' = k/d^{\frac{1}{2}}, \tag{24}$$

a result which is obtained from Eq. (22) if the density of an ignited jet varies inversely as the distance. It was noticed that the temperature of the wire, as judged from its color, appeared to increase with the distance from the orifice in the region studied.

It is generally considered that viscosity has a very small effect on the frequency of an Aeolian tone, but that the initiation of the tone is very definitely a function of viscosity. An examination of Fig. 10 shows that the increase of the orifice velocity with distance is less for the initiation of the tone than for the maintenance of a given frequency. For the initiation of vortices behind a cylinder Richardson[8] gives an average value of the quantity UD/ν the number 30. This is to be compared with the values 542 and 565 found for artificial gas and natural gas, respectively. Unless this can be accounted for on the basis of increased viscosity due to the increase in temperature then it must be concluded that higher velocities are required for the initiation of a tone with a jet than for the ordinary Aeolian tone.

In conclusion, the author wishes to thank Dr. A. L. Foley, the director of this research, for his helpful comments and suggestions during the progress of this work. The author wishes also to thank Professor W. S. Webb, of the department of physics at the University of Kentucky, for the use of apparatus and facilities required for making measurements with natural gas.

[8] F. G. Richardson, *Sound*, p. 153.

Sound Absorption and Attenuation by the Flue Method

HAWLEY O. TAYLOR AND CHALMERS W. SHERWIN
Wheaton College, Wheaton, Illinois
(Received January 21, 1938)

THE method of measuring the absorption of sound as herein outlined is the same as that developed in a former paper[1] in which the sound flue was used. The term "flue" was originally proposed in order to suggest a pipe of rather larger cross-sectional area than is usual in the case of tubes for the study of sound interference. Several writers of previous papers had noted the effect of absorption on the interference pattern in tubes, but as absorption was not of primary interest the coefficient was not developed. In the work of Eckhardt and Chrisler,[2] the effect of attenuation in the flue is taken into account as a damping factor in the wave equations, but as "exact solutions of the equations do not seem practicable" the attenuation was not evaluated. An approximate solution however "appears to be adequate," from which the following expression for the coefficient of absorption, α, is developed:

$$\alpha=1-\left[\frac{m^{\frac{1}{2}}-n_1^{\frac{1}{2}}+(n_2^{\frac{1}{2}}-n_1^{\frac{1}{2}})/2}{m^{\frac{1}{2}}+n_1^{\frac{1}{2}}-(n_2^{\frac{1}{2}}-n_1^{\frac{1}{2}})/2}\right]^2, \qquad (1)$$

where m is the intensity of the first maximum of the interference pattern in the sound flue (measuring from the material closing the end), and n_1 and n_2 are the intensities of the first two minima of this pattern. When attenuation is practically absent, this expression reduces to the simpler form developed in the former paper[1] to which reference has been made:

$$\alpha=1-\left[\frac{m^{\frac{1}{2}}-n^{\frac{1}{2}}}{m^{\frac{1}{2}}+n^{\frac{1}{2}}}\right]^2=\frac{4}{(m/n)^{\frac{1}{2}}+(n/m)^{\frac{1}{2}}+2}. \qquad (2)$$

The purpose of the present paper is to show how the sound flue may be used to determine the fraction of sound attenuated in a unit distance along the axis of the flue by the material lining its sides, and to translate the change produced in sound intensity given by this coefficient into decibels per square foot of the material when so placed in the flue.

The Sound Flue

The research utilized several sound flues, three of which had square cross sections with inside measurements of 5, 8 and 11 inches on a side and about 6 feet long. Closing one end of each flue was a cover clamped to a flange at the end. Sound absorbing material was attached to the inside of this cover and also as lining to the side walls of the flue. Hair felt, 1 inch thick, and Acousti-Celotex C1, C3 and CB were used for these linings. The source of sound at the open end of the flue was usually a telephone receiver connected to an audio-oscillator. A Magnavox connected to the oscillator was sometimes used for the frequency of 256~ because of the pure tone produced. The tone used must be practically free from harmonics for dependable results, also all cracks in the flue and end cover must be stopped with some such material as wax.

The explorer for measuring the intensity of sound along the axis of the flue was a brass tube $\frac{1}{4}$ inch in diameter and about 8 feet long, open at one end and connected to the cap of a telephone receiver at the other end. The intensity of the sound at the open end of the tube excited the telephone receiver, and the voltage generated in the receiver was measured with an amplifier and a suitable rectifier and ammeter. The exploring equipment was calibrated by comparison with a Rayleigh disk over the range of intensities encountered in the flue measurements.

Complete Attenuation in the Sound Flue

If the flue is small in cross section and lined with material of high absorbing power, the standing wave interference pattern may be inappreciable, leaving only diminishing intensities as indicated by the explorer when it was advanced from the open end of the flue inward.

[1] H. O. Taylor, "A Direct Method of Finding the Value of Materials as Sound Absorbers," Phys. Rev. **2**, 11 (1913).
[2] E. A. Eckhardt and V. L. Chrisler, "Transmission and Absorption of Sound by Some Building Materials," Sci. Papers of National Bureau of Standards, No. 526, April, 1926.

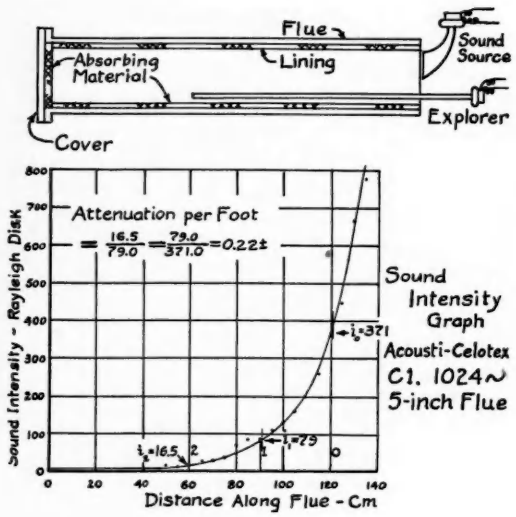

FIG. 1.

In this case there was practically no sound wave reflected from the material at the closed end of the flue—the sound energy was practically consumed before it reached this end.

A case of this type is shown in Fig. 1 which was obtained at a frequency of 1024~ for a 5-inch flue lined with ½-inch C1 Celotex. This curve shows practically the same fractional reduction in intensity, or in other words, a uniform attenuation per unit length throughout the length of the flue, amounting to 0.22 or about 6½ decibels per foot.

EFFECT OF ATTENUATION ON STANDING WAVES

If the sound energy is not too highly thinned out before the waves reach the closed end of the flue, then a standing wave pattern results, the regions of maximum or minimum intensity being one-half wave-length apart. Suppose that a sound wave p proceeds down the flue in the direction of the arrow (Fig. 2). Let its intensity at position 0 be i. (By intensity may be understood the rate at which sound energy would flow away if opportunity were given, as through the exploring tube.) Then at positions 1, 2 and 3 (the reflecting surface), its intensity will be $b_1 i$, $b_1^2 i$ and $b_1^3 i$, respectively, where b_1 is the attenuation constant for a distance along the flue equal to a quarter wave-length. At the reflecting material closing the end of the flue, the effective surface of which seems to be embedded beneath the actual surface, sound energy will be absorbed, the fraction left being given by ρ. The reflected wave r will return through the flue, its intensities at positions 3, 2, 1 and 0 being $b_1^3 i\rho$, $b_1^4 i\rho$, $b_1^5 i\rho$ and $b_1^6 i\rho$, respectively. The progressive and reflected waves combining will produce maximum and minimum regions of sound intensities, as shown in Fig. 2, the first and second minima from the reflecting surface having intensities of (say) n_1 and n_2, respectively, and the intervening maximum having an intensity of m. The distance along the flue from n_1 to m (that is, from 2 to 1) is a quarter wave-length $\lambda/4$, as is also the distance between each of the neighboring positions marked. Since intensity measurements made at these positions are used to determine the attenuation of the material lining the flue, it will be convenient to use a quarter-wave-length as the unit distance for computing the attenuation constant.

From the theory of sound waves interfering in the flue,[1] the maximum intensity m is proportional to the square of the sum of the amplitudes of the progressive and reflected waves; and the minimum intensity n is proportional to the square of their difference. Then taking the intensity of sound as proportional to the square of the amplitude of the waves:

$$\left[\frac{m}{n_2}\right]^{\frac{1}{2}} = \frac{(b_1 i)^{\frac{1}{2}} + (b_1^5 i\rho)^{\frac{1}{2}}}{(i)^{\frac{1}{2}} - (b_1^6 i\rho)^{\frac{1}{2}}} = \frac{(b_1)^{\frac{1}{2}} + (b_1^5\rho)^{\frac{1}{2}}}{1 - (b_1^6\rho)^{\frac{1}{2}}} = C \qquad (3)$$

and

$$\left[\frac{m}{n_1}\right]^{\frac{1}{2}} = \frac{(b_1 i)^{\frac{1}{2}} + (b_1^5 i\rho)^{\frac{1}{2}}}{(b_1^2 i)^{\frac{1}{2}} - (b_1^4 i\rho)^{\frac{1}{2}}} = \frac{1 + (b_1^4\rho)^{\frac{1}{2}}}{(b_1)^{\frac{1}{2}} - (b_1^3\rho)^{\frac{1}{2}}} = D. \qquad (4)$$

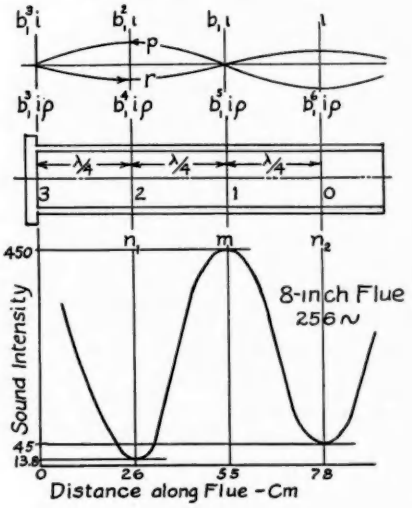

FIG. 2.

By eliminating $\rho^{\frac{1}{2}}$ and the factor (b_1^2+1) from Eqs. (3) and (4), the following quadratic equation in $(b_1)^{\frac{1}{2}}$ results:

$$b_1CD+(b_1)^{\frac{1}{2}}(D-C)-CD=0,$$

from which

$$b_1=\left[\frac{(C-D)\pm((C-D)^2+4C^2D^2)^{\frac{1}{2}}}{2CD}\right]^2$$

$$=\left[\frac{n_1^{\frac{1}{2}}-n_2^{\frac{1}{2}}}{2m^{\frac{1}{2}}}\pm\left(\left(\frac{n_1^{\frac{1}{2}}-n_2^{\frac{1}{2}}}{2m^{\frac{1}{2}}}\right)^2+1\right)^{\frac{1}{2}}\right]^2. \quad (5)$$

The data of Fig. 2 were taken from the 8 inch flue lined with Acousti-Celotex C3, $\frac{7}{8}$ inch thick, and the end of the flue was closed with the same material. Sound of frequency 256~ was used. The intensities were: $n_1=13.8$ at 26 centimeters from the closed end; $m=450$ at 55 cm; and $n_2=45$ at 78 cm. The half-wave-length is seen to be 78–26 or 52 cm, that is, 104 cm for the wave-length. In the open air, the wave-length for this frequency would be about 133 cm. This shortening of wave-length for sound in flues lined with absorbing material has already been noted.[1] By substituting values of n_1, n_2 and m in (5) we find 0.869 for the value of b_1, the fractional reduction of sound energy per quarter-wave-length.

Coefficient of Sound Absorption

The coefficient of sound absorption, α, is equal to $1-\rho$. Using the expressions for ρ obtained from Eqs. (3) and (4), we get from (3):

$$\alpha=1-\rho=1-\left[\frac{C-(b_1)^{\frac{1}{2}}}{((b_1)^{\frac{1}{2}})^5((b_1)^{\frac{1}{2}}\cdot C+1)}\right]^2 \quad (6)$$

and from (7):

$$\alpha=1-\rho=1-\left[\frac{D(b_1)^{\frac{1}{2}}-1}{((b_1)^{\frac{1}{2}})^3((b_1)^{\frac{1}{2}}+D)}\right]^2. \quad (7)$$

If there is practically no attenuation of sound in the flue, then $b_1=1$, and $C=D=(m/n)^{\frac{1}{2}}$. These values placed in Eqs. (6) and (7) reduce them to formula (2). On the same assumption, n_1 and n_2 of Eq. (1) will become equal, and the expression for α will also reduce to formula (2).

Substituting the values indicated on Fig. 2, we get $\alpha=0.356$ from (6), 0.354 from (7) and 0.348 from (1). These values are all in good agreement. On the other hand, formula (2), in which the attenuation is neglected, yields a value equal to 0.634. This is about 80 percent too large.

Sound Attenuation per Square Foot

The attenuation constant b for a square foot of lining material in position in the flue would be determined for one foot along the flue if the perimeter of the flue measured just one foot on the inside. For perimeters less than one foot, b must be found for a greater distance along the flue, and for greater perimeters a correspondingly less distance. If f is the inside width of one side of the flue, then a distance along the flue of $1/(4f)$ would be required to make one square foot of flue lining, where f is measured in feet. The attenuation coefficient B for this length along the flue would be

$$B=b^{1/(4f)}. \quad (8)$$

The relation between b and b_1 is

$$b=b_1^{4/\lambda},$$

since a quarter-wave-length is contained in a length of one foot $4/\lambda$ times, where λ is expressed in feet. Then B in terms of b_1 is:

$$B=b_1^{1/(f\lambda)}. \quad (9)$$

Eq. (9) gives the attenuation coefficient per square foot of material in position in the flue in terms of the attenuation constant b_1 determined from measurements of maximum and minimum intensities (m, n_1 and n_2) of standing waves in the flue.

Attenuation in Decibels

The decibel is a unit of change in sound intensity. If the intensity changes, because of attenuation, from i_1 to i_2, then, expressed in decibels, db, this would be

$$\text{db}=-10\log(i_2/i_1). \quad (10)$$

If this change occurred when sound swept over one square foot of material, then Eqs. (9) and (10) may be combined to give it in decibels. That is,

$$\log B=(1/(f\lambda))\log b_1=\log(i_2/i_1),$$

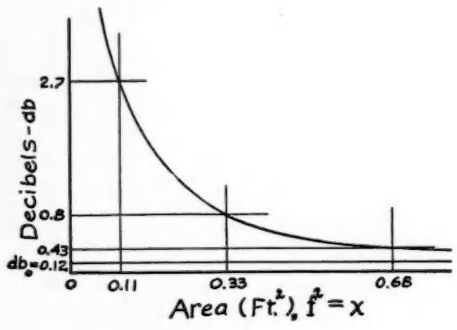

FIG. 3.

which, when multiplied by -10, gives the change in sound intensity in decibels:

$$(-10/(f\lambda))\log b_1 = -10\log(i_2/i_1) = \text{db per sq. ft.}$$

Using the data of Fig. 2, db for material C3 at 256~ would be

$$\text{db} = (-10/3.04)\log 0.869 = 0.203.$$

If the attenuation b is taken for one foot as the unit, then the expression for decibels per square foot would, from (8), be

$$\log B = (1/(4f))\log b;$$

from which $$\text{db} = (-10/(4f))\log b.$$

If decibels per square foot are plotted as ordinates against f^2 (the inside area of the square cross section of the flue) as abscissas, the resulting graph (Fig. 3) approximates a rectangular hyperbola. It is reasonable, as the graph indicates, that, as the area of the flue diminishes, the attenuation in decibels per square foot of flue lining would approach infinity; and, as the flue area approaches infinity, the attenuation would diminish to the constant, db_0. The equation of the curve is: $(\text{db}-\text{db}_0)f^2 = q$ (a constant). Plotting decibels as ordinates against the reciprocal of f^2 would give approximately a straight line. The equation of this line is

$$\text{db} = q(1/f^2) + \text{db}_0. \qquad (11)$$

Table I gives some average results from many observations made on Acousti-Celotex C1 and C3. λ is the wave-length of the sound in feet; f is the inside width of the square flue in feet; b_1 is the attenuation of sound per quarter-wave-length along the flue; and db is the attenuation of sound per square foot of flue lining.

Db and $1/f^2$ in the table were used for the graphs of Fig. 4. Knowing the slope and y-intercept for a material, its attenuation per square foot when used as a lining in a given size of flue may be calculated by means of Eq. (11). The given flue area in square feet is substituted for f^2, and the equation is solved for db, the required attenuation per square foot. The length of flue required to make a lining area of one square foot would be $1/(4f)$, where $4f$ is the inside perimeter of the flue. This is the length of flue that would produce the attenuation found.

Let us suppose that a flue of square cross section is lined with Acousti-Celotex C3. What flue area would be required to suppress 10 decibels per foot length of flue for a sound of frequency 512~?

To apply formula (11), decibels *per square foot* must be found and substituted in the formula for db. If the required area of the flue is f^2 square feet, then $4f$ is the length of its perimeter, and $1/(4f)$ is the length along the flue required to give the C3 lining an area of one square foot. Since the attenuation in decibels is proportional to the length of flue, then, if there are to be 10 decibels drop in sound intensity per foot, for a

TABLE I.

			11-INCH FLUE				8-INCH FLUE				5-INCH FLUE			
	~	λ	f	$1/f^2$	b_1	db	f	$1/f^2$	b_1	db	f	$1/f^2$	b_1	db
C1	256	3.94	0.825	1.47	0.86	0.201	0.575	3.03	0.77	0.501	0.325	9.47	0.81	0.715
C3			.760	1.73	.62	.692	.522	3.67	.73	.665	.272	13.5	.58	2.208
C1	512	1.97	.825	1.47	.85	.434	.575	3.03	.81	.808	.325	9.47	.67	2.713
C3			.760	1.73	.75	.835	.522	3.67	.59	2.223	.272	13.5	.46	6.30
C1	1024	.985	.825	1.47	.84	.932	.575	3.03	.85	1.246	.325	9.47	.68	5.23
C3			.760	1.73	.765	1.556	.522	3.67	.56	4.765				

length of $1/(4f)$ feet, the drop in decibels would be $10/(4f)$—which is the db of formula (11). From the graph (Fig. 4) for C3 512~, $db_0=0.6$ and $q=16/39$. Therefore formula (11) becomes: $10/(4f)=16/(39f^2)+0.6$, from which $f=0.171$ feet or about $2\frac{1}{2}$ inches. The quadratic equation gives also a second and larger value for f. This is true also when the formula is applied for the value of f using the data of Table I, a second value is obtained beside that given in the table, indicating two sizes of flue for the same attenuation per foot along the flue. Data on flues having these larger areas are not yet available so that the discussion of this paragraph is in the nature of a progress report.

The authors acknowledge with gratitude the valuable assistance of students who have participated in the experimental work and of others who have shown interest in the work, particularly Mr. Jacob Mazer who furnished the audiofrequency oscillator and Dr. B. E. Eisenhour who loaned the Magnavox and other equipment.

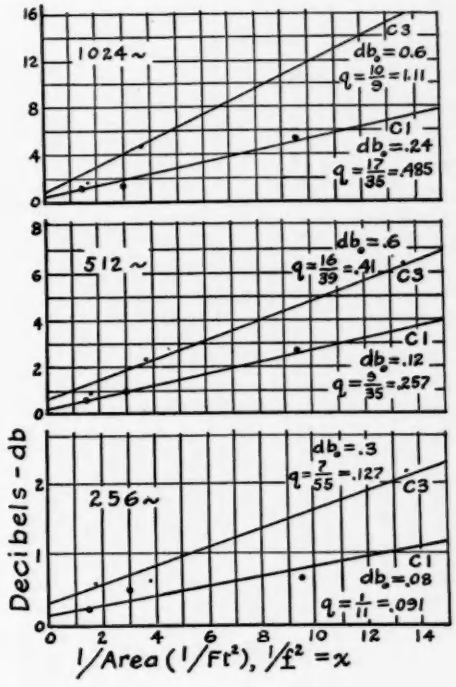

FIG. 4.

SYMBOLS USED

α, coefficient of absorption of sound reflected from a material.
B, attenuation constant per square foot of sound flue lining.
b, attenuation constant per foot along sound flue.
b_1, attenuation constant per quarter-wave-length along sound flue.
C, $(m/n_2)^{\frac{1}{4}}$.
D, $(m/n_1)^{\frac{1}{4}}$.
db, drop of sound intensity in decibels per square foot of flue lining.
db_0, drop of intensity in decibels per square foot of material lining a flue of very large cross-sectional area.
f, inside width of square section of sound flue.
i, i_1, i_2, intensity of sound under various conditions.
λ, length of sound wave.
m, maximum sound intensity of standing wave in the flue.
n, n_1, n_2, minimum sound intensity of standing wave in the flue.
p, amplitude of progressive sound wave in the flue.
π, number of radians in 180° (3.1416).
q, product of db drop per sq. ft. of flue lining and area of flue section.
r, amplitude of reflected sound wave in the flue.
ρ, coefficient of reflection of sound.
~, cycles or complete vibrations per second.

The M.K.S. System of Units Applied to Electroacoustics

A. E. KENNELLY AND JACKSON H. COOK
Harvard University and The Massachusetts Institute of Technology, Cambridge, Massachusetts
(Received August 20, 1937)

PURPOSE AND SCOPE

THE subject of electroacoustics deals with the transformation of electric energy to sound energy and *vice versa* by means of various electroacoustic transducers—microphones and loudspeakers. The quantitative investigation of such transfers requires a definite system of units for expressing the magnitudes involved. At present two sets of units are commonly employed; electric quantities are expressed in the international series of practical electric units, the *volt*, *ohm*, *ampere*, *joule*, etc.; while mechanic quantities are stated in the *centimeter*, *gram*, *second* (c.g.s.), system. These two sets of units are not homogeneous, one with the other, and their coincident use in electroacoustic work makes necessary the employment of unwieldy transformation coefficients. The *joule*, unit of energy in the practical series, is equivalent to 10^7 *ergs* of the c.g.s. system; the practical unit of power, the *watt*, is equal to 10^7 *ergs/second*, etc.

A great saving in labor on the part of electroacoustic workers would be effected if a system of mechanic units, homogeneous with the practical electric unit series, were employed. Such a system, the Giorgi *meter*, *kilogram*, *second* (m.k.s.) system of units, is available for use and its recent adoption by the I.E.C. (International Electrotechnical Commission) endows it with sufficient importance to warrant its immediate application.[1] It is the purpose of this paper to express commonly used acoustic quantities in the m.k.s. system, to note their magnitudes relative to the corresponding c.g.s. units, and to point out the advantages thereby obtained.

ACOUSTIC UNITS

The unit of length in the m.k.s. system is the *meter* (m) ($=10^2$ *cm*), the unit of mass is the *kilogram* (kg) ($=10^3$ *gm*). Time is measured in terms of the *mean solar second* (s) in both systems.

Sound wave-length is measured in *meters* (m) ($=10^2$ *cm*). The wave-length of a 1000 *c.p.s.* sound wave in air, at ordinary barometric pressure intensity and temperature, is 0.344 (m).

The velocity of propagation of a sound wave is stated in *meters/second* (m/s) ($=10^2$ *cm/s*). A free sound wave in air, under normal conditions, (20°C, 1 *standard atmosphere*) is propagated at a velocity, 344 (m/s). (This unit is almost universally used at the present time). Particle velocity is likewise expressed in (m/s).

Sound pressure (intensity) is measured in *newtons/square meter* (*newtons/m²*) ($=10$ *barye* or *dynes/cm²*) (*Newton* is the tentative name for the m.k.s. unit of force, one *joule/meter*, equals 10^5 *dynes*). The present c.g.s. reference pressure (0.2) *millibaryed*) is 2×10^{-5} *newton/m²* or 20 *micro-newtons/m²*. Normal barometric pressure is 1.0132×10^5 *newtons/m²* $=0.10132$ *mega-newton/m²*.

The unit of sound energy flow is the *watt* ($=10^7$ *ergs/s*). For an effective sound pressure, p (*newtons/m²*) in a plane or spherical free wave propagated with a velocity, c (m/s), in a gas of density, ρ (kg/m^3), the sound energy flow, P (*watts*), through an area, a (m^2), is:

$$\mathrm{P}=(p^2a/\rho c)\cos\theta \quad watts,$$

where θ is the angle of incidence of the sound wave on the area, a.

Sound intensity, the sound energy passing through unit area in unit time, is expressed in *watts/square meter* (*watts/m²*) ($=10^3$ *ergs/s·cm²*). For an effective pressure, p (*newtons/m²*), in a plane or spherical free wave propagated with a velocity, c (m/s), in a gas of density, ρ (kg/m^3), the sound intensity, I (*watts/m²*) in the direction of propagation may be written:

$$\mathrm{I}=(p^2/\rho c) \quad watts/m^2.$$

Sound energy density has the units of *joules/cubic meter* (*joule/m³*) ($=10^{+1}$ *ergs/cm³*).

[1] A. E. Kennelly, "I.E.C. Adopts M.K.S. System of Units," Elec. Eng. Dec. (1935). I.E.C. Document R.M. 118. Minutes of the I.E.C., E.M.M.U. Meeting, Scheveningen-Brussels, June (1935). Gino Sacerdote, "L'Applicazione Delle Unità M.K.S. Elettromagnetiche (Giorgi) Nel Campo Dell'Elettroacoustica," Alta Frequenza 9, 570 (1936).

Acoustic Impedance

The subject of acoustic impedance is confused by the existence in the literature of conflicting definitions of this important quantity. Crandall, Kennelly, Morse, and others define the acoustic impedance of a sound medium to a surface lying in a wave front as the product of the surface area by the ratio of sound pressure to particle velocity in the medium.

$$Z=(p/q)a.$$

From this definition it follows logically that the motion of a given piston in a sound medium is impeded more than is the motion of a similar piston having a smaller surface area. Furthermore the dimensions of acoustic impedance according to this definition, are those of a force divided by a velocity, identical with the dimensions of mechanic impedance.

$$Z=(p/q)a,$$

$$Z=\frac{[\text{Force/Area}]}{[\text{Velocity}]}\,[\text{Area}],$$

$$Z=[\text{Force}]/[\text{Velocity}].$$

Therefore in determining the behavior of a mechanic system in a sound medium (a vibrating piston in air) the acoustic impedance offered by the medium introduces a directly additive modification of the mechanic impedance of the system. In short, by this definition, acoustic impedance *is* mechanic impedance.[2]

The fundamental dimensions of this kind of acoustic impedance are a mass divided by a time.

$$Z=\frac{[\text{Force}]}{[\text{Velocity}]}=\frac{[\text{MLT}^{-2}]}{[\text{LT}^{-1}]}=[\text{MT}^{-1}].$$

The unit in the m.k.s. system is the *kilogram/second* (kg/s) ($=10^3$ gm/s). It would be advantageous if the name *mechanic ohm* should be used for the unit of mechanic *and* acoustic impedance having this magnitude.

The tentative "American Standards for Acoustical Terminology" define the acoustic impedance of a sound medium on a given surface lying in a wave front as "the complex quotient of the sound pressure (force per unit area) on that surface by the flux (volume velocity or linear velocity multiplied by the area) through the surface."[3]

$$Z=(p/q)(1/a).$$

According to this definition the motion of a given piston in a sound medium would be less impeded than would be the motion of a piston having a smaller surface area. However a definition of an acoustic impedance of this type is of use in problems in which the actual flow of sound energy through orifices is dealt with and a concept of impedance somewhat analogous to the resistance of a conductor to electric current flow is needed.[4]

The ambiguity introduced by the above duality of definition does not affect the concept of "specific acoustic impedance," defined for a plane sound wave as the ratio of the sound pressure to the particle velocity in the sound medium.

$$Z_s=p/q.$$

The unit in the m.k.s. system is the *kilogram/second square meter* ($kg/s\cdot m^2$) ($=10^{-1}$ $gm/s\cdot cm^2$ (Suggested name: *mechanic ohm per square meter*).

For the case of a plane sound wave propagated with a velocity, c (m/s), in a sound medium of density, ρ (kg/m), the specific acoustic impedance reduces very simply to:

$$Z_s=\rho c \quad kg/s\cdot m^2.$$

The density of air under normal pressure at 20°C

[2] A. E. Kennelly and J. H. Cook, "Mechanic Impedance in M.K.S. Units." Elec. Eng. **56**, 1062–63 (1937).

[3] American Tentative Standard—Acoustical Terminology 24.1 (1936). American Standards Association.

[4] It is evident that these two definitions of acoustic impedance differ because they deal with two entirely different concepts; one the impedance offered to a plate vibrating in a sound medium, the other the impedance to the flow of fluid offered by an orifice in a sound medium. These two concepts might best be discriminated between by the use of different unit names such as *piston impedance* and *orfice impedance*, Z_p and Z_a, respectively. If this latter definition (Z_a) is used exclusively for "acoustic impedance" it is necessary, when studying the motion of a vibrating piston in a sound medium, to multiply the acoustic impedance of the system by the square of the piston area in order that the contribution of the sound medium to the mechanic impedance of the system may be determined. The fundamental dimensions of acoustic impedance as defined in the "Tentative Standards" are $[\text{ML}^{-4}\text{T}^{-1}]$.

$$Z=\frac{p}{q}\frac{1}{a}=\frac{[\text{MLT}^{-2}/\text{L}^2]}{[\text{LT}^{-1}]}\,\frac{1}{[\text{L}^2]}=[\text{ML}^{-4}\text{T}^{-1}].$$

The unit in the m.k.s. system is the *kilogram/second-meter-to-the-fourth-power* ($kg/s\cdot m^4$) ($=10^{-5}$ $gm/s\cdot cm^4$).

is 1.205 kg/m^3; the velocity of propagation of a sound wave in air under these conditions is 344.0 m/s. Thus:

$Z_s = 415$ *mech. ohms*/m^2 ($kg/s \cdot m^2$) for air at 20°C, 1 *atmosphere*.

Architectural Acoustics

Reverberation time is measured in terms of the *second* (s), a unit common to both systems. Sabine's equation for the reverberation time (T), in which the energy density is reduced by a factor 10^6, is

$$T = \frac{0.16\ V}{a\bar{\alpha}}\ (s),$$

where V is the volume (m^3) of a room having a total surface area (walls, floor and ceiling) (m^2), with an average absorption coefficient, $\bar{\alpha}$.

The steady state energy density, E(*joules*/m^3), in this room when a sound source, P (*watts*), is operating in it is:

$$E = \frac{4P}{c\bar{\alpha}a}\ joules/m^3.$$

The coefficients of viscosity and of kinematic viscosity of a sound medium are used in studies of absorbing materials and of sound transmission. The coefficient of viscosity is measured in units of *kilograms/meter-second* ($kg/m \cdot s$) ($=10^1$ *gm*/$cm \cdot s$). The coefficient of kinematic viscosity has the unit, *square meter/second* (m^2/s) ($=10^4$ cm^2/s). For air at ordinary temperature and pressure:

Coefficient of viscosity $= 18.4 \times 10^{-6}\ kg/m \cdot s$
Coefficient of kinematic viscosity $= 1.32 \times 10^{-5}\ m^2/s$.

Conclusions

Electroacoustics embodies two branches of applied science, namely, (1) mechanics, (2) electrics including electromagnetics, electrostatics, piezoelectrics and thermoelectrics.

If mechanic quantities are expressed in c.g.s. units it is also necessary to measure electromagnetic quantities in c.g.s. electromagnetic units if homogeneity is to be maintained. It is however, almost impossible to avoid using the practical series of electric units (*volt*, *ohm*, *ampere*, etc.) because these are invariably used in electric measurements as well as in commercial specifications and descriptions. This fact leads to the use of a dual system of units, mechanic measures being made in the c.g.s. system, electromagnetic magnitudes being expressed in the practical series. These two systems are not homogeneous, a given quantity having units of different sizes in the two systems, (e.g. the unit of energy in the c.g.s. system is the *erg* and is equal to 10^{-7} *joule*, the m.k.s. unit of energy). Thus the use of dual systems makes necessary unwieldy transformation coefficients that obscure the physical facts being investigated and complicate the numerical calculations.

When, however, the m.k.s. unit system is used for both mechanic and electric quantities all transformation coefficients disappear.

A further advantage of m.k.s. mechanic units is their size which is suitable for engineering work.[5]

At least one textbook[6] has thus far been published using the m.k.s. system of units exclusively, and several others are in preparation.

[5] A. E. Kennelly, "The M.K.S. System of Giorgi as Adopted by the International Electrotechnical Commission (I.E.C.) in June 1935," J. Eng. Ed. Dec. (1936).

[6] P. Vigoureux and C. E. Webb, *Principles of Electric and Magnetic Measurements* (Blackie & Son, Ltd., Glasgow; Prentice-Hall, Inc., New York, 1936).

Appendix I

Table I. *A comparative table of mechanic, acoustic, and electric units of use in electroacoustics.*

Quantity	Symbol	m.k.s. Unit	c.g.s. Unit	c.g.s. Units in 1 m.k.s. Unit	m.k.s. Units in 1 c.g.s. Unit
Mass	M, m	kilogram, kg	gram, gm	10^{3}	10^{-3}
Length	L, l	meter, m	centimeter, cm	10^{2}	10^{-2}
Time	T, t	second	second	1	1
Density		kilogram per cu. meter kg/m³	gram per cu. centimeter, gm/cm³	10^{-3}	10^{3}
Velocity	V, v	meters per second, m/s	centimeters per second, cm/s	10^{2}	10^{-2}
Force	F, f	newton, kg·m/s²	dyne, gm·cm/s²	10^{5}	10^{-5}
Pressure (intensity)	p	kg/s·m	barye, gm/s·cm	10^{1}	10^{-1}
Sound Energy Flow	P*	watt	erg/s	10^{7}	10^{-7}
Sound Intensity	I	watt/m²	erg/s·cm²	10^{3}	10^{-3}
Sound Energy Density	E	joule/m³	erg/cm³	10^{1}	10^{-1}
"Diaphragm" Acoustic Impedance	Z_p	m.k.s. mechanic ohm, kg/s	c.g.s. mechanic ohm, gm/s	10^{3}	10^{-3}
"Orifice" Acoustic Impedance	Z_a	kg/s·m⁴	acoustic ohm, gm/s·cm⁴	10^{-5}	10^{5}
"Specific" Acoustic Impedance	Z_s	kg/s·m²	gm/s·cm²	10^{-1}	10^{1}
Viscosity		kg/s·m	poise, gm/s·cm	10^{1}	10^{-1}
Kinematic Viscosity		m²/s	cm²/s	10^{4}	10^{-4}
Work	W	joule	erg	10^{7}	10^{-7}
Power	P, P	watt	erg/s	10^{7}	10^{-7}
Elastic Coefficient	S	newton/m	dyne/cm	10^{3}	10^{-3}
Mechanic Impedance	Z	mechanic ohm, kg/s	mechanic abohm, gm/s	10^{3}	10^{-3}
Force Factor	$\mathfrak{A}$	newton/ampere	dyne/abampere	10^{6}	10^{-6}
Electric Current	I, i	ampere	abampere	10^{-1}	10^{1}
Electric Resistance	R	ohm	abohm	10^{9}	10^{-9}
Electric Inductance	L	henry	abhenry	10^{9}	10^{-9}
Magnetomotive Force	$\mathfrak{F}$	ampere turn		$4\pi\times10^{-1}$	$\frac{1}{4\pi}\times10^{+1}$
Magnetic Intensity	$\mathfrak{IC}$	ampere-turn per meter	oersted	$4\pi\times10^{-2}$	$\frac{1}{4\pi}\times10^{2}$
Magnetic Flux Density	$\mathfrak{B}$	weber/square meter	gauss	10^{4}	10^{-4}
Magnetic Reluctance	$\mathfrak{R}$	ampere-turn/weber		$4\pi\times10^{-9}$	$\frac{1}{4\pi}\times10^{9}$
Magnetic Permanence	$\mathfrak{P}$	weber/ampere-turn		$\frac{1}{4\pi}\times10^{9}$	$4\pi\times10^{-9}$

* J is sometimes used for this quantity.

Appendix II

An electroacoustic problem illustrating the use of the m.k.s. system of units

The diaphragm of an electrodynamic loudspeaker is assumed to act as a rigid piston. We shall consider the behavior of this device operating first in a vacuum and secondly in air. We shall further subdivide each of these cases into operation with an applied mechanic vibromotive force and operation under the influence of an alternating electromotive force applied to the voice coil terminals inducing a mechanic vibromotive force. Mechanic friction in the diaphragm and its supports is neglected in the analysis. The following constants of the loudspeaker are assumed:

Radius of diaphragm	$0.1m$
Area of diaphragm	$a=0.01\pi\ m^2$
Mass of diaphragm (including attached voice coil)	$M=5\times10^{-3}\ kg$
Elastance of diaphragm support	$S=5\times10^{3}\ newton/m$
Force factor of electromagnetic drive	$\mathfrak{A}=2\ newton/amp.$
Electric resistance of voice coil	$R_c=20\ ohms$
Inductance of voice coil	$L_c=10^{-2}\ henrys$

Case I$_a$ Loudspeaker in a vacuum
Mechanic vibromotive force applied
$F=2$ *newtons* r.m.s.

The mechanic impedance of the system is:

$$Z_d=0+j(M\omega-S/\omega)\ \ mech.\ ohms\ (kg/s).$$

With an r.m.s. force, F *newtons*, applied the r.m.s. velocity of the diaphragm is:

$$V=F/Z\ \ m/s.$$

This system is purely reactive, no active power being absorbed from the driving agency. (See Table II.)

We must first determine the impedance to electric current flow offered by the moving coil. This impedance includes the electric impedance of the coil, when stationary, and the motional electric impedance of the device. The motional electric impedance is given by:

$$Z_M=\mathfrak{A}^2/Z\ \ ohms.$$

The electric impedance of the voice coil, when stationary, is:

$$Z_c=R_c+jL_c\omega\ \ ohms.$$

The total electric impedance of the moving voice coil is:

$$Z_E=Z_M+Z_c\ \ ohms.$$

TABLE II.

Case Ia. Loudspeaker in a vacuum.
Mechanic vibromotive force applied; F = 2 *newtons* r.m.s.

ω	Z	V
rad/s	*mech. ohms = kg/s*	*m/s*
100	$-j4.5$	$j.445$
316	0	∞
1000	$j4.5$	$-j.445$
10000	$j50$	$-j.040$

Case Ib. Speaker in a vacuum.
Alternating electromotive force applied to voice coil $E = 10$ *volts* r.m.s.

TABLE III.

Case Ib. Loudspeaker in a vacuum.
Alternating e.m.f. applied to voice coil $E = 10$ *volts* r.m.s.

ω *rad/s*	Z_c *ohms*	Z_M *ohms*	Z_E *ohms*
100	$20+j1.0$	$j.89$	$20+j1.89$
316	$20+j3.16$	∞	∞
1000	$20+j10.0$	$-j.89$	$20+j9.11$
10000	$20+j100.0$	$-j.08$	$20+j100$

I *amp.*	F *newtons*	V *m/s*
$0.496-j.047$	$0.992-j.094$	$0.021+j.221$
0	0	—
$.414-j.089$	$.828-j.178$	$-.0396-j.184$
$.019-j.096$	$.038-j.192$	$-.0038-j.00076$

Case IIa. Loudspeaker in air.
Mechanic vibromotive force applied F = 2 *newtons* r.m.s.

TABLE IV.

Case IIa. Loudspeaker in air.
Mechanic vibromotive force applied F = 2 *newtons* r.m.s.

ω *rad/s*	Z *mech. ohms = kg/s*	V *m/s*	P *watts*
100	$13.0-j4.5$	$0.137+j.048$	0.272
316	13.0	.154	.308
1000	$13.0+j4.5$	$.137-j.048$	.272
10000	$13.0+j50$	$.0097-j.0375$	.0195

Case IIb. Loudspeaker in air.
Alternating electromotive force applied to voice coil $E = 10$ *volts* r.m.s.

Hence the electric current that flows in the voice coil may be calculated:

$$I = E/Z_E \quad amp.$$

TABLE V.

Case IIb. Loudspeaker in air.
Alternating e.m.f. applied to voice coil $E = 10$ *volts* r.m.s.

ω *rad/s*	Z *mech ohms = kg/s*	Z_M *ohms*	Z_E *ohms*	I *amp*
100	$13.0-j4.5$	$0.275+j.095$	$20.275+j1.095$	$0.491-j.0267$
316	13.0	.308	$20.308+j3.16$	$.480-j.0748$
1000	$13.0+j4.5$	$.275-j.095$	$20.275+j9.905$	$.398-j.195$
10000	$13.0+j50$	$.0195-j.075$	$20.0195+j99.925$	$.0193-j.096$

F *newtons*	V *m/s*	P *watts*	η %
$0.982-j.0534$	$0.0688+j.0197$	0.0667	1.36
$.960-j.149$	$.0738-j.0115$	.0726	1.51
$.796-j.390$	$.0454-j.0457$	.0539	1.36
$.0386-j.192$	$-.00341-j.00166$	.000187	.097

This current flowing in the voice coil gives rise to a mechanic force acting on the diaphragm:

$$F = \mathfrak{A} I \quad newtons.$$

The diaphragm, vibrating in a vacuum, dissipates no energy by its motion. The power supplied to the circuit is absorbed in the electric resistance of the voice coil. (See Table III.)

The computations for this case are carried through in the same manner as those delineated in case Ia except that the mechanic impedance of the vibrating diaphragm contains a dissipative term accounting for the tendency of the system to supply acoustic energy to the surrounding medium, air. The magnitude of this mechanic or acoustic resistance is calculated from:

$$R = \rho c a \quad mech.\ ohms\ (kg/s),$$

where ρ = density of air = 1.205 kg/m^3 at 1 *atmos.*, 20°C,
c = velocity of propagation of sound in air,
= 344.0 m/s at 1 *atmos.*, 20°C,
a = area of diaphragm = 0.0314 m^2,
whence R = 13.0 *mech. ohms* (*kg/s*).

The power dissipated in the mechanic system in this case may be determined from:

$$P = V^2 R \quad watts.$$

This power is supplied to the air as acoustic power. (Table IV.)

The computations for this case parallel those of case Ib with the exception noted above that the mechanic impedance of the system is altered by the air load on the diaphragm.

The efficiency of transfer of electric power to acoustic power is the ratio of acoustic power (= mechanic power dissipation for this case of frictionless supports) to electric power input to the voice coil and is given in the column headed η in Table V.

The Position of the Vibrator in the Experiments of Melde and Kundt

B. J. Miller and L. O. Olsen
State University of Iowa, Iowa City, Iowa

(Received November 10, 1937)

It is shown that the point of application of the obligatory motion in the experiments of Melde and Kundt is at a displacement "node" in the driven medium. The word "node" means a point of minimum amplitude in the standing wave in the tube or string. This result agrees with that of Rayleigh but is obtained in a simpler manner. The discussion is presented briefly to make the results more available as current textbooks indicate a nearly universal misunderstanding of these two well-known experiments.

AN examination of a number of widely used college physics texts shows a quite general misunderstanding of the position of the vibrator in the Kundt's tube experiment. Many writers locate the end of the vibrating rod at a displacement loop of the standing wave in the tube. Others locate it "near a node." Still others avoid any statement but indicate graphically an agreement with one of these locations or a position midway between a node and a loop.

The purpose of this discussion is to point out the correct view, namely, that at resonance the distance from the piston to the nearest displacement node is zero except for terms involving the second and higher powers of the damping constant. Here the word "node" implies a point of minimum amplitude in the standing wave in the tube. These minimum amplitudes differ from zero except at the fixed end of the air column.

Discussions of Melde's experiment in these texts do not usually include the point here considered; the illustrations presented are, for the most part, correct in this respect. It is probably not generally realized however that the end of the fork is located so precisely at a displacement node when the string is tuned for resonance. Thus it is worth while to point out that the treatment here presented applies equally well to the transverse form of Melde's experiment. (Fork vibrating at right angles to the length of the string.)

We make the following assumptions and conventions:

(1) The fixed end (of the air column or string) is located at $x=0$.

(2) The vibrator is at $x=l$ and executes a vibrator described by

$$u=a\sin\omega t,$$

where u is the displacement. The reaction of the driven medium is thus neglected.

(3) A damping force proportional to the particle velocity is assumed.

Under these assumptions the wave equation takes the form:

$$\frac{\partial^2 u}{\partial x^2}-\frac{2K}{c}\frac{\partial u}{\partial t}=\frac{1}{c^2}\frac{\partial^2 u}{\partial t^2}, \tag{1}$$

where c is the $(T/m)^{\frac{1}{2}}$ in the case of the string and $(\gamma p/\rho)^{\frac{1}{2}}$ for the air column. In order to simplify the subsequent algebra, the constant of proportionality is written in the form $2K/c$. This equation is to be solved subject to the boundary conditions.

$$\text{At } x=0,\ u=0 \text{ for all } t, \tag{2}$$

$$\text{At } x=l,\ u=a\sin\omega t. \tag{3}$$

A solution which satisfies these conditions can be derived from the solution

$$u=Ae^{-\alpha x}\sin k(x-\beta t)+Be^{-\alpha x}\cos k(x-\beta t)+Ce^{\alpha x}\sin k(x+\beta t)+De^{\alpha x}\cos k(x+\beta t). \tag{4}$$

Here $\alpha=\dfrac{K}{(1+K^2/k^2)^{\frac{1}{2}}}$ and $\beta=\dfrac{c}{(1+K^2/k^2)^{\frac{1}{2}}}$

$k=2\pi/\lambda$, where $\lambda=2\pi(\beta/\omega)$; and the positive square root is used for α and β.

Application of the boundary conditions gives:

$$A=C,\quad B=-D,$$
$$A\tan kl=B\tanh \alpha l,$$
$$a/2=A\cos kl\sinh \alpha l+B\sin kl\cosh \alpha l.$$

This gives u in the following form:

$$u=a/(\cos^2 kl\sinh^2\alpha l+\sin^2 kl\cosh^2\alpha l)$$
$$\times\begin{cases}\cos\omega t(\sin kx\cosh\alpha x\cos kl\sinh\alpha l\\ \quad-\cos kx\sinh ax\sin kl\cosh\alpha l)\\ +\sin\omega t(\cos kx\sinh ax\cos kl\sinh\alpha l\\ \quad+\sin kx\cosh ax\sin kl\cosh\alpha l).\end{cases}\tag{5}$$

This can be further reduced if we set the coefficient of $\cos\omega t$ equal to $-R\sin\gamma$ and the coefficient of $\sin\omega t$ to $R\cos\gamma$. This gives

$$u=\frac{aR\sin(\omega t-\gamma)}{\cos^2 kl\sinh^2\alpha l+\sin^2 kl\cosh^2\alpha l}.\tag{6}$$

R reduces to

$$R=\frac{(\sinh^2\alpha x\cos^2 kx+\cos^2\alpha x\sin^2 kx)^{\frac{1}{2}}}{(\sinh^2\alpha l\cos^2 kl+\cosh^2\alpha l\sin^2 kl)^{\frac{1}{2}}}\tag{7}$$

and γ is given by

$$\tan\gamma=\frac{\tanh\alpha x\tan kl-\tanh\alpha l\tan kx}{\tanh\alpha x\tanh\alpha l+\tan kx\tan kl}.\tag{8}$$

Finally u becomes[1]

$$u=\frac{a(\sinh^2\alpha x\cos^2 kx+\cosh^2\alpha x\sin^2 kx)^{\frac{1}{2}}}{(\sinh^2\alpha l\cos^2 kl+\cosh^2\alpha l\sin^2 kl)^{\frac{1}{2}}}\sin(\omega t-\gamma).\tag{9}$$

In this form the physical interpretation is evident. Each particle of the air column or string executes a simple harmonic vibration with the frequency of the vibrator and with an amplitude

$$\frac{a(\sinh^2\alpha x\cos^2 kx+\cosh^2\alpha x\sin^2 kx)^{\frac{1}{2}}}{(\sinh^2\alpha l\cos^2 kl+\cosh^2\alpha l\sin^2 kl)^{\frac{1}{2}}}=\frac{aF(x)}{F(l)}\tag{10}$$

and with a phase given by γ.

The solution differs from that for an undamped medium in that the dependence of the displacement on x is not sinusoidal and the phase of the vibration is a function of x.

For any frequency of the vibrator there is a vibration in the string or air column having minima and maxima. The points of minimum amplitude are the minima of $F(x)$ given by

$$\alpha\sinh 2\alpha x=-k\sin 2kx.\tag{11}$$

If α is small

$$-2\alpha^2 x=k\sin 2kx.$$

If we set $x=n\pi/k+\epsilon_1$ where $2k\epsilon_1\ll 1$

$$\epsilon_1=(-n\pi\alpha^2)/k^3.\tag{12}$$

Thus the nodes are at $x=n\pi/k$ if α^2/k^2 is very small compared to unity, and are uniformly spaced to an even closer approximation.[2]

The location of the vibrator ($x=l$) relative to these minima is as yet not fixed as we have not used the condition of resonance. We define the resonant frequency as that which leads to a maxima displacement amplitude. This can be determined by minimizing $F(l)$ with respect to k. This gives

$$\sin 2kl=(2\alpha^3/k^3)\sinh 2\alpha l\tag{13}$$

or for small α

$$\sin 2kl=2\alpha^4 l/k^3$$

setting
$$kl=n\pi+k\epsilon_2\tag{14}$$
$$2k\epsilon_2=(n\pi/k+\epsilon_2)(2\alpha^4/k^3)$$
$$\epsilon_2=n\pi\alpha^4/k^5.\tag{15}$$

Thus at resonance

$$k=(n\pi/l)(1+\alpha^4/k^4),\tag{16}$$

which expression is identical for all practical purposes, with that calculated by more elementary means.

The distance of the vibrator from the nearest node can now be exhibited. From (14)

$$l=\frac{n\pi}{k}+\frac{n\pi\alpha^4}{k^5},\quad\text{or,}\quad\text{if}\ \frac{\alpha^2}{k^2}\ll 1,$$
$$=\frac{n\pi}{k}.$$

From (12) the nearest node is at $x=n\pi/k-n\pi\alpha^2/k^3$

$$l-x=d=\frac{n\pi\alpha^2}{k^3}=\frac{n\alpha^2\lambda^3}{8\pi^2}\tag{17}$$

if we neglect higher powers of α.

[1] The result agrees with that of Rayleigh, *Theory of Sound*, second edition, Vol. I, page 198.

[2] To a closer approximation

$$\epsilon_1=-\frac{n\pi\alpha^2}{k^3}\left[1+\frac{\alpha^2}{k^2}\left(\frac{2n^2\pi^2}{3}-1\right)\right].$$

Thus we have a linear dependence of ϵ_1 on n if $\alpha^4/k^4\ll 1$.

Thus the node at resonance is in front of the vibrator a distance proportional to α^2 and to the number of nodes.

An estimate of the value of α can be obtained from the following considerations. If we insert "k" from (16) in Eq. (9), and neglect higher powers of α/k, we may write

$$u=\frac{aF(x)}{\sinh \alpha l}\sin(\omega t-\gamma). \qquad (18)$$

Also, to an approximation close enough for this computation (first power of α)

$$\sin kx=1$$

at a loop. At such a point the amplitude is given by $a/\alpha l$. The amplitude of the vibrator is a and the ratio of the amplitude of the driven medium to that of the driven is thus $1/\alpha l$.

Suppose we use as an example some actual data on Melde's experiment. The string used was a high grade of fishing tackle, but inhomogeneities were apparently not entirely absent. However it gave more consistent results than various other strings and wires tried. The amplitude of the string at resonance was conservatively estimated to be ten times that of the fork. For a length of 200 cm this gives $\alpha=5\times10^{-4}$. In the most adverse case $\lambda=100$ cm $n=4$. From Eq. (17) then "d" $=0.013$ cm.

Thus the distance from the fork to the nearest node is theoretically 0.013 cm. This is entirely negligible in view of the fact that the various internodal distances differed from each other by one or two cm.

In the case of Kundt's experiment the amplitude ratio is much greater and the customary wave-length much shorter. leading to even smaller values of d.

In Melde's experiment it is usually found that the resonance point is not sharply determined by the amplitude which is essentially constant over a fairly wide range of load. Experimentally it is found that the resonance load can be much more sharply determined by requiring that the final node coincide with the end of the fork.

The phase factor γ is of some interest. In the vicinity of a node, from Eqs. (8), (12) and (15), $\tan\gamma=\infty$. That is, the vibration at the nodes is $\pi/2$ radians out of phase with the vibration of points remote from the node. This was first noticed and discussed by C. V. Raman.[3]

Summary and Conclusion

(1) An expression has been developed for a standing wave in a dissipative medium with an obligatory simple harmonic motion imposed at a point.

(2) It has been shown that the points of minimum amplitude in the driven medium are equally spaced if powers of the damping constant higher than the second are neglected. This spacing is equal to that for the undamped case if the square of the damping coefficient is negligible.

(3) At resonance, the mean position of the vibrator coincides with that of a minimum if $\alpha^2/k^2\ll1$.

(4) A method of estimating damping constants and a method of tuning to resonance have been suggested

The authors wish to acknowledge their indebtedness to Professor G. W. Stewart who called their attention to the general misunderstanding and the correct view.

[3] C. V. Raman, Phys. Rev. **32**, 309 (1911).

The Sound of Bells

Jottings from my Experiences in the Domain of the Sound of Bells

JAN ARTS
"Huize Ruwenberg" St. Michielsgestel, the Netherlands

(Received September 25, 1937)

THE STRIKE NOTE OF BELLS

THE strike note of bells has been discussed by A. T. Jones,[1] and it may be assumed therefore that the reader is acquainted with the strike note problem.

It is some ten years ago now that I wrote to the late P. Griesbacher as follows: "I wonder why you don't mention the seventh partial in *Glockenmusik*. Yet experience of the last few years taught me that this apparently unsignificant matter is of great importance for the exact determination of the strike note."[2]

From the moment that I noticed this phenomenon, originally strange but explainable, I have always, whenever an opportunity offered, noted the seventh partial together with the fifth partial with a view to be able to make out whether the mysterious strike note might be explainable as difference tone. But soon I verified that this could not be true, the tone-relations of the 5th and 7th partials being usually of such a nature as to exclude the possibility of the strike note being a difference tone.

In order not to take up too much space I submit three tables, which will sufficiently prove and explain my allegation. I confine myself to these three though I could add a dozen similar cases.

Table I shows the octaves below the fifth partials and the frequencies of the fifth and seventh partial of two bells in the tower at Maestricht, Limburg, the Netherlands; when these bells sound together, the two strike notes are heard in the interval of a minor third. Careful experimenting showed that the 5th and 7th of bell I are represented as d″ 8/16–a″ 10/16, respectively, the 5th and 7th of bell II as f″ 7/16–c‴ 5/16.

This table clearly shows that if the strike note should be originated by the fifth–seventh, the strike note as difference tone is excluded; should this be the case, not a minor third would be heard when the two bells rang together, but the major second d′ 13/16–f′ 0/0. The octaves d′ 8/16–f′ 7/16 below the fifth partials on the other hand are quite concordant with the minor third interval heard.

Table II shows the octaves below the 5th partials and the tone relations of the 5th and 7th of two bells in the tower of Vlokhoven, Noord-Brabant. When the two bells are rung together, a good major second interval is heard. Were the difference tones e♭′ 7/16–e′ 13/16 to decide of the strike notes, not a major but a minor second would be heard. So here too the octaves below the fifth partials are in favor of the strike note hypothesis.

The tone relations of the 5th and 7th in Table III are of two bells, of Breda, Noord-Brabant. When rung together, here too the major second is heard. Again, were the difference tones b♭′ 7/16–d♭″ 1/16 to decide of the strike notes, the minor third and not the major second would be heard.

Conclusion: "The results of this test appear to favor the octave hypothesis rather than the difference tone hypothesis."

I for one am of opinion that the fifth partial, both in the case of small bells and of big ones, originates the strike note. In defining the objectively nonexisting strike note, my only guide is the fifth; a guide fully to be relied on even in the most critical cases.

TABLE I.

	BELL I		BELL II	
	CYCLES/SEC.	NOTE*	CYCLES/SEC.	NOTE*
Seventh	901.6 =	a″ 10/16	1053.6 =	c‴ 5/16
Fifth	597.6 =	d″ 8/16	708.2 =	f″ 7/16
Difference tone	304.0 =	d′ 13/16	345.4 =	f′ 0/0
Octave below the fifth partial	298.8 =	d′ 8/16	354.1 =	f′ 7/16

* The fraction beside the name of the note is part of a half-step of an equally tempered tuning fork. The fraction on the left of the note-name points to a minus, the fraction on the right to a plus.

[1] A. T. Jones, J. Acous. Soc. Am. **8**, 199–202 (1937).
[2] P. Griesbacher, *Glockenmusik* (Nachtrag, 1929), p. 43.

TABLE II.

	BELL I		BELL II	
	CYCLES/SEC.	NOTE	CYCLES/SEC.	NOTE
Seventh	935.2 =	b♭″ 4/16	1042.0 =	c‴ 2/16
Fifth	619.6 =	e♭″ 2/16	700.6 =	f″ 4/16
Difference tone	315.6 =	e♭′ 7/16	341.4 =	e′ 13/16
Octave below the fifth partial	309.8 =	e♭′ 2/16	350.3 =	f′ 4/16

TABLE III.

	BELL I		BELL II	
	CYCLES/SEC.	NOTE	CYCLES/SEC.	NOTE
Seventh	1421.6 =	f‴ 8/16	1618.8 =	g‴ 12/16
Fifth	948.8 =	b♭″ 8/16	1068.8 =	c‴ 9/16
Difference tone	472.8 =	b♭′ 7/16	550.0 =	d♭″ 1/16
Octave below the fifth partial	474.4 =	b♭′ 8/16	534.4 =	c″ 9/16

TABLE IV.

	A BELL	*B* BELL
Fifth	c⁗ 12/16	c⁗ 11/16
Fourth	g‴ 12/16	g‴ 12/16
Third	e♭‴ 10/16	e♭‴ 12/16
Second	c‴ 5/16	2/16 c‴
First	2/16 c″	c″ 7/16

The late P. Griesbacher once asked me:[3] "Just tell me: How do you test bells higher than a″? As our tuning forks reach only to a‴, the method with the fifth leaves you in the lurch already at b″. *And is it your opinion too, that at that height the strike note somewhat loses its influence on the sound and that often the second and oftener still the first partial is predominant?*"

My answer: Last year I was sent two small bells for examination, bells of exactly the same diameter (pl.m. 40 cm) but formed after different profiles. The two bells were before me with mouths turned upwards. When struck respectively with a mallet there was no doubt about the strike note of the *A* bell being decidedly a quarter of a step below that of the *B* bell. After careful experimenting I obtained the tone relations as shown in Table IV. As the 5ths of the two bells were both of the same frequency the strike note concordance must be all right, I thought. At my request I had the two bells mounted for ringing and lo: when the two bells rang together it was as if only one bell was ringing, so perfect was the concordance between the two strike notes. So originally the distinct coming forth of the two first partials, differing about a quarter of a step, was misleading.[4]

IS A BELL TONE, OBTAINED WITH A FORK, TUNED AN OCTAVE LOWER, AN ABSOLUTELY RELIABLE PICTURE OF THE FREQUENCE RELATION 1 : 2?

For many years I have been using a set of tuning forks (Edelmann) with a total range of F♯ to a‴ included, to investigate bell tones, of both church bells and carillon bells. As I could not afford to acquire the whole set at once on account of the great expense, I bought only one fork, the fork with a range of d♯′ to a′. As the range of the fork was rather small, the fork was of little use to me; the range of the tones of church bells and carillon bells being very extensive. Therefore I asked myself the question: Is it possible to bring forth the bell tones lying outside my tuning fork, as a harmonic overtone. And behold, by my first experiment I found that with a fork tuned an octave or duodecimo lower, the bell tone, which was an octave or duodecimo higher, reacted clearly and distinctly upon it. But a second question arose: Is the result arrived at in this way to be trusted; is the aliquot tone produced in this way, an absolutely reliable picture of the frequence relation: 1 : 2, 1 : 3?

Gradually I came into the possession of the whole set of nine forks. I thought now to be able, to prove the reliability of my method. I experimented on the bell in the belfry of our college, with a diameter of about 38 cm. This bell has the 4 following partial tones: first: c″ 8/16; second: b″ 15/16; third: e♭‴ 7/16; fourth: g♭‴ 15/16.

[3] Letter: 20, X (1930).

[4] My Dutch readers are informed that the firm of Petit & Fritsen, bell-founders at Aarle-Rixtel, N.B. found the case so interesting and convincing that they keep the two bells mounted in their show room in order to give those interested at any time an opportunity to verify the fact.

TABLE V. *The tones in column 1, were acquired with the normally pitched tuning fork. The fork tones in columns 2, 3, 4 and 5, bring forth as first aliquot tones, the tones of column 1.*

	1	2	3	4	5
Fifth	c'''' 6/16	c''' 6/16	f'' 6/16	c'' 5/16	a♭' 8/16
Fourth	g♭''' 15/16	g'' 0/0	b' 15/16	g♭' 15/16	e♭' 0/0
Third	e♭''' 7/16	e♭'' 7/16	a♭' 8/16	e♭' 7/16	b 9/16
Second	b'' 15/16	c'' 0/0	e' 15/16	c' 0/0	a♭ 4/16
First	c'' 8/16	c' 8/16	f 10/16	c 10/16	A♭ 10/16

When setting the fork an octave lower to the first, so to c' 8/16, the first partial very distinctly was brought out.[5] The second b'' 15/16 reacted very weakly on b' 15/16 but distinctly came out when the fork was tuned on c'' 0/0. The third e♭''' 7/16 clearly answered the setting e♭'' 7/16. The fourth g♭''' 15/16 on the other hand, only clearly came forth on a g'' 0/0 setting. Now I tried whether I could elicit the same partials (plus the fifth) also as 3rd, 4th and 5th aliquot tones. In this I succeeded perfectly, but, as Table V shows the results are not all in the exact frequence relations: 1 : 2, 1 : 3, 1 : 4, 1 : 5.

In all my subsequent experiments I observed the peculiar phenomenon, that sometimes a fork tuned a pure octave lower, produced the pure over-octave and sometimes not. How to account for it, that the results are so different? Is the cause to be found in the physical nature of the bell or of the tuning fork? (Table VI.)

AN UNKNOWN (?) BELL TONE

I am in the possession of a small bell (weight about 12 kg). One day as I was experimenting on this bell I suddenly noticed a tone I had not heard so far. Since that time I regularly meet with this unknown (?) tone in small bells. This tone has the peculiarity (a) it is very modest in its appearance, (b) it does not react upon the tuning fork. It is possible, however, to make it free of beats to respond to the tuning fork and consequently its pitch exactly definable. Its singing-out time is of the same length or nearly so as that of the 3rd partial and therefore I presume that it is closely related with the third partial.

[5] In order to arrive at a wholly reliable result especially in the case of the lower bell tones, such as the first and the second, it is desirable to put a piece of thin cloth on the soundbow, to prevent the fork from jumping up.

TABLE VI. *The partial tones in column 1 were acquired with the normally tuned fork; the fork tones in column 2 bring forth (with a fork tuned a pure (?) octave lower) the tones of column 1.*

		1.	2.
Bell I	Third	f♯'' 5/16	f♯' 5/16
	Second	d♯'' 5/16	d♯' 3/16
	First	d♯' 7/16	d♯ 8/16
Bell II	Fourth	g♯''' 11/16	g♯'' 11/16
	Third	e''' 8/16	e'' 5/16
	Second	c♯''' 7/16	c♯'' 4/16
	First	c♯'' 7/16	c♯' 7/16
Bell III	Fourth	g''' 8/16	g'' 8/16
	Third	e♭''' 10/16	e♭'' 8/16
	Second	4/16 c'''	2/16 c''
	First	c'' 6/16	c' 8/16
Bell IV	Fourth	g''' 11/16	g'' 10/16
	Third	e♭''' 9/16	e♭'' 7/16
	Second	c''' 4/16	c'' 4/16
	First	4/16 c''	1/16 c'
Bell V	Fourth	f''' 1/16	1/16 f''
	Third	d♭''' 7/16	d♭'' 4/16
	Second	b♭'' 1/16	b♭' 2/16
	First	b♭' 1/16	b♭ 2/16
Bell VI	Fifth	g♯''' 0/0	g♯'' 0/0
	Fourth	d♯''' 0/0	6/16 d♯''
	Third	b'' 0/0	b' 0/0
	Second	1/16 g♯''	3/16 g♯'
	First	1/16 g♯'	2/16 g♯

I should be inclined to call it the "acoustic tone" on account of its objective nonexistence. The first and second partial of my study-object are affected with beats. The third too has this defect. Now it is a well-known fact, that, if a partial sings out with beats, there are two sector groups, which each of them send out separate tones, only slightly differing in pitch.

As it happens, with my bell the sectors of the 1st and 2nd are quite congruent.[6] If I make the bell vibrate by means of the clapper in one of

TABLE VII.

SINGING-OUT SECONDS	*A* SECTORS	PARTIALS ACOUSTIC	*B* SECTORS	SINGING-OUT SECONDS
0.5	f'''' 15/16	Fourth	f'''' 15/16	0.5
3.	d'''' 4/16	Third	d'''' 3/16	3.
5.	b''' 1/16	Second	b''' 5/16	5.
3.	g''' 2/16	*Acoustic*	g♯'''' 0/0	3.
15.	5/16 b''	First	8/16 b''	15.

[6] Incidentally I wish to draw the reader's attention to the possibly unknown fact that the position of the nodal meridians and specially that of the nodal circles is equally well definable by means of the adjustable tuning forks as with the resonators or any other instruments adapted to the purpose.

TABLE VIII.

	Bell 1		Bell 2		Bell 3		Bell 4		Bell 5		Bell 6		Bell 7	
P.A.	N.	S.S.	N.	S.S.	N.	S.S.	N.	S.S.	N.	S.S.	N.	S.S.	N.	S.S.
Third	c''' 0/0	9	e♭''' 10/16	7	e♭''' 9/16	7	e♭''' 1/16	7	f''' 0/0	6	d♭''' 7/16	11	0/0 b''	11
Second	1/16 a''	12	4/16 c'''	11	c''' 4/16	9	5/16 c'''	10	d''' 7/16	10	b♭'' 1/16	13	1/16 g#'''	14
Acoust.	f'' 0/0	8	g'' 1/16	7	a♭'' 4/16	6	g'' 10/16	7	a♭'' 0/0	6	f#'' 2/16	11	e'' 1/16	10
First	a' 1/16	27	c'' 6/16	25	4/16 c''	26	3/16 c''	30	12/16 d''	22	b♭' 1/16	47	1/16 g#'	36

The initials P.A., N. and S.S. respectively indicate: partial/acoustic, note and singing-out seconds.

the *A* sectors, the elusive tone comes forth as g''' 2/16; if the bell is struck in the middle of one of the *B* sectors another tone presents itself, namely g#''' 0/0. In the beginning you have to strain your ears to discern it from the other bell tones; once its acquaintance thoroughly made, it is rather easily discernable.

A synoptic table of the tone relations and singing-out-time is given in Table VII. For clearness sake of the above-said, I shall call the two sector groups *A* and *B*. Now I began experimenting on a 50 kilogram bell and discovered between the 1st partial c'' and the second partial c''' a tone of analogous character g'', which took up 4 seconds in singing-out. Since that time I have often been observing this "super" but have not succeeded so far in defining its origin. I met it not only in bells of Netherlands make, but also in many bells, found abroad.

I give by way of elucidation (Table VIII) the 1st, 2nd and 3rd partials, besides the acoustic tones with the singing-out times proper to them, of seven bells. May I have stimulated hereby to the study of this problem, of which, up till now, I have not been able to give a satisfactory explanation.

TEMPERATURE INFLUENCE ON BELLS

The late Griesbacher came by experiments[7] to the conclusion that the bell is not subject to temperature changes.[8]

Some years ago—it was an exceptionally hot August—I took in the evening a bell into a room and tuned the forks carefully i.e., free of beats to the 1st, 2nd and 3rd partial. The next day in the forenoon, the thermometer in the room where the tuning forks and the bell had spent the night, pointed to 18° Celsius. I controlled the fork tones together with the bell tones and the agreement was complete as the evening before. The forks were left in the room (18°C) and bell and thermometer were exposed to the sun for an hour. After an hour the thermometer pointed to 31°C. Now I brought the forks into contact with the bell one after another and counted

for the 1st partial 14 beats per 10 seconds
" " 2nd " 29 " " " "
" " 3rd " 33 " " " "

Some time afterwards I came to the same result on another bell:

for the 1st partial 10 beats per 10 seconds
" " 2nd " 20 " " " "
" " 3rd " 24 " " " "

These results clearly prove the influence of the temperature on the bell body and consequently on the tones produced. Incidentally I wish to draw my readers attention to the ratio of beats: 14, 29, 33, and 10, 20, 24 which is in agreement with frequence proportion: 1 : 2 (first–second) 1 : 2, 4 (first–minor third).

[7] If one wants to make this experiment by means of the tuning forks, it is necessary to handle it carefully as it is rather sensitive to temperature changes.

[8] Reference 2, pages 46–47.

The Velocity of Sound in Single Crystals of Bismuth

A. B. Focke, R. B. Lindsay and C. R. Wilks
Brown University, Providence, Rhode Island

(Received December 10, 1937)

The velocity of compressional waves in single crystals of bismuth of two orientations (P_1 and P_3) of the principal axis has been measured. The specimen to be tested (around 10 cm in length) is inserted between two longer steel rods, one of which is driven by a loudspeaker coil while the other has a free end. The velocity is computed from the observed distance between two nodes when all or part of the crystal is included between them. For the P_1 and P_3 orientations the velocities are found to be 2028 meters/sec. and 1541 meters/sec., respectively, and the corresponding Young's moduli come out to be 4.043×10^{11} dynes/cm^2 and 2.245×10^{11} dynes/cm^2.

Introduction

THE present paper contains the results of the measurement of the velocity of compressional waves in single crystals of bismuth of various orientations of the principal axis. The measurements not only possess acoustical interest but yield a valuable method for the calculation of Young's modulus and its dependence on crystal orientation. The method is believed to be particularly adapted to acoustical wave velocity determinations in small specimens of soft and brittle substances which are able to stand but little strain.

Theory of the Method

Consider a solid rod of length l_2 and cross-sectional area S_2 inserted between two long rods of cross-sectional areas S_1 and S_3, respectively (see Fig. 1). The middle rod is the crystal to be tested, while for convenience the other two rods are of some standard easily prepared metal, e.g., steel or brass. If the rods are the seat of compressional waves traveling lengthwise through them, the particle displacement ξ and excess tension T at the boundary between S_1 and S_2 will be given in terms of these quantities at a point 1, distant l_1 from the boundary A, by the relations[1]

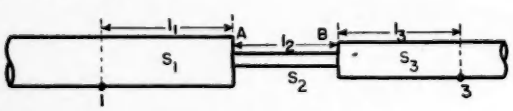

Fig. 1.

$$\begin{aligned}\xi_{12}&=\xi_1\cos k_1l_1+(T_1/\rho_1c_1\omega)\sin k_1l_1,\\ T_{12}&=T_1\cos k_1l_1-\rho_1c_1\omega\xi_1\sin k_1l_1,\end{aligned}\tag{1}$$

where the quantities ξ_1 and T_1 are taken at point 1 and ξ_{12} and T_{12} are taken at the boundary A but *in* the first rod. The density of the first rod and the velocity of sound in it are given by ρ_1 and c_1, respectively. As usual $k_1=\omega/c_1$.

Denoting quantities at the boundaries A and B of the specimen rod by the subscripts 21 and 23, respectively, we have the similar equations

$$\begin{aligned}\xi_{23}&=\xi_{21}\cos k_2l_2+(T_{21}/\rho_2c_2\omega)\sin k_2l_2,\\ T_{23}&=T_{21}\cos k_2l_2-\rho_2c_2\omega\xi_{21}\sin k_2l_2,\end{aligned}\tag{2}$$

where $k_2=\omega/c_2$ and ρ_2 and c_2 refer to the specimen being tested. Denoting by the subscript 3 the displacement and excess tension at a point distant l_3 in the rod of cross section S_3 from the boundary B, we finally have the third pair of relations

$$\begin{aligned}\xi_3&=\xi_{32}\cos k_1l_3+(T_{32}/\rho_1c_1\omega)\sin k_1l_3,\\ T_3&=T_{32}\cos k_1l_3-\rho_1c_1\omega\xi_{32}\sin k_1l_3.\end{aligned}\tag{3}$$

The boundary conditions at A and B, respectively, are

$$\begin{aligned}\xi_{12}&=\xi_{21}\quad;\quad \xi_{23}=\xi_{32}\quad;\\ S_1T_{12}&=S_2T_{21};\quad S_2T_{23}=S_3T_{32}.\end{aligned}\tag{4}$$

With the use of (4) we can express ξ_3 in terms of ξ_1 and T_1. The result is

$$\xi_3=\xi_1\left[\cos k_1l_1\left(\cos k_2l_2\cos k_1l_3-\frac{S_2\rho_2c_2}{S_3\rho_1c_1}\sin k_2l_2\sin k_1l_3\right)\right.$$

[1] Cf., e.g., Lindsay and White, J. Acous. Soc. Am. **4**, 155 (1932), particularly Eqs. (8) with necessary change in notation.

$$-S_1 \sin k_1 l_1 \left(\frac{\rho_1 c_1}{\rho_2 c_2 S_2} \sin k_2 l_2 \cos k_1 l_3 + \frac{1}{S_3} \cos k_2 l_2 \sin k_1 l_3 \right) \Bigg]$$

$$+T_1 \Bigg[\frac{\cos k_2 l_2}{\rho_1 c_1 \omega} \left(\sin k_1 l_1 \cos k_1 l_3 + \frac{S_1}{S_3} \cos k_1 l_1 \sin k_1 l_3 \right)$$

$$- \frac{\sin k_2 l_2}{\rho_2 c_2 \omega} \left(\frac{S_2 \rho_2^2 c_2^2}{S_3 \rho_1^2 c_1^2} \sin k_1 l_1 \sin k_1 l_3 - \frac{S_1}{S_2} \cos k_1 l_1 \cos k_1 l_3 \right) \Bigg]. \quad (5)$$

Suppose now that the points 1 and 3 are *nodes*. Then $\xi_1 = \xi_3 = 0$ and hence the coefficient of T_1 in (5) must vanish. The condition that 1 and 3 are nodes is therefore (taking the special case where $S_1 = S_3$)

$$\tan k_2 l_2 = - \frac{\tan k_1 l_1 + \tan k_1 l_3}{1/A - A \tan k_1 l_1 \tan k_1 l_3} \quad (6)$$

with $A = S_2 \rho_2 c_2 / S_1 \rho_1 c_1$. Let us now introduce the parameters η_1 and η_3 where

$$\begin{aligned} \tan \eta_1 k_1 l_1 &= A \tan k_1 l_1, \\ \tan \eta_3 k_1 l_3 &= A \tan k_1 l_3. \end{aligned} \quad (7)$$

This enables us to write (6) finally in the form

$$k_2 l_2 + \eta_1 k_1 l_1 + \eta_3 k_1 l_3 = n\pi, \quad (8)$$

where n is an integer and in particular is equal to unity if 1 and 3 are *successive* nodes. Eq. (8) can be used to calculate k_2 and hence c_2 from a knowledge of the physical quantities already specified and measurement of l_1, l_2, l_3.

Experimental Procedure

The bismuth single crystals used were grown by a method described by one of the authors in a previous paper[2] and hence no discussion of this need be given here. Two types of crystal orientation were employed, *viz.*, (1) the P_1 orientation in which the principal axis of the crystal is perpendicular to the length of the rod, and (2) the P_3 orientation with the principal axis parallel to the length of the rod. The crystal rods used were all of the order of 10 cm in length and 0.04 cm² in cross section.

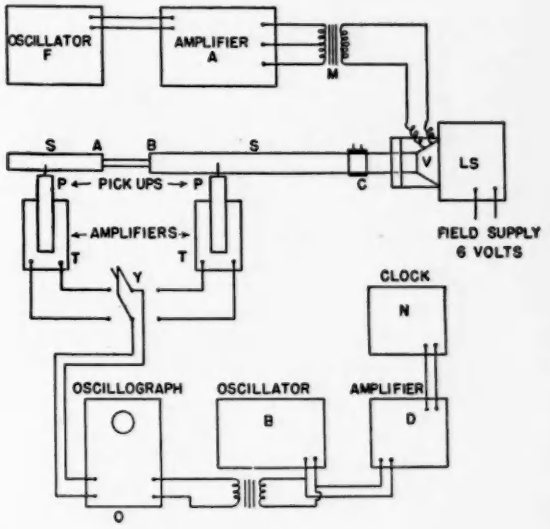

FIG. 2.

The actual experimental arrangement is indicated in Fig. 2 which shows the crystal rod AB soldered between two sections of steel, S and S'. The former section S is fixed by a collar C to a specially constructed voice coil attachment, V, of a dynamic speaker unit L. S. This was driven by a 15-watt amplifier, A, with a practically constant output over the audible range. The General Radio oscillator F gave a continuous variation of frequencies in the desired range with fair frequency stability.

As vibration detectors two piezoelectric (Rochelle salt) phonograph pick-ups (P in Fig. 2) were employed. These have a very nearly uniform response up to 12,000 cycles. Since their output is small it must be amplified. This was done by feeding the current into the amplifiers T, the first stage of which was located in a metal shielded can on top of which the pick-ups were mounted. In this stage a type 6C6 tube was used. The output of the amplifiers was impressed on the vertical plates of a cathode-ray oscillograph, O, through resistance coupling. By means of the double pole, double throw switch Y, the pick-ups could be connected in turn to the oscillograph. To measure the frequency of the

[2] Cf. A. B. Focke and J. R. Hill, Phys. Rev. **50**, 179 (1936).

vibrations of the crystal, the output of a beat frequency oscillator, B, was placed across the horizontal plates of the oscillograph. The frequency of this oscillator was varied between 700 and 1500 cycles until a simple Lissajous figure was observed on the fluorescent screen. This made possible the determination of the ratio of the frequencies of the crystal and the oscillator. At the same time the output of the oscillator was fed into a two-stage amplifier, D, which drove a 1000 cycle synchronous clock, N. If the time required by the second hand to make a complete revolution is denoted by t, the frequency of the oscillator is

$$\nu' = 60{,}000/t.$$

If μ is the Lissajous ratio the frequency of vibration of the crystal ν is then given by

$$\nu = \mu\nu'.$$

In the experimental procedure the rod S was set in vibration by the oscillator F through the voice coil V, the pick-ups P were moved along the rod and the nodal points noted. With the indicated arrangment it was possible to locate the nodes to within less than one millimeter. It was found that the nodes could be most easily located with the rod vibrating in a resonance mode.

The velocity of sound in steel enters into the formula (8). This was measured by the simple method of determining the distance between two successive nodes in the vibrating steel rod and using the relation $c = c_1 = \lambda_1\nu$. This simple method cannot, of course, be used successfully in general in the bismuth crystal because of the short length and great fragility of the latter.

TABLE I.

Crystal No.	Length in cm	Orientation	Freq. ν	l_1 cm	l_2 cm	l_3 cm	n (in Eq. (8))	c_2 in m/sec.
1	12.3	P_1	6860	16.8	12.3	22.3	2	2140
			6900	16.7	8.1	0	1	1848
			6950	17.2	7.5	0	1	1775
2	11.3	P_1	6860	16.55	7.8	0	1	1753
			7420	20.7	11.3	14.5	2	1900
3	10.8	P_1	10220	10.2	10.8	14.5	2	2130
			11520	17.1	10.8	41.1	3	2070
			8330	0	9.9	9.4	1	1910
			6850	16.7	9.2	0	1	2040
4	11.1	P_1	7490	0	6.9	17.0	1	2025
			11320	15.3	11.1	18.6	3	1960
			11840	19.2	11.1	14.0	3	2035
			4860	0	9.6	27.5	1	2050
5	11.6	P_3	6850	16.7	7.3	0	1	1525
			8520	17.65	11.6	27.0	3	1490
			8460	56.9	11.6	17.4	4	1460
			9270	2.9	11.6	13.5	2	1560
6	9.6	P_3	9270	4.4	9.6	18.4	2	1583
			10120	8.7	6.3	0	1	1630
7	11.0	P_3	6300	11.2	10.5	0	1	1500
			6780	15.7	8.0	0	1	1517
			11700	0	6.85	0	1	1610
			11280	0	6.8	0	1	1532

Results and Conclusions

The averaging of twelve measurements ranging in frequency from 3300 cycles to 8700 cycles gave for the velocity of the compressional wave in the steel rod used the value $c_1 = 5141$ meters/sec. All the individual values were within 1 percent of the mean.

The following data were used in the reduction of the experimental observations. For the steel $\rho_1 = 7.753$ gram/cm^3, $S_1 = 0.0445$ cm^2; for the bismuth crystal $\rho_2 = 9.83$ g/cm^3, $S_2 = 0.04$ cm^2.

In the application of the experimental measurements to Eq. (8) it was found desirable to use linear interpolation. To render this practicable without undue error it was necessary to take the readings in such a way that $k_1 l_1$ and $k_1 l_3$ are not close to 0 or $\pi/2$ (or higher multiples of $\pi/2$). In general it was found advantageous to have $\tan k_1 l_1$ and $\tan k_1 l_3$ differ in sign. Moreover the choice of $A < 1$ (by proper choice of the cross-sectional areas) helps to avoid large variations in c_2 due to small errors in the measurements.

The probable error of the frequency measurements was 0.25 percent, and that in the length measurement approximately 1 percent.

The bismuth crystals are extremely fragile and twin lamellae were apt to be produced by straining the crystal. Any twinning of a crystal in the P_1 orientation changes the orientation in the direction of the P_3 orientation and *vice versa*.

Seven crystals were tested, four in the P_1 orientation and three in the P_3. Table I contains the results of the measurements in the order in which they were actually carried out for each crystal. The occurrence of $l = 0$ in the table means that in the particular measurement concerned no node was used in the rod in question. The fundamental equation (8) still remains valid in this special case. The last two measurements listed are of interest because in them both nodes were located in the crystal, and the formula (8) thus reduces to a particularly simple form,

for l_2 in these cases is simply a half-wave-length. It will be observed that l_2 is equal to the actual length of the crystal only when $n>1$.

Examination of the table discloses that the velocity c_2 for the P_1 orientation is definitely greater than that for the P_3 orientation. Moreover, for all crystals save 1 and 2 the results for various frequencies and l values are reasonably consistent. In the case of crystal 1, the great discrepancy between the second and third values and the first (which agrees fairly well with the average of 3 and 4) can be accounted for by the assumption that the strain on the crystal produced twinning which would result in a lowering of c_2 in the direction of the value for the P_3 orientation. This assumption was verified by actual etching and microscopic examination of the crystal. A similar situation was found to exist in the case of crystal 2. With care, twinning was to a large extent avoided in the remaining cases and the velocities may be taken to represent those for relatively pure orientations.

TABLE II.

ORIENTATION	AVERAGE VELOCITY c_2	YOUNG'S MODULUS
P_1	2028 m/sec.	4.043×10^{11} dynes/cm^2
P_3	1541 m/sec.	2.245×10^{11} dynes/cm^2

Table II presents the final results with average velocities computed using crystals 3–7 inclusive. The corresponding values of Young's modulus $Y=\rho c^2$ are also included. These results are consistent with the known lattice structure of bismuth in the two orientations in question.

An Improved Method for Obtaining Photographs of Ripple Wave Actions

M. E. RAQUET AND F. R. WATSON
University of Illinois, Urbana, Illinois
(Received February 21, 1938)

THE use of ripple waves to show reflection, diffraction and other actions of waves is well known.[1] Light shining upward through the glass bottom of a tank containing a shallow layer of water will be modified by the waves on the water surface and will show a pattern of the waves when striking a frosted glass surface, of which photographs may be taken.

Figure 1 pictures the arrangement of the apparatus. Puffs of air directed perpendicularly against the surface of the shallow water in the tank set up waves that proceed outward in concentric circles. These are made visible stroboscopically by flashes of light that pass up through the glass bottom of the tank and cast a shadow of the waves on the frosted glass above the water. The puffs of air and the flashes of light are regulated by the number of holes in the rotating wheel. If both pass through the same ring of holes, the waves appear to stand still; that is, the waves are shown in one position by the flash of light and then all is dark until each wave moves forward to the position of its predecessor when another flash illuminates them. If the flashes of light come less frequently than the waves by passing the light through another ring with fewer holes, the waves appear to move forward slowly.

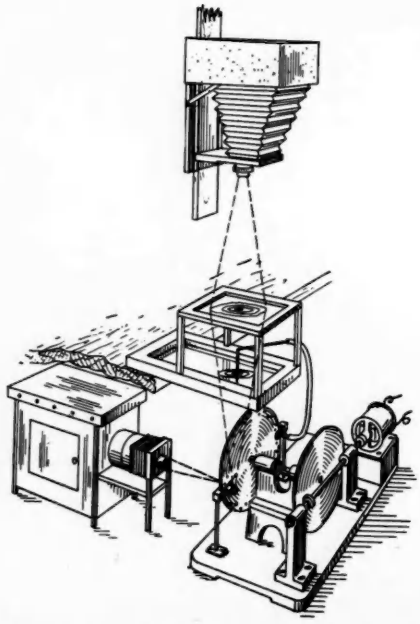

FIG. 1. Apparatus for photographing ripple waves.

[1] Vincent, Phil. Mag. **43**, 411 (1897); **45**, 191 (1898).

Figures 2 and 3 show the distorting effect of surface tension on the pattern of waves. In Fig. 2, two obstacles placed on the bottom of the tank to reflect waves project slightly above the water surface so that the water meniscus formed by the surface tension at the sides of the obstacles makes a sort of concave lens that distorts the direct light, while in Fig. 3, the water level is slightly above the top of the obstacles with a rounded edge of water, since the oily top of the obstacle prevents the water from covering it. Figs. 4 and 5 show clear outlines of the obstacles and no distortion of the waves; these being obtained by the method described later. Fig. 6 shows a photograph of waves in a miniature

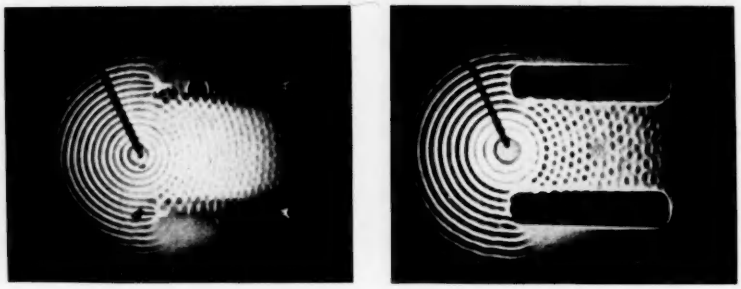

FIGS. 2 (left) AND 3 (right). Photographs showing distortion of water waves by surface tension. Fig. 2, Water too shallow. Fig. 3, Water too deep.

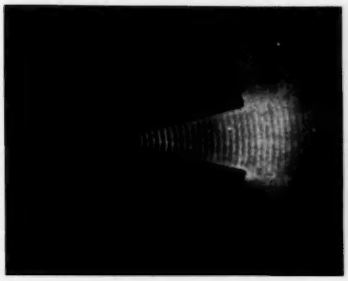

FIGS. 4 (top) AND 5 (bottom). Photographs of water waves without distortion. Fig. 4, megaphone with short waves. Fig. 5, diffraction with long waves.

FIGS. 6 (left) AND 7 (right). Photographs of auditorium models. Fig. 6, distortion due to surface tension. Fig. 7, surface tension distortion eliminated.

model of an auditorium. The irregular outline of the model is due to the surface tension action which draws the water into irregular drops. Water waves reflected from this irregular surface are distorted. Fig. 7 shows the same model with the surface tension effects overcome, with a clear outline of the model and a regular undistorted reflection of the waves.

The method followed in eliminating the surface tension distortion was as follows. The reflecting obstacles were made plane parallel. These were placed on the plate glass bottom of the tank which had been carefully leveled; then the water which completely covered the obstacles was slowly siphoned off until the layer of water over the obstacle was so thin that the waves could not pass but were completely reflected. (This suggestion was made to F. R. Watson by F. V. Hunt.) A series of photographs was made while the water was being lowered to secure the best condition,—too much water or too little water gave distorted photographs. It was necessary to clean the tank of all traces of oil, to use distilled water and to make the obstacles scrupulously clean. This latter condition was obtained by the application of a special cleaning solution of acid-alcohol (95 percent alcohol, 5 percent glacial acetic acid) using a clean cloth and not touching the objects with the fingers, which always seem to have some oil traces on them. This procedure was followed by washing the obstacles with plain alcohol and wiping them with a clean cloth, after which they were placed in the tank, covered with water, and photographs taken as described.

Letter to the Editor

A "Foaming Tone" Obtained from Vibrating Strings and Rods

In a contribution to the editor, the author states that a novel "foaming tone" may be obtained by two types of instrument, and suggests several different arrangements for generating the tones.

In one arrangement, a sonometer box is used that is 80 cm long, 30 cm wide, and is equipped with 154 strings of metal or silk with a space between adjacent strings of about 2 mm. When an operator scrapes a finger nail or small metal object across the strings, a foaming-like tone should be obtained, depending on the velocity of scraping. The strings can either be tuned in unison or adjusted to give 22 octaves, each octave being the same as every other octave and covering the same frequencies. As a substitute for the finger nail, a stream of air from a tube may be used.

In another type of construction, a row of teeth in a copper bar is drawn across a single string to generate the tones. The arrangement calls for 350 teeth in a copper bar, 1 meter long, 3 cm×3 cm in cross section, the teeth being confined in a space of 70 cm of the bar; the string being 80 cm long and is to be stroked at right angles at a point 8 cm from one end. For ease of operation, the bar should be equipped with a handle and a supporting guide. The teeth can be tuned in unison or in octaves. Various tones will depend on the velocity of scraping and on the segments of the string which are adjusted by hand.

The author states that he has obtained the tones by apparatus roughly similar to the suggested instruments; but adds that he is not acquainted with the musical principles, and that the details of arrangement await the advice of musicians. He "hopes that the problem will be investigated and completely developed."

TAI CHUNG-LING
(formerly named Tai Chen)

Soochow University,
Soochow, China,
October 15, 1937.

Acoustical Society News

THE Spring meeting of the Acoustical Society is to be held in Washington, D. C. on May 2–3, 1938. Those who attended the last Washington meeting will remember what an excellent program we had and will be glad to know that Mr. V. L. Chrisler is again in charge and is already laying plans for the Spring meeting. Address all correspondence pertaining to the meeting to Mr. V. L. Chrisler, Department of Commerce, National Bureau of Standards, Washington, D. C. The present plans call for a symposium on acoustic standards. On Monday evening a trip is planned through the Department of Justice Building, where we will hear about the "G-Men" and their work. The Wardman Park Hotel will be headquarters.

On March 14–15, a symposium on "Physics in the Automotive Industry," arranged by the American Institute of Physics, was held in Ann Arbor, Michigan, the department of physics of the University of Michigan acting as host.

The fall meeting of the Acoustical Society will be held in November at Harvard University, Cambridge, Massachusetts. Professor F. A. Saunders is Chairman of the Program and Arrangements Committee.

Current Publications on Acoustics

F. A. FIRESTONE

147 East Physics Building, University of Michigan, Ann Arbor, Michigan

Reviews of Contemporary Papers

MEMBERS who have occasion to translate important papers from foreign journals will be doing a real service to those members who do not read the foreign languages easily, if they will prepare a review of such articles for publication in this section.

These reviews should be of the nature of a lengthy abstract (500 to 1500 words) rather than a critique or apprais al, and should attempt to set forth in this limited space as much of the original author's contribution as possible. One or two figures may be included if desired.

To avoid duplication of effort it is desirable to arrange with the office of this department before writing a review.

On the Vibration Insulating by Means of Springs and Damping Materials. E. MEYER, L. KEIDEL. Zeits. f. techn. Physik **18**, 299–304 (1937).—To insulate vibrating apparatus, springs, layers of rubber or cork, etc., are used. Fig. 1 shows the equivalent diagram and the electrical

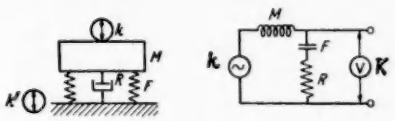

FIG. 1. Mechanical and electrical analogy of an insulated vibrating system.

analogy of an insulated vibrating system. "k" is the periodic force producing the vibration, M the mass of the system, F its compliance, R the dissipation resistance and K the force exerted on the ground. Using a logarithmic scale, the transmission U will be given by

$$U=10\log_{10}\left|\frac{K}{k}\right|^2=10\log_{10}\frac{R^2+1/\omega^2F^2}{R^2+(\omega M-1/\omega F)^2}.$$

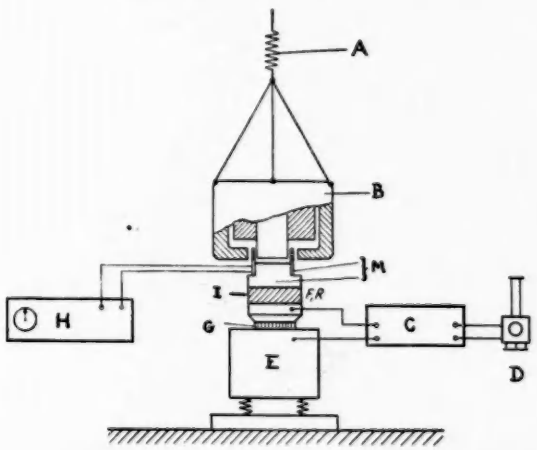

FIG. 2. Experimental arrangement. *A*, suspension; *B*, pot shaped magnet; *M*, moving coil, vibrating mass (aluminum or iron); *C*, amplifier cog valve voltmeter; *D*, recording instrument; *E*, case plate; *G*, quartz crystal; *H*, heterodyne oscillator; *I*, test piece.

Putting

$$\omega_0=1/(MF)^{\frac{1}{2}},\qquad \alpha=\omega_0/\omega,\qquad \beta=R/(M/F)^{\frac{1}{2}}$$

this can be written

$$U=10\log_{10}(\alpha^2\beta^2+\alpha^4)/[\alpha^2\beta^2+(1-\alpha^2)^2]. \quad \text{db.}$$

When $\alpha=\omega_0/\omega=1$, the transmission curve shows a resonance peak, and for $\omega/\omega_0=1/\alpha=\sqrt{2}$, $k=K$, everything is the same as if the system would not be insulated. For greater values of ω/ω_0, the transmission decreases at a rate which is the greater the smaller R. For most of the materials used in practice, R is not a fluid resistance, but is due to hysteresis in the material and consequently decreases as $1/\omega$ approx. Then $\alpha\beta=\gamma$ is a constant, and for $\omega/\omega_0>\sqrt{2}$ the transmission becomes practically independent of R, decreasing 12 db for the frequency twice as great. Fig. 2 represents the experimental arrangement. A moving coil in the air gap of a pot shaped magnet serves as generator. The force exerted on the base plate is registered by means of a quartz crystal and a logarithmic voltmeter. The mechanical parts have been cemented together to ensure close contact, and great care had to be taken to avoid resonances. Leaving out the test piece (short circuit test) the force exerted on the quartz crystal should be independent of the frequency, which gives a means of controlling the working of the apparatus.

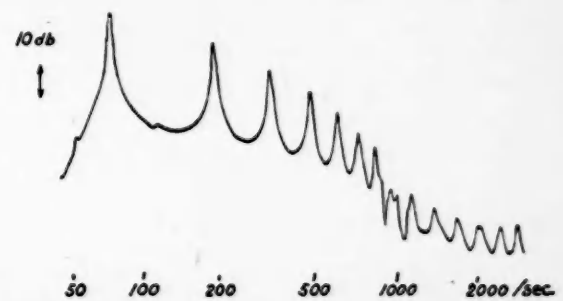

FIG. 3. Transmission curve for a spring insulating.

Figure 3 gives a record obtained with a screw-spring insulating. The great number of resonances greatly decreases the vibration insulation. They are still present, if the fundamental period of the system is lowered by means of a heavier mass. Only a specially constructed annular spring showed the exact insulation as demanded by the theoretical curve. Also layers of cork and rubber have natural periods of their own, which will fall into the working range if the layer is thick. The lowest natural frequency of such a system is proportional to the thickness of the layer, whilst the first resonance of the layer occurs, when its thickness is equal to $\lambda/2$, λ being the wave-length in the particular material. The transmission curve for hair felt shows a very damped resonance peak, and the insulation is not good, even for high frequencies. Apparently the dissipation mechanism of felt is different from the usual hysteresis loss. Fiber board shows a nonlinear behavior but its insulation is good (nonlinear resonance curve). A mechanical low pass filter consisting of four sections gave a very great decrease of the transmission for the higher frequencies. Each section was made up of a mass ($M=600$ grams) and a compliance (rubber disk, 4 ohms dia., thickness 10 mm).

In conclusion, it can be said that above the fundamental resonance, springs or layers of rubber or cork insulate equally well (12 db increase in the insulation for a frequency twice as great), but if the material has any additional resonances within the frequency range under consideration the transmission is greatly increased.

E. J. SKUDRZYK

The Theoretical Derivations of the Laws of Reverberation. H. CREMER, L. CREMER. Akustische Zeits. **2**, 225–241, 296–302 (1937).—This paper gives a critical survey of the various methods of deriving the reverberation formulae, pointing out the approximations and the limits of validity in every case.

(1) To obtain Sabine's law on statistical considerations, it is necessary to assume that every ray of sound crosses all points of space, and that it crosses every one of them in all directions. This last assumption is not necessary if the so called cosine law holds for the absorber:

$$a^1(\vartheta) = -\log\,[1-a(\vartheta)] = \text{constant}/\cos\vartheta,$$

where $a(\vartheta)$ is the absorption factor of the wall and ϑ the angle of incidence. a^1 is generally called the absorption exponent. Let us prove this for a rectangular chamber the edges of which are l_1, l_2, l_3. Let $\cos\vartheta_1$, $\cos\vartheta_2$, $\cos\vartheta_3$ be the direction cosines of the sound ray with regard to the three faces. (The same ray always strikes the same face under the same angle of incidence.) Then the number of times the ray will strike the three walls during one second will be given by

$$c\cos\vartheta_1/2l_1, \qquad c\cos\vartheta_2/2l_2, \qquad c\cos\vartheta_3/2l_3,$$

respectively. Hence we obtain for the energy at the time t

$$T_t = T_0(1-a_{10})^{c\cos\vartheta_1 t/2l_1}(1-a_{11})^{c\cos\vartheta_1 t/2l_1} \cdots (1-a_{3l})^{c\cos\vartheta_3 t/2l_3}. \quad (1)$$

where a_{10}, $a_{11}\cdots a_{30}$, a_{3l} are the absorption factors of the six walls. This can be written

$$T_t = T_{0l}^{-2\delta t} \quad \text{with} \quad 2\delta = (c/4V)\sum_n 2a_n(\vartheta_n)\cos\vartheta_n F_n. \quad (2)$$

Different rays will thus be damped differently, according to their angle of incidence. Only if (1) holds δ becomes independent of ϑ and Sabine's formula holds exactly. Most of the absorbers show an increase of absorption with the angle of incidence so that the cosine law frequently will be a fair approximation.

(2) If our calculations are based on the wave equation, reverberation is identified with the dying out of the damped modes of vibration. Let us first consider the natural functions of an undamped rectangular chamber. They are

$$\cos k_1 x \cos k_2 y \cos k_3 z\, l^{i\omega_\nu t} \qquad (k_\nu = n_\nu\pi/l_\nu).$$

Every one of these can be decomposed into eight waves of the form

$$l^{i(\pm k_1 x \pm k_2 y \pm k_3 z + \omega t)}.$$

The resonance frequencies are given by

$$f = (c/2)[(n_1/2l_1)^2 + (n_2/2l_2)^2 + (n_3/2l_3)^2]^{\frac{1}{2}}.$$

They can be obtained graphically as the distance from the origin to a point n_1, n_2, n_3 of a rectangular network, the units of which are $c/2l_1$, $c/2l_2$, $c/2l_3$ in the x, y, and z direction, respectively. The direction of the resonance in space is the same as that of the ray connecting the origin to the corresponding point of the network. If the frequency is large, the number of resonances between the frequencies f and $f+\Delta f$ asymptotically is equal to the volume contained in an octant of the spherical shell with the radii f and $f+\Delta f$, divided by $(c/2)^3(1/l_1)(1/l_2)(1/l_3)$, the volume of one cell of the network. Similarly the number of resonances between f and $f+\Delta f$ in the direction $\Delta\Omega$ is asymptotically given by

$$\Delta n = \frac{f^2\Delta f\Delta\Omega}{(c/2)^3(1/l_1)(1/l_2)(1/l_3)} = \frac{8V}{c^3}f^2\Delta f\Delta\Omega$$

and this is independent of the angle Ω, no particular direction being favored in the limit. Thus every mode of vibration leads to a uniform distribution of energy and the sound field is diffuse, if within a certain frequency range the modes are excited with equal amplitudes. These considerations are not limited to a rectangular chamber, but as can be shown apply to any shape of space.

(3) M. J. Strutt introduces a resistive force $r(xyz)v$, "v" being the particle velocity. Using Rayleigh's method for small perturbations, his results are obtained as follows: The energy dissipated each second in the whole space is

$$N = \int r(x, y, z)v^2(xyz)\,dV$$

and the total energy will be given by

$$EV = \int \rho v^2(x, y, z)\,dV,$$

where E is the average energy density. Putting

$$v^2 = v_0^2 l^{-2\delta t}$$

we get $$N = -(d/dt)(EV) = 2\delta EV.$$

Hence $$2\delta = \int r v^2 dV / \rho \int v^2 dV.$$

If the energy density is uniform and $r(xyz)$ spread over a number of wave-lengths, v^2 can be canceled out in numerator and denominator, giving Strutt's formula

$$2\delta = \int r dV / \rho V. \qquad (3)$$

For porous absorbers of thickness d_n and area F_n we get, performing the integration,

$$2\delta = \frac{c}{4V} \Sigma \frac{4 r_n d_n}{\rho c} F_n.$$

It follows from above that d_n should be a few wave-lengths but in no case less than $\lambda/4$. Also, the energy calculation was based on the undisturbed vibration which is only allowable if $(r/\rho\omega) \ll 1$. Under these conditions (3) may even be used to calculate the frequency variation of the absorption of porous absorbents. There is no difficulty in showing that the cosine law

$$a^1(\vartheta) = 2rd/\rho c \cos \vartheta$$

applies to such absorbers.

(4) Schuster and Waetzmann introduce a complex wall resistance and Van den Dungen derived the reverberation formula for great values of wall impedance, with the aid of a perturbation method. The exponential law is found to hold, if the wall resistance is independent of the angle of incidence. This takes the place of the previously mentioned cosine law, and always holds for porous absorbents of large streaming resistance at the low frequencies. For other values of streaming resistance and frequencies deviations from Sabine's law are to be expected.

(5) The rectangular chamber lends itself to calculation, even if any wall resistance is admitted. The general solution of the wave equation can again be split up into eight waves of the type

$$l^{\pm(ik_1 - s_1)x \pm (ik_2 - s_2)y \pm (ik_3 - s_3)z + (i\omega - \delta)t}.$$

By a few calculations we get (2) again. The only assumption we require is that

$$(s_1^2 + s_2^2 + s_3^2)^{\frac{1}{2}} \ll (k_1^2 + k_2^2 + k_3^2)^{\frac{1}{2}},$$

which is true in all practical cases. Previously we have derived Eq. (2) for very short wave-lengths; we now find that this equation is still valid even if the wave-length is of the same order of magnitude as the dimensions of the chamber.

The authors also treat the case of a prismatic chamber the cross section of which is a right angled bilateral triangle. Such a chamber results if one of square section is divided into two halves along the diagonal. The partition wall has no effect on the sound field, as the particle velocity perpendicular to it is zero (the two resonances of the square chamber which have the same frequency but different directions being excited equally). Hence such a triangular chamber has the same natural frequencies as the square chamber. The triangular chamber is of practical importance, as it is free from flutter echoes.

(6) The rectangular chamber could be used to determine the absorption factor at low frequencies and various angles of incidence. This would be done by exciting one mode at the time, measuring the reverberation time and calculating the corresponding angle of incidence.

E. J. SKUDRZYK

Construction and Investigation of a Damped Room. W. JANOVSKY, F. SPANDÖCK. Akustische Zeits. **2**, 322–331 (1937).—The cross section of the damped room is irregular, approaching the shape of a triangle. Its sides are about 8 m long and the distance floor to ceiling is 3 m. The walls are lined with Heraklith plates, then comes a 10 cm thick layer of slag wool, a 10 cm layer of cotton wool and finally a 30 cm layer of cotton wadding suspended edgewise. The slag wool is held in position by means of a wire grating which at the same time acts as electrical screen. Perpendicular to the wall, strips of wire gauze are fixed at distances of one meter. Their object is to prevent the rapid spread of fire. They are supposed to act similar to Davy's safety lamp.

A measurement of the propagation along the axis of the room gave the same results as have already been described by E. H. Bedell in this journal.[1] The free air propagation could be obtained up to a distance of $2\frac{1}{2}$ m, the point source being placed in the middle of the room. For greater distances the pressure decreased at a greater rate than $1/r$. E. H. Bedell suggested that along the damped surface the wave velocity is reduced, and the

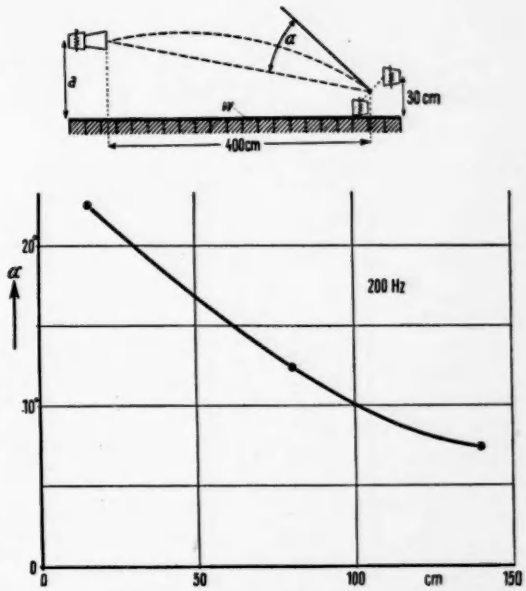

FIG. 1. Difference between the acoustical and optical angle of incidence plotted against the height of the loudspeaker from the floor.

wave front bent or diffracted towards the absorbing surface, more energy being absorbed than if the wave remained spherical. To prove this, the height of a loudspeaker was varied from 15 to 150 cm whilst the angle of incidence at which the sound was striking the floor was determined, at a distance of 4 m from the speaker. This was done by means of two microphones one close to the floor, the other movable in a plane 30 cm from the ground. The output of the two separate microphone amplifiers was coupled together in antiphase and the movable microphone adjusted to the minimum of loudness. This gave the planes of equal phase and hence the direction of the incident sound. The result is represented in Fig. 1. A quantitative idea of the equivalent damping due to the bending of the waves could be obtained by measuring the intensity of sound whilst the height of sound source and receiver were varied. The result depends to a great extent on the directional characteristics of the sound source. On the other hand a loudspeaker of uniform direction characteristics showed marked directivity when placed close to the damped wall.

Finally the absorption coefficient of the damped wall was measured. The loudspeaker was placed at the floor and the microphone suspended at a mean height. A short electrical impulse was sent through the loudspeaker coil, and the microphone output, corresponding to the direct impulse and its first reflection, was oscillographed. 14 percent of the pressure amplitude was reflected, giving an absorption coefficient of 98 percent.

E. J. SKUDRZYK

[1] E. H. Bedell, J. Acous. Soc. Am. **8**, 118–125 (1936).

Magnetic Strip Recording with Tapes and Circular Recording and Reproducing Heads. H. LÜBECK, Akustische Zeits. **2**, 273–295 (1937).—The object of this work was to investigate the circular recording and reproducing heads in conjunction with nonmagnetic tapes covered with ferromagnetic powder.

The circular recording head (recording horseshoe magnet) consists of a ferromagnetic ring with a very narrow air gap (0.03 mm), the ring carrying a coil. The ring is usually made from isoperm, but it is shown in this publication that much better results can be obtained with substances that have a very large permeability, remanence being reduced to a negligible value by means of an additional air gap. The flux leaking out from the air gap, and only that portion, magnetizes the tape which is drawn in front of it. Such an arrangement leads to a very sharp definition of the magnetic field in front of the air gap, and with quite simple means tape velocities as low as 60 cm/sec. still give a linear reproduction of the frequency range 50–10,000 c/sec. Nonmagnetic tapes covered with ferromagnetic powders are of advantage as they are cheaper and lighter than steel wire and at a junction they are simply pasted together. Even after playing a tape 10,000 times wearing could hardly be noticed.

The recorded sound is erased by magnetizing the tape to about its saturation value. By means of an additional d.c. current in the recording head, when the next recording takes place, the new working point is brought back to the straight portion of the magnetization characteristics.

A consideration of the magnetic intensity following one particle of the tape leads to an expression for the highest frequency recorded without great distortion. This frequency is proportional to the tape velocity and inversely proportional to the a.c. amplitude of the recording current, and is the greater the sharper the magnetic definition of the air gap. It is therefore necessary to reduce the a.c. amplitudes when recording high frequencies. These conclusions are confirmed by measurements. A consideration of the erasing and recording process leads to an analysis of the most favorable working point and shows that the minimum of distortion corresponds to a maximum of intensity on the record. It is found that the hysteresis loop of the tape is a direct characteristic of the recording process.

The receiving head is similar to the recording head. For an understanding of the receiving process the tape is best considered as a series of elementary magnets. Those facing the air gap send a magnetic flux through the induction coil, those opposite the solid portion of the ring are short circuited by the latter. A short calculation gives an approximate expression for the e.m.f. induced in the receiving head and extensive measurements show how to correct it. It is found that the induced e.m.f. essentially is determined by the wave-length recorded on the tape and the tape velocity, also that there is a certain amount of demagnetization taking place, increasing exponentially with the frequency, at a rate which is the greater the higher the permeability of the tape. For small slits the frequency response becomes independent of the length of the air gap.

The ferromagnetic powder on the tape is not quite uniform, therefore, there is a certain amount of background noise, but it is hoped, that improvement in this respect soon will be obtained.

E. J. SKUDRZYK

CORRECTION

Disturbance Produced by Nonlinear Distortion. H. J. V. BRAUNMUHL AND W. WEBER. Akustische Zeits. **2**, 135–147 (1937). In the review of this paper published in this journal (**9**, 170 (1937)) it was stated that the sounds were picked up from high quality records, whereas the authors inform us that the sounds were picked up directly from the studios.

References to Contemporary Papers on Acoustics

MOST of the titles of papers appearing in other languages than English have been translated; the clue as to the language in which the article is written can usually be found by noting the name of the journal in which it appears. Abstracts in English of many foreign papers have appeared or soon will appear in Science Abstracts, Section A. Where references are made to Science Abstracts, the reference is to the volume number and abstract number. The abbreviations of the names of journals are those used in Science Abstracts and can be found in any annual index to those abstracts.

The numbers appearing at the head of each entry are the numbers which identify the subject headings in the Cumulative Index of this journal which is to appear soon.

---

2. Architectural Acoustics

2.3 **Investigation of Vibration of City Hall in Philadelphia and of the Subway Structure Beneath.** J. E. Shrader. J. Frank. Inst. **224**, 757–766 (1937).

2.4 **Construction and Investigation of a Damped Room.** W. Janovsky and F. Spandöck. Akustische Zeits. **2**, 322–331 (1937). (See review in this issue.)

2.7 **Reverberation Control. How to add echo, without distortion, to sound movie tracks.** John K. Hilliard. Electronics **11**, 15, Jan. (1938).

2.7 **The Theoretical Derivations of the Laws of Reverberation.** H. Cremer and L. Cremer. Akustische Zeits. **2**, 225–241, 296–302 (1937).

2.9 **Technical Researches on the Sound Transmission of Wall Constructions.** Claus Feck. (Book, in German.) (T. H. Braunschweig, 1936.)

2.9 **The Transmission of Sound Through Multiple Metal Partitions.** L. Renault. Revue d'Acoustique **6**, 69–101, May–July (1937).

4. Ear and Hearing

4.1 **Transient Sound Phenomena.** H. Backhaus. Ergeb. d. exakt. Naturwiss. **16**, 237–294 (1937). Sci. Abs. 5415 (1937).

4.6 **On Loudness and Pitch.** Marek Kwiek. Akustische Zeits. **2**, 170–178 (1937).

4.9 **On Loudness and Pitch.** Marek Kwiek. Akustische Zeits. **2**, 170–178 (1937).

5. Instruments and Apparatus. Applied Acoustics

5.1 **Acoustical Interferometers.** H. K. Schilling. Am. Phys. Teacher **5**, 280–282 (1937).

5.1 **Action of Intense Sounds on Molten Metal.** G. Schmid and L. Ehret. Zeits. f. Elektrochem. **43**, 869–874, Nov. (1937). Sci. Abs. 5408 (1937).

5.1 **Flame as a Tone Amplifier.** Z. Gyulai. Zeits. f. Unterr. **50**, 146–147 (1937).

5.1 **A Projection Apparatus for Compounding Harmonic Vibrations.** R. M. Archer. J. Sci. Inst. **14**, 408–410 (1937).

5.1 **A Mechanical Analyzer for the Solution of Secular Equations and the Calculation of Molecular Vibration**

5.1 **Acoustic Vibrations and Internal Combustion Engine Performance. I. Standing Waves in the Omtale Pipe System.** Philip M. Morse, R. H. Boden and Harry Schecter. J. Appl. Phys. **9**, 16–23 (1938).

5.1 **Demonstration Apparatus for Wave Motion; Group and Phase Velocities.** (In German). H. Greinacher. Helv. Phys. Acta. **10**, 490–494 (1937).

5.1 **Study of Vibrated Concrete.** Tucker, Pigman, Pisapia, and Rogers. Nat. Bur. Stand. J. Research. **19**, 575–592 (1937).

5.1 **An Anomaly in the Elastic Behavior of India Rubber.** A. N. Puri. (In English.) Nat. Acad. Sci. India. **7**, 45–51 (1937).

5.2 **Flame as a Tone Amplifier.** Z. Gyulai. Zeits. f. Unterr. **50**, 146–147 (1937).

5.3 **Advanced Laboratory Experiments in Acoustics, Including a New Method for Measuring the Absorption of Sound in Tubes.** C. K. Stedman. Am. Phys. Teacher **5**, 252–259 (1937).

5.4 **Frequency Discrimination by Inverse Feedback.** George H. Fritzinger. I. R. E., Proc. **26**, 207–225, Feb. 1938.

5.4 **A New Type of Selective Circuit and Some Applications.** H. H. Scott. I. R. E., Proc. **26**, 226–235 (1938).

5.7 **A Direct-Reading Pitch Recorder and its Applications to Music and Speech.** (In English.) J. Obata and R. Kobayashi. Imp. Acad. Japan, Proc. **13**, 247–250 (1937).

5.9 **On the Distortion of Low Frequency Condenser Microphones.** Arch. f. Elektrot. **31**, 487–494 (1937).

5.9 **Construction and Investigation of a Damped Room.** W. Janovsky and F. Spandöck. Akustische Zeits. **2**, 322–331 (1937). (See review in this issue.)

5.10 **Optimum Frequency for Sound Signals.** W. Janovsky and A. Rechten. Wiss. Veroff. a. d. Siemens-Werken. **16**, 84–91 (1937). Sci. Abs. 5951 (1937).

5.11 **A New Type of Selective Circuit and Some Applications.** H. H. Scott. I. R. E., Proc. **26**, 226–235 (1938).

5.12 **Cathode-Ray Phasemeter.** S. Bagno and A. Barnett. Electronics **11**, 24 (1938).

5.14 **On the Steady Force of a Sound Field on Suspensions of Particles Not Spherical in Shape.** R. Pohlman. Zeits. f. Physik **107**, 497–508 (1937).

5.16 **Magnetic Strip Recording with Tapes and Circular Recording and Reproducing Heads.** H. LUBECK. Akustische Zeits. **2**, 273–295 (1937). (See review in this issue.)

5.16 **A Turntable Wobble Indicator.** WILLIAM F. WICHART. Electronics **11**, 13 (1938).

5.16 **Reverberation Control.** How to add echo, without distortion to sound movie tracks. JOHN K. HILLIARD. Electronics **11**, 15 (1938).

5.16 **A Magnetic Recorder.** T. J. MALLOY. Electronics **11**, 30 (1938).

6. MUSICAL INSTRUMENTS AND MUSIC

6.1 **Transient Sound Phenomena.** H. BACKHAUS. Ergeb. d. exakt. Naturwiss. **16**, 237–294 (1937). Sci. Abs. 5415 (1937).

6.5 **On the Self-Oscillation of Jets entering the Same Medium.** F. J. BOURRIERES. Comptes Rendus. **205**, 111–113 (1937).

6.6 **The Natural Vibrations of Inhomogeneous Strings.** K. KARAS. Akad. Wiss. Wien. Ber. **145**, 797–826 (1936).

7. NOISE

7.1 **Methods and Results of Subjective and Objective Noise Measurements.** ERNEST LUBCKE. Naturwiss. **26**, 17–20 (1938).

7.6 **On the Problems of Preventing Vibration** (1st report). (Using Paper, Gum, Cloth, Sand, Compressed Pith of Kaoliang, etc. as Damping Materials.) Trans. Soc. Mech. Eng. Japan. **3**, 103–109 (1937).

7.7 **Attenuation of the Intake and Exhaust Noises of Diesel Engines in Ships.** M. PIENING. Zeits. d. Ver. d. Ing. **81**, 770–776 (1937).

7.7 **A Proposed Test Code for Apparatus Noise Measurement.** Electr. Engineering **56**, 1079–1082 (1937).

9. SPEECH AND SINGING

9.1 **Beginning of a Vowel Sound and Shock of the Glottis.** W. TRENDELENBERG. Preuss. Akad. Wiss. Berlin. Ber. **13**, 127–143 (1937). Sci. Abs. 5050 (1937).

10. SUPERSONICS

10.1 **Relation Between Frequency and Sound Absorption in Aerosols.** O. BRANDT. Kolloid Zeits. **81**, 2–6 (1937). Sci. Abs. 5406 (1937).

10.1 **Employment of Supersonics in Colloidal Investigations.** H. A. WANNOW. Kolloid Zeits. **81**, 105–113 (1937).

10.1 **Ultrasound and its Scientific and Technical Applications.** LUDWIG BERGMANN. (Book.) Berlin. VDI-Verlag GmbH. (1937).

10.1 **Bibliography on Supersonics.** HARRY SCHECTER. Electronics **11**, 34 (1938).

10.1 **Note on the Paper "On an Interference Phenomenon with Ultrasonic Waves."** E. SCHREUER AND K. OSTERHAMMEL. Zeits. f. Physik. **107**, 560 (1937).

10.1 **On Periodicity of Diffracted Images of Ultrasonic Waves.** E. HIEDEMANN AND E. SCHREUER. Zeits. f. Physik **107**, 463–473 (1937).

10.1 **The Chemical Action of Ultrasound.** L. R. SSOLOWJERVA. Shurnal technitscheskoi Fisiki (Russian) **6**, 2059–2064 (1936).

10.1 **A Remark on the Absorption of Ultrasound in Tubes.** J. CLAYS AND H. SACK. (In German.) Bull. Belgique. (5) **23**, 659–671 (1937).

10.1 **The Intramolecular Vibrations in Gases and Mixtures Excited by Collisions. IV. Sound Dispersion and Absorption Measurements in N_2O and CO_2 at High Temperatures.** A. EUCKEN AND E. NUMANN. Zeits. f. phys. Chem. **B36**, 163–183 (1937).

10.1 **Measurement of Elastic Constants with Ultrasound.** L. BERGMANN. Zeits. d. Ver. d. Ing. **81**, 878–882 (1937).

10.2 **Experimental Determination of Ultrasonic Velocity in Several Gases at Pressures Between One and One Hundred Atmospheres.** ALFRED H. HODGE. J. Chem. Phys. **5**, 974–977 (1937).

11. WAVES AND VIBRATIONS

11.1 **Acoustic Vibrations and Internal Combustion Engine Performance. I. Standing Waves in the Intake Pipe System.** PHILIP M. MORSE, R. H. BODEN AND HARRY SCHECTER. J. Appl. Phys. **9**, 16–23 (1938).

11.3 **On the Pressure of Acoustical Radiation.** (In French.) A. D. FOKKES. Physica **5**, 31–38 (1938).

11.3 **A Method of Measuring the Velocity of Sound in Air.** (60 pulses per second detected by cathode ray oscillograph.) R. C. COLWELL, A. W. FRIEND, AND D. A. MCGRAW. Paper No. 60 on Program for Feb. 1938 meeting of Am. Phys. Soc. See Phys. Rev.

11.5 **The Shock Wave and Explosion Products from Detonating Solid Explosives.** W. PAYMAN AND D. W. WOODHEAD. Proc. Roy. Soc. **163**, 575–591 (1937).

11.5 **Action of Intense Sounds on Molten Metal.** G. SCHMID AND L. EHRET. Zeits. f. Elektrochem. **43**, 869–874 (1937). Sci. Abs. 5408 (1937).

11.5 **Acoustic Radiation Pressure and Waves of Large Amplitude.** E. F. GHIRON. Alta Frequenza, **6**, 640–653 (1937). Also (in French) in Revue d'Acoustique. **6**, 118–127 (1937). Sci. Abs. 5045 (1937).

11.6 **Speed of Pulses Along Tubes with Elastic Walls—An Artificial Artery.** NOEL C. LITTLE. Am. Phys. Teacher **6**, 30–32 (1938).

11.6 **Advanced Laboratory Experiments in Acoustics, Including a New Method for Measuring the Absorption of Sound in Tubes.** C. K. STEDMAN. Am. Phys. Teacher **5**, 252–259 (1937).

11.7 **The Calculation of the Natural Vibrations of Spherical Shells.** K. FEDERHOFER. Akad. Wiss. Wien. Ber. **146**, 57–50 (1937).

11.7 **The Natural Vibrations of an Axially Compressed Circular Cylindrical Shell.** K. FEDERHOFER. Akad. Wiss. Wien. Ber. **145**, 681–688 (1936).

11.7 **The Natural Vibrations of Inhomogeneous Strings.** K. KARAS. Akad. Wiss. Wien. Ber. **145**, 797–826 (1936).

11.7 **Variable Frequency Electric Circuit Theory with Application to the Theory of Frequency Modulation.** JOHN R. CARSON AND THORNTON C. FRY. Bell System Techn. J. **16**, 513–540 (1937).

11.7 **Theoretical and Experimental Research on the Transverse Vibrations of Free Elliptical Plates.** BOHUSLAV PAVLIK. Zeits. f. Physik **107**, 458–462 (1937).

11.7 **On the Steady Force of a Sound Field on Suspensions of Particles Not Spherical in Shape.** R. POHLMAN. Zeits. f. Physik **107**, 497–508 (1937).

11.7 **Verification of Stokes' Theory of a Sphere Oscillating in a Liquid.** (In English.) D. S. SUBRAHMANYAM. Indian J. Phys. **11**, 307–318 (1937).

11.7 **Effects of Tuned Circuits Upon a Frequency Modulated Signal.** HANS RODER. I. R. E., Proc. **25**, 1617–1647 (1937).

11.7 **A Mechanical Analyzer for the Solution of Secular Equations and the Calculation of Molecular Vibration Frequencies.** D. P. MACDOUGALL AND E. BRIGHT WILSON, JR. J. Chem. Phys. **5**, 940–944 (1937).

11.7 **The Phenomenon of Auto-Oscillation in Acoustics.** Y. ROCARD. Revue d'Acoustique **6**, 102–117 (1937).

11.7 **On the Self-Oscillation of Jets entering the Same Medium.** F. J. BOURRIERES. Comptes Rendus. **205**, 111–113 (1937).

11.7 **Research on the Transverse Vibrations of Rhombic Plates with Free Edges.** BOHUSLAV PAVLIK. Akustische Zeits. **2**, 161–169 (1937).

11.7 **Resonance and Non-Linear Oscillations.** R. IGLISCH. Zeits. f. angew. Math. u. Mechanik. **17**, 249–258 (1937). Sci. Abs. 5403 (1937).

11.7 **The Differential Equations of Sound Fields.** OTTO HEYMAN. Akustische Zeits. **2**, 193–202 (1937).

11.7 **The Frequencies and Nodal Systems of Circular Plates.** R. C. COLWELL AND H. C. HARDY. Phil. Mag. **24**, 1041–1054 (1937).

11.7 **Fourier Expansions obtained Operationally.** N. W. MCLACHLAN. Phil. Mag. **24**, 1055–1058 (1937).

11.7 **Radial and Torsional Vibrations of Annular Quartz Plates.** A. ZACEK AND V. PETRZILKA. Phil. Mag. **25**, 164–174 (1938).

11.7 **On the Pressure of Acoustical Radiation.** (In French.) A. D. FOKKES. Physica **5**, 31–38 (1938).

11.7 **The Shock Wave and Explosion Products from Detonating Solid Explosives.** W. PAYMAN AND D. W. WOODHEAD. Proc. Roy. Soc. **163**, 575–591 (1937).

INDEX TO VOLUME 9

A

ABBOTT, E. J.: On the Noise Inspection and Noise Rating of Mechanical Equipment, (Abstract) 272
ACOUSTICAL SOCIETY NEWS: 59, 165, 270, 354
ARTS, JAN: Sound of Bells, 344–347

B

BACHEM, A.: Various Types of Absolute Pitch, 146–151
BELL, D. T.: New Continuous Frequency Audiometer, (Abstract) 76
BLACK, R.: (see Muller, G. G.) 273
BLOOMENTHAL, S.: Amplification of Sound Received by Horns, (Abstract) 77
BOOK REVIEWS
VIBRATIONS AND SOUND, Philip M. Morse, 59
OBJECTIVE ANALYSIS OF MUSICAL PERFORMANCE, Carl E. Seashore, 165
SOUND, Arthur Taber Jones, 165
SOUND WAVES, THEIR SHAPE AND SPEED, Dayton Clarence Miller, 166
BRAY, CHARLES W.: (see Wever, Ernest Glen) 227–233
BRUDERLIN, HENRY H.: Sound Frequencies from an Airplane Exhaust System, (Abstract) 77

C

CARY, B.: Some Acoustic Problems of the Automotive Fan, (Abstract) 272
COOK, JACKSON H.: (see Kennelly, A. E.) 336–340
COOP, J. J.: Tones Produced by a Wire Placed in an Ignited Gas Jet, 321–330
COTTON, JACK C.: Vocal Resonance and Puff Oscillations, (Abstract) 78
COWAN, MILTON: (see Lewis, Don) (Abstract) 79
CURRENT PUBLICATIONS ON ACOUSTICS
Reviews of Contemporary Papers, 51–56, 168–172, 265–268, 355–358
References to Contemporary Papers on Acoustics, 56–58, 172–174, 268–270, 359–361

D

DAVIS, H.: (see Newman, E. B.) 107–118
DAVIS, T. E.: (see Muller, G. G.) 273
DORSEY, H. G.: Demonstration of Dorsey Fathometer, (Abstract) 74

F

FAIRBANKS, GRANT: (see Lewis, Don) (Abstract) 79
FARNSWORTH, D. W.: (see Herriott, W.) (Abstract) 274
FARNSWORTH, PAUL R.: Approach to the Study of Vocal Resonance, 152–155
FIRESTONE, F. A.: (see Trimmer, J. D.) 24–29
—— Current Publications on Acoustics, 51–58, 168–174, 265–270, 355–361
FLETCHER, HARVEY: Loudness, Masking and Their Relation to the Hearing Process and the Problem of Noise Measurement, 275–293
FLETCHER, HARVEY AND W. A. MUNSON: Relation Between Loudness and Masking, 1–10; (Abstract) 78
FOCKE, A. B.: (see Lindsay, R. B.) (Abstract) 76
——, R. B. LINDSAY AND C. R. WILKS: Velocity of Sound in Single Crystals of Bismuth, 348–351
FREDERICK, H. A.: American Tentative Standard Acoustical Terminology, 60–71
FRICKE, E.: (see Knudsen, V. O.) (Abstract) 273

G

GARDNER, MARK B.: (see Steinberg, John C.) 11–23
GHOSH, R. N.: Theory of the Clarinet, 255–264
GILL, IRVING L.: Loudness Factors of Sound-in-Air Fog Signal Units, (Abstract) 74
GREENE, PAUL C.: Violin Intonation, 43–44
GREENTREE, C. D.: Vibration Instruments, (Abstract) 75

H

HERRIOTT, W. AND D. W. FARNSWORTH: High Speed Motion Pictures of the Vocal Cords, (Abstract) 274
HICKMAN, C. N.: Magnetic Recording and Reproducing, (Abstract) 77
HOELZLE, F. C.: Requirements of the Bureau of Marine Inspection and Navigation for Emergency Announcer Systems, (Abstract) 74
HULSWIT, WILLIAM H., JR.: Effect of Containing Tubes on Ultrasonic Velocities in Benzene, 224–226
HUNT, F. V. AND J. A. PIERCE: Preliminary Report on a High Fidelity Reproducer for Lateral Cut Disk Records, (Abstract) 274

J

JACK, WILLIAM AND JOHN S. PARKINSON: Method for Evaluating Compliant Materials in Terms of Their Ability to Isolate Vibrations, 141–145, (Abstract) 76
JANEWAY, R. N.: Coordinated Treatment of Automobile Noise and Vibration, (Abstract) 75
JARNAK, POUL: Acoustics of the Telephone Receiver with a New Earcap, (Abstract) 77
JONES, ARTHUR TABER: Resonance in Two Types of Non-Uniform Tubes, (Abstract) 271

K

KAGAN, S.: Reviews of Contemporary Papers, 267
KENNELLY, A. E. AND JACKSON H. COOK: M. K. S. System of Units Applied to Electroacoustics, 336–340
KLEIN, ELIAS: Absolute Sound Intensity in Liquids by Spherical Torsion Pendula, 312–320
—— Radiation Pressure by Torsion Pendulum and by "Weighing" on Spring Balance (With Demonstrations), (Abstract) 75
KNAUSS, HAROLD P.: Empirical Formula for the Loudness of a 1000-Cycle Tone, 45–46
KNOWLES, HUGH: Acoustic Networks in Loudspeaker Cabinets, (Abstract) 271

KNUDSEN, VERN O.: Some Cultural Applications of Modern Acoustics, 175–184
—— AND E. FRICKE: Absorption of Sound in Carbon Dioxide—Effects of Impurities, (Abstract) 273
KOBAYASHI, RYÛJI: (see Obata, Jûichi) 156–161
KOCK, WINSTON E.: New Interpretation of the Results of Experiments on the Differential Pitch Sensitivity of the Ear, 129–134

L

LAIDLER, T. J. AND E. G. RICHARDSON: Absorption of Supersonics in Smokes, 217–223
LEWIS, DON: On the Phase and Magnitude of Subjective Tones, (Abstract) 274
——, MILTON COWAN AND GRANT FAIRBANKS: Pitch Variations Arising from Certain Types of Frequency Modulation, (Abstract) 79
—— AND CURTIS TUTHILL: Resonant Frequencies and Damping Constants of Vocal Resonators, (Abstract) 273
LINDSAY, R. B. (see Focke, A. B.) 348–351
—— Book Review, 59
—— AND A. B. FOCKE: Finite Solid Acoustic Filters, (Abstract) 76
LOOMIS, ALLEN: (see Young, Robert W.) 79

M

MILLER, B. J. AND L. O. OLSEN: Position of the Vibrator in the Experiments of Melde and Kundt, 341–343
MORISON, G. E.: Predetermination of Speech Levels in Auditoria with Coupled Spaces, 244–254
MORRIS, R. M., G. M. NIXON AND J. S. PARKINSON: Variations in Sound Absorption Coefficients as Obtained by the Reverberation Chamber Method, 234–243; (Abstract) 76
MULLER, G. G., R. BLACK AND T. E. DAVIS: Diffraction Produced by Cylindrical and Cubical Obstacles (Title only) 273
MUNSON, W. A.: (see Fletcher, Harvey) 1–10; (Abstract) 78
—— (see Steinberg, J. C.) 272

N

NELSON, C. E.: Muffler and Silencer Design, (Abstract) 272
NEWMAN, E. B., S. S. STEVENS AND H. DAVIS: Factors in the Production of Aural Harmonics and Combination Tones, 107–118
NIXON, G. M.: (see Morris, R. M.) 234–243, (Abstract) 76
NORRIS, R. F.: Are Automobiles Not Quiet? (Abstract) 272
NOYES, ATHERTON, JR. (see Pierce, G. W.) (Abstract) 74; 185–192; 193–204; 301–307
—— AND G. W. PIERCE: Apparatus for Acoustic Research in the Supersonic Frequency Range, 205–211

O

OBATA, JÛICHI AND RYÛJI KOBAYASHI: Direct-Reading Pitch Recorder and Its Applications to Music and Speech, 156–161
OLSEN, L. O.: (see Miller, B. J.) 341–343
OLSON, HARRY F.: Horn Consisting of Manifold Exponential Sections, (Abstract) 271

P

PARKINSON, JOHN S.: (see Jack, William) (Abstract) 76; 141–145
—— (see Morris, R. M.) (Abstract) 76; 234–243
PHELPS, WILLIAM D.: Role of the Speaker Impedance in Resonance in a Closed Pipe, 308–311
PIELEMEIER, W. H.: Acoustical Detection of Electrically Weak Vibrations in Quartz Plates, 212–216
PIERCE, G. W.: (see Noyes, Atherton, Jr.) 205–211
—— AND ATHERTON NOYES, JR.: Acoustic Signaling Along the Plane Boundary Between Two Media, (Abstract) 74
—— AND ATHERTON NOYES, JR.: Improved Magnetostriction Oscillator, 185–192
—— AND ATHERTON NOYES, JR.: Theoretical and Experimental Investigation of the Transmission of Sound Over Reflecting Surfaces, 193–204
—— AND ATHERTON NOYES, JR.: Periods of Longitudinal Vibration of Steel Cones and Truncated Cones, 301–307
PIERCE, J. A.: (see Hunt, F. V.) (Abstract) 274
POTWIN, C. C.: (see Stanton, G. T.) (Abstract) 77
PROGRAM OF THE SEVENTEENTH MEETING, May 3–4, 1937, Washington, 74–79; Eighteenth Meeting, November 29–30, 1937, Ann Arbor, 271–274
Proposed Specifications for Audiometers for General Diagnostic Purposes, 72–73

R

RAILSBACK, O. L.: Chromatic Stroboscope, 37–42
—— Scale Temperament as Applied to Piano Tuning, (Abstract) 274
RAMER, L. G.: (see Sabine, Paul E.) (Abstract) 273
RAQUET, M. E. AND F. R. WATSON: Improved Method for Obtaining Photographs of Ripple Wave Actions, (Abstract) 271; 352–353
RICHARDS, WILLIAM T.: Recent Progress in Supersonics, (Abstract) 273
RICHARDSON, E. G.: (see Laidler, T. J.) 217–223
RIEBER, FRANK: Complex Elastic Wave Patterns in the Earth and Their Directional Analysis, (Abstract) 75
ROGERS, ROBERT AND F. J. WILLIG: Pressures of Sound Waves Measured by a Condenser Microphone and Oscillope for Continuously Varying Frequency, (Abstract) 271
RUSSELL, G. OSCAR: Pedagogical Hearing Tests of Large Groups, (Abstract) 78

S

SABINE, PAUL E.: Effects of Cylindrical Pillars in a Reverberation Chamber, (Abstract) 272
—— AND L. G. RAMER: Absorption Effects in Sound Transmission Measurements, (Abstract) 273
SAUNDERS, F. A.: Mechanical Action of Violins, 81–98
—— Mechanical Action of Violins of High Quality, (Abstract) 79
—— Book Review, 165

SHERWIN, CHALMERS W.: (see Taylor, Hawley O.) 331–335
SIVIAN, L. J.: Sound Propagation in Ducts Lined with Absorbing Materials, (Abstract) 77; 135–140
SKUDRZYK, E. J.: Reviews of Contemporary Papers, 168–172; 265–267; 355–358
SMALL, ARNOLD: Harmonic Structure of the Violin Tone as a Function of Bow Speed and Bow Pressure, (Abstract) 79
STANTON, G. T.: Sound Measuring Instruments as Applied to Noise Reduction, (Abstract) 272
—— AND C. C. POTWIN: Kansas City Municipal Auditorium Acoustics and Sound Reinforcement, (Abstract) 77
STEINBERG, JOHN C. AND MARK B. GARDNER: Dependence of Hearing Impairment on Sound Intensity, 11–23
—— AND W. A. MUNSON: Some Practical Considerations of the Effect of Noise Upon Speech Intelligibility (Title only) 272
STEVENS, S. S.: (see Newman, E. B.) 107–118
STUHLMAN, OTTO, JR.: Dynamics of the Auditory Ossicles, (Abstract) 78
—— Nonlinear Transmission Characteristics of the Auditory Ossicles, 119–128

T

TAI, CHUNG-LING: "Foaming Tone" Obtained from Vibrating Strings and Rods, (Letter to the Editor) 354
TAYLOR, HAWLEY O. AND CHALMERS W. SHERWIN: Sound Absorption and Attentuation by the Flue Method, 331–335
THOMAS, D. H.: Reviews of Contemporary Papers, 267
THURAS, A. L.: Sensitive Method of Measuring Magnetic Flux in Small Areas, (Abstract) 74
TRIMMER, JOHN D.: Sound Waves in a Moving Medium, 162–164
TRIMMER, JOHN D. AND F. A. FIRESTONE: Investigation of Subjective Tones by Means of the Steady Tone Phase Effect, 24–29
TUTHILL, CURTIS: (see Lewis, Don) (Abstract) 273

V

VIETH, L.: (see Wiebusch, C. F.) (Abstract) 273

W

WARNER, GLEN W.: Study of the Effect of Frequency and Temperature on the Velocity of Ultrasonic Waves in Gases, 30–36
WATSON, F. R.: (see Raquet, M. E.) (Abstract) 271; 352–353
—— Book Reviews, 165–167
WATSON, NORMAN A.: Limits of Audition for Bone Conduction, (Abstract) 274; 294–300
—— Hearing of Speech by Bone Conduction, 99–106
WEVER, ERNEST GLEN AND CHARLES W. BRAY: Distortion in the Ear as Shown by the Electrical Responses of the Cochlea, 227–233
WHITE, WILLIAM BRAID: Practical Tests for Determining the Accuracy of Pianoforte Tuning, 47–50
WIEBUSCH, C. F. AND L. VIETH: Application of Negative Feedback to Electromechanical Devices, (Abstract) 273
WILKS, C. R.: (see Focke, A. B.) 348–351
WILLIG, F. J.: (see Rogers, Robert) (Abstract) 271

Y

YOUNG, L. H.: Vibration Problems in Buildings, (Abstract) 75
YOUNG, ROBERT W. AND ALLEN LOOMIS: Improved Chromatic Stroboscope, (Abstract) 79